Hydrometallurgical Recovery of Gold from Waste Printed Circuit Boards - a Process Development, Process Plant Design, and Early-stage Feasibility Study

Dissertation Submitted for the Degree of

Master of Science in Engineering (MScEng),

Specialising in Chemical Engineering

By

Marco Ngeleka Mukuna

Supervisor

Prof. Jochen Petersen

Co-Supervisor

Dr. Thandazile Moyo

The University of Cape Town,

Department of Chemical Engineering,

Hydrometallurgy,

Minerals to Metals Research Group

2023

Declaration

I, Marco Ngeleka Mukuna, declare that:

- I know the meaning of plagiarism and that all the work in this dissertation, save for that which is properly acknowledged, is my own.
- This thesis/dissertation has been submitted to the Turnitin module (or equivalent similarity and originality checking software) and I confirm that my supervisor has seen my report and that any concerns revealed by such have been resolved with my supervisor.
- All sources referenced in this dissertation are correctly acknowledged and referenced using the UCT Author date system.
- This dissertation has not been submitted before for any degree or examination.

Signature: Signed by candidate

Date: 21 December 2023

Acknowledgements

I would like to express my sincere thanks to my lord and saviour Jesus Christ, and the following people:

- My supervisor, Prof. Jochen Petersen, for his technical advice, encouragement, patience, and guidance, and for all the effort he put into my work.
- My co-supervisor, Dr Thandazile Moyo, for her wealth of knowledge and guidance.
- My family and friends, for their support and understanding.
- Fernando Ortega Jiménez, Ameen Jakoet, and Kathija Shaik, for their technical advice in the laboratory.
- The South African National Research Foundation and the University of Cape Town, for their funding.

Table of Content

Chapter 1: Introduction 1

1.1 Background and Motivation 1

1.1.1 Waste Printed Circuit Boards (WPCBs) 1

1.1.2 Motivations for Industrial-scale WPCB Recycling Operations 5

1.1.3 Conventional Processing Plants for Metal Recovery from WPCB's 8

1.1.4 Drawbacks of Conventional Processing Plants for Au Recovery from WPCB's 10

1.1.5 Hydrometallurgical Processing Plants for Au Recovery from WPCB's 11

1.2 Problem Statement 13

1.3 Aim and Objectives 14

1.4 Limitations 16

1.5 Structure of Dissertation 17

Chapter 2: Literature Review 19

2.1 Base Metal (BM) Leaching from WPCBs 20

2.2 Au Leaching from WPCBs 22

2.2.1 Cyanide Lixiviants 22

2.2.2 Thiosulphate Lixiviants 23

2.2.3 Thiourea Lixiviants 24

2.2.4 Halide Lixiviants 24

2.3 Au Concentration by Liquid-Liquid Extraction (LLE) 27

2.4 Au Concentration by Solid-Liquid Extraction (SLE) 30

2.5 Au Recovery by Electrowinning (EW) 34

2.5.1 Au EW Fundamentals 34

2.5.2 Practical Au EW Considerations 35

2.5.3 Previous Investigations into Au EW 38

2.6 Simultaneous Au Concentration and Recovery by Ion-exchange Extractant Membrane (IEM) SLE and EW 41

2.7 IEMs and IEM Separation 43
2.7.1 IEM Classification 43
2.7.2 IEM Design Principles 44
2.7.3 IEM Production 45
2.7.4 IEM Separation Fundamentals 45
Chapter 3: Technical Feasibility 49
3.1 Materials and Apparatus 51
3.1.1 WPCB I^--I_2-Au Electrolyte Solution, and I^--I_2 Electrolyte Solution 51
3.1.2 Au Selective Ion Exchange Extractant Membrane (Au-IEM) 53
3.1.3 Anion-Exchange Membrane (AEM) 56
3.1.4 Experimental IX-EW Cell 57
3.2 Method 59
3.3 Results and Discussion 61
3.3.1 Au and BM Concentrations in WPCB's 61
3.3.2 Au and BM Concentrations in Leachates and Leaching Yields 62
3.3.3 Au Concentration and Recovery by IEM-SLE and EW 64
Chapter 4: Process Development and Process Plant Design 69
4.1 Plant Capacity, Availability, and Operation 69
4.2 Feed Composition 71
4.3 Size-reduction Circuit 71
4.4 Leaching Circuit 73
4.5 Concentration-Recovery Circuit 79
Chapter 5: Economic Feasibility 87
5.1 Methodology 87
5.1.1 Net Present Value (NPV) 88
5.1.2 Profitability Indices and Pay Back Period (PBP) 89
5.1.3 Financial Considerations 90

5.1.4 Financial Cost Estimations 93

5.2 Results and Discussion 96

5.2.1 Capital Investment 96

5.2.2 Revenue 100

5.2.3 Production Cost 102

5.2.4 Discounted Cash Flow and Profitability (DCFP) Assessment 106

5.2.5 Sensitivity Analysis 109

Chapter 6: Conclusions and Recommendations 115

References 120

Appendix 138

List of Figures and Tables

Table 1.1.1 WEEE categories, and examples of waste items in each category (Ogunseitan et al, 2009) 1

Table 1.1.2 Concentration and market value of common economically valuable metals found in typical WPCBs (Vermesan et al., 2019; Yazıcı and Deveci, 2016). 8

Table 2.1.1 Summary table of previous studies investigating the leaching of BMs from WPCBs ((a) Le et al., 2011, b) Vijayaram et al., 2013, c) Bas et al.,2014, d) Birloaga et al., 2013, e) Jadhav and Hocheng, 2015, f) Kumari et al., 2016, g) Deveci et al, 2010, h) Oh et al, 2003)) 21

Table 2.4.1 Metal loading performance onto Purogold S992 and activated carbon (Van Deventer et al., 2012) 32

Table 3.1.1 Technical specifications of the PVC and Purogold S992 resin used to synthesise the Au-IEM employed in the laboratory experiment (Sasol, n.d.; Purolite, n.d.) 54

Table 3.3.1 Au and BM concentrations in WPCB's 62

Table 3.3.2 Au and BM concentrations in leachates 62

Table 3.3.3 Au and BM leaching yields 63

Table 3.3.4 Metal concentrations in 2.0 L electrolyte solutions in IX-EW cell 65

Table 3.3.5 Summary of key results 68

Table 4.2.1 Processing plant's WPCB feed composition 71

Table 4.4.1 Processing plant's daily leachate metal compositions 76

Table 4.5.1 Processing plant's IX-EW cell specifications 83

Table 5.1.1 Ratio factors for estimating capital investment items of solid-fluid processing plants based on delivered-equipment cost (Peter and Timmerhaus, 2003) 94

Table 5.1.2 Ratio factors for estimating direct production cost, fixed production cost, and general production cost of solid-fluid processing plants (Peter and Timmerhaus, 2003) 95

Table 5.1.3 Number of operating labours per process section in a batch operation chemical processing plant with automatic controls (Seider et al., 2019) 96

Table 5.2.1 Processing plant's start-up equipment costs 97

Table 5.2.2 Processing plant's total capital investment..... 98

Table 5.2.3 Processing plant's annual revenue 101

Table 5.2.4 Processing plant's electricity costs.....102

Table 5.2.5 Processing plant's raw material and production consumable cost 103

Table 5.2.6 Processing plant's production cost.....105

Table 5.2.7 Processing plant's discounted cash flow and profitability assessment results 107

Table 5.2.8 Comparison of processing plant's profitability indices with alternative projects 108

Table 5.2.9 Corporate tax rate, discount rate, bond interest rate, total capital investment, annual production cost, and annual revenue used in the processing plant's sensitivity analysis 112

Table 5.2.10 Processing plant's sensitivity analysis results 112

Figure 1.1.1 Schematic illustration of concentrations (in ppm) of common chemical elements found in WPCBs (note, elemental content decreases with colour intensity) 3

Figure 2.5.1 Schematic illustration of the EW cell used by Meng et al. (2019) 40

Figure 2.6.1 Schematic illustration of the IX-EW cell used by Sun et al. (2020)..... 42

Figure 2.7.1 Categorized IEMs. (a) Positive or negatively charged monopolar IEM, (b) Amphoteric IEM, (c) Bipolar IEM and (d) Mosaic IEM (adapted from Asante-Sackey et al., 2021) 43

Figure 2.7.2 Ion pathway through a (a) homogeneous IEM and (b) heterogeneous IEM (Asante-Sackey et al., 2021) 48

Figure 3.1 Simplified overall block flow diagram of the processing plant 49

Figure 3.1.1 Scheme of leaching set-up..... 51

Figure 3.1.2 10 cm x 15 cm WPCB used in the laboratory experiment 53

Figure 3.1.3 Schematic illustration of the side view (bottom) and isometric view (top) of the experimental cell used 58

Figure 4.1 Overview of the processing plant's daily mass and energy flow..... 70

Figure 4.3.1 Processing plant's size-reduction circuit flowsheet 71

Figure 4.4.1 Processing plant's leaching circuit flowsheet. 73

Figure 4.4.2 SJ8.5x9.0 Tank (Xinhai, n.d.) 77

Figure 4.4.3 Sinus Jevi Type D-8800, W 3161-30 immersion heater (sinusjevi, n.d.)..... 78

Figure 4.4.4 Ishigaki Lasta MC filter press (Ishigaki, n.d.) 79

Figure 4.5.1 IEM-SLE and EW circuit flowsheet 82

Figure 4.5.2 Schematic illustration of the IX-EW cell 82

Figure 4.5.3 Visual illustration of the IX-EW cell showing specifications 84

Figure 5.2.1 Change in processing plant's NPV vs percentage change in variable 113

Abbreviations

Anion-exchange membrane: AEM

Au selective ion-exchange extractant membrane: Au-IEM

Base metals: BMs

Bed volumes per hour: BV/h

Cathode ray tube: CRT

Chemical engineering plant cost index: CEPCI

Direct current: DC

Discounted cash flow and profitability: DCFP

Divinylbenzene: DVB

Diethylene glycol dibutyl: DBC

Di-isobutyl ketone: DIBK

Di-(2-ethylhexyl)phosphoric acid: D2EHPA

Double declining balance: DDB

Electrical and electronic components: EECs

Electrical and electronic equipment: EEE

Electrowinning: EW

Fixed capital investment: FCI

High-density polyethylene: HDPE

IEM-SLE and EW cell: IX-EW cell

Inductively coupled optical emission spectroscopy: ICP-OES

Internal rate of return: IRR

Ion-exchange extractant membrane solid-liquid extraction and electrowinning: IEM-SLE and EW

Ion exchange: IX

Light emitting diodes: LEDs

Liquid-liquid extraction: LLE

Magnetic resonance imaging: MRI

Medium-base anion: MBA

Methyl isobutyl ketone: MIBK

Metric ton per annum: tpa

Metric tons: t

N-di-n-octylacetamide: DOAA

Net present value: NPV

N,N-di-n-octylauramide: DOLA

Parts per million: ppm

Payback period: PBP

Poly-vinyl-chloride: PVC

Printed circuit boards: PCBs

Return on investment: ROI

Revolutions per minute: rpm

Revolutions per second: RPS

Solid-liquid extraction: SLE

Solid-to-liquid ratio: S/L

Special Economic Zone: SEZ

Strong-base anion: SBA

Tetrahydrofuran: THF

Total Capital Investment: TCI

Tributyl phosphate: TBP

Tributyl phosphine oxide: TBPO

United States of America Dollar: US$ or $

Waste EEE: WEEE

Waste PCBs: WPCBs

2-ethyl hexyl phosphonic acid mono-2-ethylhexyl ester: PC-88A

Summary

Au recovery is one of the most important aspects of an industrial-scale waste printed circuit board (WPCB) recycling operation because Au is a highly economically valuable metal which is present in WPCBs in appreciable concentrations, often tens to hundreds of times greater than in naturally occurring ore deposits. Unfortunately, significant value loss and resource wastage occurs when Au is recovered from WPCBs in conventional processing plants which use various pyrometallurgy and physical separation techniques. The primary aim of this project was to contribute knowledge to the development of a hydrometallurgical processing plant for Au recovery from WPCBs, which can be applied in real-life industrial-scale WPCB recycling operations, in a technically and economically feasible manner, as an alternative to conventional processing plants. To achieve this aim, findings from literature were used to successfully design a theoretical hydrometallurgical processing plant for Au recovery from WPCBs, which uses a non-toxic and recyclable iodide lixiviant for Au leaching and the novel ion-exchange extractant membrane solid-liquid extraction and electrowinning (IEM-SLE and EW) technique for Au concentration and recovery. The designed processing plant's early-stage technical feasibility assessment was supported by a laboratory experiment investigating the recovery of Au from WPCB iodide leachates using the IEM-SLE and EW technique. This laboratory experiment commenced by loading 2.0 L of WPCB iodide leachate into the feed tank of the experimental IEM-SLE and EW cell (IX-EW cell) and loading 2.0 L of KI^{-}-I_2 electrolyte solution into the electrolyte solution tanks hosting the cathode and anode. Thereafter, electrical power was provided to the electrodes at a constant cell voltage of 12.9 V, temperature of 25 ^{o}C, 250 rpm agitation speed, average current of 5 A, and 1429 A/m^2 equivalent current density. Once the experiment was complete/electrical power had been provided for 6.0 hrs, the brown Au deposit on the cathode was chemically analysed together with the sample electrolyte solutions collected from each of the IX-EW cell's tanks (after 2 hrs, 4 hrs, and 6 hrs). The laboratory experiment results demonstrated that Au recovery from WPCB iodide leachates using the IEM-SLE and EW technique is technically feasible since it was possible to concentrate and recover Au under the given conditions

with a high yield (95.5 %) while recycling/recovering an iodide solution with an 82 % I_2 recovery yield and 89 % I^- recovery yield. However, due to the high voltages applied (12.9 V) and due to the loss of Au (~4 %) to the Au-IEM, it is evident that more research is required to optimise the developed processing plant before it can be subjected to a thorough technical and/or economic feasibility assessment, for application in a real-life industrial-scale WPCB recycling operation, in a technically and economically feasible manner. Through a discounted cash flow and profitability (DCFP) assessment, the early-stage economic feasibility of the processing plant under ideal conditions was successfully determined within a South African context. Results of the DCFP assessment showed that the processing plant's estimated NPV was $5,812,000,000 at a bond interest rate of 9 %, a cash flow discount rate of 17.86 %, and a corporate tax rate of 15 %. While the processing plant's ROI, PBP, net margin, and ebitda margin were estimated to be 76.00 %, 0.03 years, 34.74 % and 48.37 %, respectively. The observed short PBP and large positive NPV, ROI, net margin, and ebitda margin, suggest that the developed processing plant is economically feasible under the ideal specified plant design conditions. However, the sensitivity analysis of the processing plant's early-stage economic feasibility assessment shows that the developed processing plant is likely to be economically unfeasible for industrial-scale application under non-ideal conditions in a real-life setting since the annual revenue obtained from the recovery of Au from typical/ non-ideal WPCBs is unlikely to result in pay back or produce a large positive NPV, ROI, ebitda margin, or net margin. The results of the sensitivity analysis showed that the processing plant's economic feasibility is highly sensitive to the key assumptions used in the design and development, and economic feasibility assessment, and in particular assumptions relating to annual revenue. Therefore, any future research and development should carefully review and ensure that any assumptions used are as accurate as possible. From the findings presented in this thesis, it is evident that the developed processing plant justifies further research and development for future application in real-life industrial-scale WPCB recycling operations. This is because the developed processing plant has the potential to be applied industrially in a technically and economically feasible manner as evidenced by the results of the project's early-stage technical and economic feasibility assessment.

Chapter 1
Introduction

1.1 Background and Motivation

1.1.1 Waste Printed Circuit Boards (WPCBs)

Electrical and electronic equipment (EEE) is defined as equipment dependent on an electric current or electromagnetic field to function, and equipment for the generation, transfer, or measurement of such currents and fields (Williams, 2011; Ogunseitan et al., 2009). An essential constituent of almost all EEE is the printed circuit board (PCB), which is used to support and interconnect an assortment of electrical and electronic components (EECs) such as resistors, capacitors, and semiconductors (Bhunia and Tehranipoor, 2019; Grout, 2008; Hirvikorpi et al., 2005). When EEE has reached its end-of-life (becomes obsolete) and has been discarded by its owner, it is referred to as waste EEE (WEEE). PCBs found within WEEE are referred to as waste PCBs (WPCBs). Grouped into 10 categories (Table 1.1.1), WEEE includes a variety of waste items such as waste mobile phones, televisions, and ovens (Ogunseitan et al., 2009).

Table 1.1.1 WEEE categories, and examples of waste items in each category (Ogunseitan et al, 2009)

No.	WEEE category	Examples of waste items
1	Large household appliances	Refrigerators, ovens, washing machines
2	Small household appliance	Toasters, microwaves, vacuum cleaners
3	IT[a] and telecommunications equipment	Mobile phones, desktop computers
4	Consumer equipment	Televisions, radios, speakers
5	Lighting equipment	LEDs[b], CRT[d], gas discharge lamps
6	Electrical and electronic tools	Power drills, electric screwdrivers
7	Toys, leisure, and sports equipment	Treadmills, game consoles
8	Medical devices	MRI[c] scanners, pacemakers
9	Monitoring and control instruments	Thermocouples, smoke detectors
10	Automatic dispensers	Vending machines, automated teller machines

[a] information technology, [b] light emitting diodes, [c] magnetic resonance imaging, [d] cathode ray tube

WPCB Classification

WPCBs are typically classified based on 'layers', 'form', or 'population'. In terms of layers, WPCBs are classified as single-layer, double-layer, or multi-layer. Single-layer WPCBs are comprised of a solitary non-conductive substrate/ laminate, with a conductive circuit (layers, pads, tracks, or single traces) printed or etched on one side. These conductive circuits are often coated with a protective solder mask and/or silkscreen. Single-layer WPCBs are found in simple WEEE such as waste calculators, radios, and printers (Bhunia and Tehranipoor, 2019). Double-layer WPCBs are similar to single-layer WPCBs, however, in these types of WPCBs, conductive circuits are printed or etched on both sides of the non-conductive substrate. Double-layer WPCBs are found in complex WEEE such as waste computers and automotive dashboards. Multi-layer WPCBs are essentially two or more double-layer WPCBs stacked on top of each other, with the different layers joined together by a specialized adhesive. Multilayer WPCBs are found in high-end WEEE such as waste satellites (Hadiet et al., 2015). In general, conductive circuits in double-layer and multi-layer WPCBs are electrically interconnected by conductive pathways known as vias (Grout, 2008).

In terms of form, WPCBs are classified as rigid, flexible, or flex rigid. Rigid WPCBs are those with firm non-conductive substrates, while flexible WPCBs are those with free-bending non-conductive substrates. Rigid WPCBs are found in WEEE such as waste mobile phones and desktop computers, while flexible WPCBs are found in WEEE with complicated shapes such as waste sports watches. Flex-rid WPCBs are a combination of rigid and flexible WPCBs and are found in lightweight WEEE such as waste cell phones and digital cameras (Hirvikorpi et al., 2005).

In terms of population, WPCBs are classified as populated or non-populated. Populated WPCBs are those with EECs mounted onto their conductive circuits by various joining materials and mechanisms such as press-fitting using socket pedestal devices, soldering using through-hole devices or surface mount devices, screw jointing, rivet jointing, glueing using electrically conductive adhesives, etc. (Lee et al., 2012), while non-populated WPCBs are those without mounted EECs. Populated WPCBs are usually enclosed in protective casings (housing units) and are generally

equipped with structural components such as heat sinks and standoffs. Populated WPCBs are generally found in WEEE, while unpopulated WPCBs usually occur as waste products of primary PCB production (Grout, 2008; Hirvikorpi et al., 2005).

WPCB Chemical Elements

WPCBs are highly complex heterogeneous resources comprised of over 60 different chemical elements, which include non-metals such as Cl, Br, and I, base metals (BMs) such as Fe, Sn, and Zn, precious metals such as Au, Ag, and Pd, rare earth metals such as Y, Ce, and La, and metalloids such as Si, B, and Bi. Figure 1.1.1 shows the relative concentration (in parts per million/ppm) of some of the common chemical elements found in WPCBs (Waldir et al., 2014).

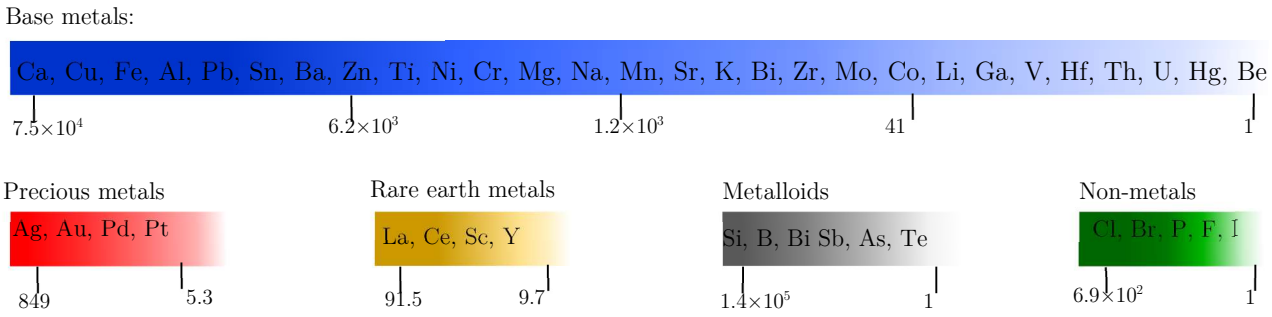

Figure 1.1.1 Schematic illustration of concentrations (in ppm) of common chemical elements found in WPCBs (note, elemental content decreases with colour intensity) (adapted from Waldir et al., 2014)

WPCB Materials

Chemical elements are present in WPCBs as an assortment of over 1000 different materials, which are broadly characterised as organic or inorganic WPCB materials. In principle, plastics are the most common organic WPCB materials, constituting approximately 40-70 wt.% of all WPCB materials. Plastics in WPCBs are found in a variety of locations. For example, nylon, polyvinyl chloride, polyethylene, polypropylene, and polycarbonate are found in protective casings and thermal and electrical insulation coatings on EECs such as electrical wires and cables. Polytetrafluoroethylene, polyethersulphone, epoxy resins, cyanate resins, and phenolic resins are found in non-conductive

substrates. Polyester resins and polyimide resins are found in conductive circuit silk screens. Plastics in WPCBs are normally found together with additive organic WPCB materials. These include brominated or chlorinated flame retardant additives such as polychlorinated biphenyls, tetrabromobisphenol-A, polybrominated biphenyls, hexabromocyclododecane, and polybrominated diphenyl ethers heat stabiliser additives such as hydroxyphenyltriazines, benzotriazoles, oxanilides, and benzophenones, plasticizer additives such as phthalates, curing additives such as 4,4'-diaminodiphenyl sulfone, 4,4'-diaminodiphenyl methane, and dicyanodiamide, anti-static additives such as ethoxylated amines, glycerol monostearate, and polyethylene glycol esters, colourant/pigment additives such as anthraquinones, and impact modifier additives such as methyl-butadiene-styrene and chloropolyethylene (Rajesha et al., 2019; Biswal et al., 2015; Marques et al., 2013; Xiong et al., 2020).

In principle, metals are the most common inorganic WPCB materials, constituting approximately 20-40 wt.% of all WPCB materials. Metals are normally found as pure metals or alloys in a variety of locations in WPCBs. For example, pure Cu is found in conductive circuits, Au alloys containing metals such as Sn, Ag, Pd, and Ni are found on electrical conductive coatings in EECs such as contact pins, Pb and Sn alloys containing metals such as Cd, In, Ag, Bi, An, and Zn are found in soldering joining materials, Al alloys containing metals such as Mg, Mn, and Ti are found in heat sinks, Fe alloys containing metals such as Ni and Cr are found in protective casings, Ga alloys containing metals such as In, Zn and As are found in EECs such as semiconductors, Cd alloys containing metals such as Co, Al and Cu are found in EECs such as batteries, while Nd alloys containing metals such as Dy and Tb are found in EECs such as hard disc drive magnets. (O'Connor et al., 2016; Ghosh et al., 2015). Ceramics and glasses are another common class of inorganic WPCB materials, they are known to constitute approximately 20-30 wt.% of all WPCB materials. In WPCBs, ceramics and glasses are found in a variety of locations, for example, silica (SiO_2) and alumina (Al_2O_3) are found in non-conductive substrates (Guidolin et al., 2017), while rare earth metal oxides (e.g., Y_2O_3 and CeO_2), BM oxides (e.g., BaO, Na_2O, MgO, CaO, K_2O, PbO etc.), and

non-metal oxides (e.g., B_2O_3) are found in EECs such as cathode ray tubes, fluorescent screens, lamps, and bulbs (Iniaghe and Adie, 2015; Iniaghe and Adie, 2017).

1.1.2 Motivations for Industrial-scale WPCB Recycling Operations

Abundance of WPCBs

The quantity of WEEE produced globally per annum has increased dramatically in recent years, from 46.4 million metric tons (t) or 6.6 kg per capita in 2015 to 53.6 million t or 7.3 kg per capita in 2019 (Forti et al., 2020). With an annual growth rate of 3–5 wt.%, WEEE is the fastest-growing waste stream in the world, growing at a rate almost 3 times faster than any other waste stream. It is thus unsurprising that the amount of WEEE generated globally per annum is expected to exceed 74 million t in 2030 (Forti et al., 2020). The exponential increase in the quantity of WEEE generated globally per annum has been attributed to a surge in EEE supply and demand, which is driven by population growth, economic development, technological advancement, and decreasing EEE product life span (Forti et al., 2020). WPCBs are known to constitute approximately 4–7 wt.% of WEEE, though this proportion is considerably higher in consumer equipment and in IT and telecommunications equipment (WEEE categories 3 and 4), where for example WPCBs constitute 20-30 wt.% of waste mobile phones, ~20 wt.% of waste desktop computers and ~10 wt.% of waste televisions (Ogunseitan et al., 2009; Bhunia et al., 2019; Grout, 2008). Thus, by considering that WEEE is produced globally per annum in millions of t, it can be presumed that WPCBs are produced globally per annum in at least hundreds of thousands of t. This presents a strong motivation for industrial-scale WPCB recycling operations, as it suggests that there is an abundance of WPCB material available for beneficiation in these operations.

Hazardous Nature of WPCBs

At present, landfill dumping is the most common WPCB disposal method (Forti et al., 2020). Although most modern-day landfills are equipped with impermeable covers and liners, these typically crack or break over time due to large confining pressures, errors in construction, or poor management

and maintenance (Yedla, 2005; Danthurebandara et al., 2013). Therefore, when WPCBs are disposed of in landfills, rainwater may percolate through broken landfill covers and leach any hazardous organic and inorganic WPCB materials present, and as a result, produce an aqueous leachate containing these hazardous WPCB materials. This presents a potential hazard to human health as the aforementioned aqueous leachate may flow through cracks in broken landfill liners and contaminate surrounding soil, crops, and/or groundwater with hazardous WPCB materials (Spalvins et al., 2008). Hazardous organic WPCB materials are mainly those containing toxic brominated or chlorinated flame-retardant additives such as polychlorinated or polybrominated biphenyls, polybrominated diphenyl ethers, tetrabromobisphenol-A, and hexabromocyclododecane, while hazardous inorganic WPCB materials are mainly those containing toxic chemical elements such as Pb, Cd, Sn, Hg, As, In, Li, Ni, Ba, Be and Cr. If food or water containing hazardous WPCB materials is ingested by humans, then deleterious health effects such as hormonal dysfunction, liver damage, heart disease, or even death may occur (Spalvins et al., 2008; O'Connor et al., 2016; Gosh et al., 2015).

After landfill dumping, incineration and open-air burning are the most common WPCB disposal methods (Forti et al., 2020). When WPCBs are disposed of by incineration or open-air burning, toxic off-gas dusts containing hazardous chemical elements such as Pb, Cd, As, Hg, In, Li, Ni, Sn, Ba, Be and Cr are released after the thermal decomposition of hazardous inorganic WPCB materials. Moreover, toxic exhaust off-gases containing hazardous compounds such as polybrominated or polychlorinated dibenzofurans and dibenzo-p-dioxins, Br_2, and Cl_2 are released after the thermal decomposition of hazardous organic WPCB materials (Cesaro et al., 2019). This presents a potential hazard to human health, as these toxic exhaust off-gas dusts may be discharged into the air and subsequently inhaled by humans (with this resulting in deleterious health effects such as emphysema, lung cancer, liver damage, muscle failure, bone damage, or spleen damage) (Sivaramanan, 2013).

Though uncommon in most parts of the world (particularly developing countries), the beneficiation of WPCBs during industrial-scale WPCB recycling operations is also a WPCB disposal method. It

has been reported that most industrial-scale WPCB recycling operations have strong motivations (namely, due to stringent governmental legislation) to reduce the quantity of WPCB material which can be disposed of by improper methods such as incineration, open-air burning, and landfill dumping so that the deleterious human health hazards imposed by these methods can be mitigated (Forti et al., 2020; Cesaro et al., 2019; Sivaramanan, 2013).

Economic Value of Metals in WPCBs

Most metals found in WPCBs are originally recovered from ores after a beneficiation process during industrial-scale mining and minerals processing operations. Unfortunately, metal recovery from ores is faced with several drawbacks such as the high consumption of energy and water, generation of large quantities of waste, land destruction, and pollution of surrounding environments with harmful gases (e.g., sulphur and carbon dioxide) and effluents (Thompson, 2009; Norgate et al., 2006; Makua and Kola, 2017; Pichtel, 2016). Ores are also obtained from natural ore reserves which are finite resources, and with high-quality ore reserves diminishing, more energy, water, and capital is being required to recover metals from ores derived from low-quality ore reserves (this also results in greater environmental pollution) (Makua and Kola, 2017; Pichtel, 2016). Furthermore, ore reserves are primarily concentrated in a handful of countries, some of which are politically unstable, thus, creating a supply risk (Nasser et al., 2020).

Fortunately, some metals found in WPCBs can also be recovered from WPCBs after a beneficiation process during an industrial-scale WPCB recycling operation. In comparison to metal recovery from ores, metal recovery from WPCBs is typically achieved with less waste generation and land destruction, minimal environmental pollution, and lower consumption of energy, water, and capital. Moreover, metal recovery from WPCBs reduces the pressure on the use of finite and supply-risk natural ore reserves and can generate profits since metals can be sold after recovery. Profits realised from metal recovery from WPCBs are mainly obtained from the recovery of economically valuable metals such as Au, Pd, and Cu which are often present in typical WPCBs in significant concentrations, often tens to hundreds of times greater than in ores (Table 1.1.2) (Vermesan et al.,

2019; Yazıcı and Deveci, 2016). Hence, it can be concluded that metal recovery from WPCBs during industrial-scale WPCB recycling operations presents a key motivation for these operations as it allows for the generation of profit and recovery of metals with significantly fewer drawbacks than metal recovery from ores.

Table 1.1.2 Concentration and market value of common economically valuable metals found in typical WPCBs (Adapted from Vermesan et al., 2019; and Yazıcı and Deveci, 2016)

Metal	Market value (US$/kg)	Concentration in WPCBs (%)	Concentration in Ores (%)	Market value (US$/kg WPCB)
Ag	870.0	8×10^{-3} - 100×10^{-3}	5×10^{-5} - 10×10^{-5}	0.070 - 0.870
Au	62,600	3×10^{-3} - 35×10^{-3}	5×10^{-5} - 10×10^{-5}	1.883 - 21.96
Pd	75,200	3×10^{-3} - 20×10^{-3}	1×10^{-5} - 10×10^{-5}	2.257 - 15.05
Fe	6.520	5.00 - 11.0	30.0 - 60.0	0.326 - 0.717
Cu	6.761	12.0 - 35.0	0.50 - 3.00	0.811 - 2.366
Al	1.781	1.50 - 5.00	20.0 - 24.0	0.027 - 0.089
Pb	1.883	0.90 - 5.00	3.00 - 15.0	0.017 - 0.094
Ni	14.90	1.00 - 7.00	1.00 - 5.00	0.149 - 1.043
Sn	18.15	0.30 - 3.00	0.50 - 3.00	0.054 - 0.545
Zn	2.466	0.10 - 2.50	0.15 - 0.65	0.062 - 0.200

1.1.3 Conventional Processing Plants for Metal Recovery from WPCBs

In principle, the main objective of most industrial-scale WPCB recycling operations is to recover economically valuable metals. This is typically achieved in conventional processing plants comprised of mechanical, physical separation, and hybrid end-processing stages (Hadiet et al., 2015; Fujita et al., 2014). Currently, all industrial-scale WPCB recycling operations commence with a mechanical processing stage. During this stage, WPCBs (obtained from dismantled WEEE) are firstly stripped from their structural housing units and casings. Functioning EECs are subsequently depopulated from stripped WPCBs and refurbished (after which they are sold for reuse). Thereafter, EECs with an abundance of hazardous substances (e.g., batteries, capacitors, CRTs, LEDs, etc.) are also depopulated from stripped WPCBs, however, these components are either discarded in landfills dedicated for hazardous waste or recycled in more specialised facilities. Finally, WPCBs are size

reduced (using a combination of mechanical shredding, crushing and/or grinding techniques) so as to yield a WPCB particulate comprised of an assortment of liberated organic and inorganic material grains. Subsequent to size-reduction, WPCBs often undergo a screening process to separate the crushed particles into uniformly sized sample fractions. (Nekouei et al., 2018)

In most modern industrial-scale WPCB recycling operations, the mechanical processing stage is succeeded by a physical separation processing stage which often commences with the treatment of WPCB particulates using gravity (and in some instances particle shape) separation techniques to produce two separate fractions. Namely, a metallic particulate (mixture of ferrous and non-ferrous metal grains) and non-metallic particulate (mixture of ceramic, glass, and organic material grains) fraction. In general, the aforementioned metallic particulate is further separated into a ferrous metal and non-ferrous metal particulate fraction through the use of magnetic separation techniques, while an Al particulate fraction is often separated from the non-ferrous metal particulate, with the use of eddy-current separation techniques. (Nekouei et al., 2018; Dias et al., 2019)

A hybrid end-processing stage for metal recovery is typically the final processing stage in most modern-day WPCB recycling operations. Metal recovery in this end-processing stage is achieved after the treatment of WPCBs (which have undergone a mechanical and often physical separation processing stage) using a combination of pyrochemical processes (e.g., pyrolysis, gasification and pyrometallurgy) and hydrometallurgy to yield pure metals (e.g., Au and Cu) and alloys (e.g., steel). (Fujita et al., 2014; Nekouei et al., 2018; Dias et al., 2019). The blister smelter process is an example of a commercially applied hybrid end-processing method which is used for metal recovery from WPCBs, and in particular Cu and precious metals. During this process, a WPCB feed (typically comprised of WPCB-derived non-ferrous metal particulate fractions) is firstly mixed with a Cu concentrate such as a Cu matte and in some instances Cu or precious metal scrap. The resulting mixture is then charged into a furnace where it is smelted by combustive heat generated from a redox reaction which occurs when hot O_2 gas is injected into the furnace and reacts with the coke or coal which is also added into the furnace. The aforementioned smelting process produces blister

Cu, which is subsequently tapped from the furnace and cast into anodes which are subjected to an electro-refining process for the recovery of high-purity Cu. Following this electro-refining process, an anode slime containing precious metals (Au, Pt, etc.) is obtained as a by-product. Precious metals are typically recovered from this anode slime after the use of various hydrometallurgical refining processes (Vidyadhar, 2015).

1.1.4 Drawbacks of Conventional Processing Plants for Au Recovery from WPCBs

Au is arguably the most important metal which is recovered during an industrial-scale WPCB recycling operation. This is because Au is a highly economically valuable metal which is present in WPCBs in appreciable concentrations, often tens to hundreds of times greater than in naturally occurring ore deposits. In terms of economic value per kg of WPCB, Au accounts for 60-80 % of the total economic value of WPCBs. It is for this reason that the profitability of most industrial-scale WPCB recycling operations is intrinsically linked to successful Au recovery (Gloe et al., 1990). Unfortunately, significant value loss and resource wastage occurs when conventional processing plants are used for Au recovery from WPCBs, since Au is not recovered with maximum yield. This primarily occurs because, during the mechanical processing stage in such conventional processing plants, some non-ferrous metal grains containing Au are not completely liberated from the other non-metallic, ferrous metal and Al material grains after the size-reduction step of the mechanical processing stage (mainly due to the strongly interlocking nature of WPCB materials). As a consequence, >40 wt.% of Au can concentrate in the non-metallic, ferrous metal, and/or Al particulates obtained after the physical separation processing stage (United Nations University, 2012). For example, Yazici et al. (2015) reported that following the physical separation of size reduced WPCBs (using magnetic separation) into a non-ferrous metal and ferrous metal fraction, more than 60 % of Au was lost into the ferrous metal fraction. When the non-metallic, ferrous metal or Al WPCB particulates obtained after the physical separation processing stage are end-processed, the >40 wt.% of Au present is not recovered and is instead lost in the by-product slags or residues

produced. Minor quantities (up to 5 wt.%) of Au is also lost during the end-processing of the non-ferrous metal WPCB particulate. However, in this instance, Au loss stems from the poor selectivity of pyrochemical processes. Another problem with using conventional processing plants for the recovery of Au from WPCBs is that hazardous exhaust off-gases are released as a by-product when pyrochemical processes are used during the end-processing stage. This necessitates the use of expensive state-of-the-art off-gas treatment systems (which convert off-gas into fine furnace dust which can be responsibly disposed), which require millions of US$ in capital investment for installation, which in some instances can be more than 150 million US$ (Ortuño et al., 2014). It is for these reasons that conventional processing plants for Au recovery from WPCBs must be operated at very large industrial scales to be economically viable.

1.1.5 Hydrometallurgical Processing Plants for Au Recovery from WPCBs

In response to the drawbacks associated with the use of conventional processing plants for Au recovery from WPCBs (Section 1.1.2), there has been increased research into the development of alternative hydrometallurgical processing plants which can be used for Au recovery from WPCBs during industrial-scale WPCB recycling operations (Ashiq, 2019). Most hydrometallurgical processing plants for Au recovery from WPCBs commence with the leaching of a size-reduced WPCB particulate in a strongly oxidising and complexing aqueous lixiviant. This liberation improves both leaching yield and kinetics. A strongly oxidising lixiviant is required for Au leaching since Au possesses a large positive reduction potential, owing to the relativistic contraction of its 6s orbitals, while a strongly complexing lixiviant is required since leached Au (as Au^{3+} and/or Au^{+} ions) is thermodynamically unstable unless it is complexed by a suitable ligand such as cyanide (CN^{-}), chloride (Cl^{-}), iodide (I^{-}), bromide (Br^{-}), or thiosulphate ($O_3S_2^{-2}$) (Zhang et al., 2012). During the aforementioned leaching process, Au, and other metals (namely Ag, Pd, Fe, Ni, Zn, Sn, Sb, Mn, and Al) present in the WPCBs encounter the lixiviant are subsequently leached into the lixiviant, thus, producing a leachate from which Au is recovered after a refining process utilising techniques such as solvent extraction and electrowinning. (Ashiq, 2019; Singh and Prasad, 2007)

Currently, most previously developed hydrometallurgical processing plants for Au recovery from WPCBs have been developed to utilise conventional cyanide or chloride lixiviants for Au leaching, which are unfortunately toxic and/or corrosive, and difficult to recycle. Hence, on the consideration that a low solid-to-liquid (S/L) ratio is typically necessary for optimal metal leaching from WPCBs using conventional cyanide or chloride lixiviants (which in some instances can be as low as 20 g/L as reported by Hao et al., 2022), it is expected that the use of such lixiviants for Au leaching in a hydrometallurgical processing plant for Au recovery from WPCBs would generate excessive amounts of difficult to recycle, toxic and/or corrosive waste water (effluent) if the processing plant is employed in a real-life industrial-scale WPCB recycling operation. For example, the cyanide leaching of just 5 t of WPCB feed is expected to produce approximately 100 kL of cyanide effluent (assuming ~5% solids loading), which is toxic and difficult to recycle.

The high toxicity and/or corrosivity of effluents generated after leaching with conventional cyanide or chloride lixiviants presents an environmental health risk since humans and wild-life may be harmed if exposed to these effluents. Furthermore, effluents generated after leaching with conventional cyanide or chloride lixiviants are difficult to recycle due to the high cost and complexity of the required recycling techniques. For example, effluents generated by the use of conventional chloride lixiviants are typically recycled using advanced thermolytic technologies requiring capital-intensive fluidized bed and thermal roasting reactors which can cost more than $200,000 (Bruns et al., 2019), while the recycling of effluents generated by the use of conventional cyanide lixiviants requires complex regeneration steps which require careful control of pH and redox potential (Parga et al., 2011).

As a solution to the aforementioned drawbacks of using conventional cyanide or chloride lixiviants, there is a strong motivation to develop a hydrometallurgical processing plant for Au recovery from WPCBs which utilises a non-toxic iodide lixiviant for Au leaching which can be recycled using a simple technique. Previous research has shown that in comparison to conventional cyanide and chloride lixiviants, iodide lixiviants offer the advantage of being non-toxic and more easily recyclable

using simple electrochemical or chemical regeneration techniques (Xu et al., 2010; Sahin et al., 2015; Batnasan et al., 2019). It has also been reported that iodide lixiviants are capable of leaching Au from WPCBs with high leaching efficiencies (>95%) and rapid kinetics (<1 hr) at ambient temperatures (~25 °C), slow agitation speeds (<200 rpm), under non-corrosive conditions/ mild pH (4-7), and without the emission of toxic fumes (Xu et al., 2010; Sahin et al., 2015; Batnasan et al., 2019). Despite their high reagent costs, iodide lixiviants can be regarded as cost-effective since they can be recycled using simple processing techniques (Xu et al., 2010; Sahin et al., 2015; Batnasan et al., 2019).

1.2 Problem Statement

The main problem with many previously developed hydrometallurgical processing plants for Au recovery from WPCBs is that most of these processing plants are not techno-economically feasible for industrial-scale application, given that they have been designed to utilise more conventional cyanide or chloride lixiviants which are toxic and/or corrosive. For this reason, there has been limited application of hydrometallurgical processing plants for Au recovery from WPCBs in commercial WPCB recycling operations (to the author's knowledge), despite the potential for effective Au recovery without the drawbacks presented by the use of physical separation and/or pyrochemical techniques as in conventional processing plants (these drawbacks are discussed in more detail in section 1.1.5).

As a potential solution to the aforementioned problem, this project developed a hydrometallurgical processing plant for Au recovery from WPCBs which utilises a non-toxic iodide lixiviant for Au leaching, which is recycled using a simple electrochemical process.

It is important to emphasise that the processing plant developed in this study is mainly focused on Au recovery and not extensively concerned with the recovery of rare earth metals, other precious metals (e.g., Pd, Pt, and Ag), or BMs, because:

- Au recovery requires different chemistry compared to that of BMs, rare earth metals or other precious metals, and thus the recovery of these other metals would necessitate the use of significantly different recovery techniques whose investigation was beyond the scope of the present work.
- Rare earth metals are not consistently found in appreciable concentrations in a wide range of WPCBs.
- Au carries most of the value of WPCBs, accounting for 60-80% (Gloe et al., 1990).
- Au is more easily recovered from WPCBs in comparison to BMs since it is mostly surface bound on connectors and contacts while BMs such as Cu are typically covered by a non-conductive substrate/ laminate (i.e., Au is more readily exposed to lixiviant).

However, it must also be noted that the fate/ recovery of BMs (namely, Cu, Al, Ni, and Fe) as a mixed precipitate sponge is included in the design of the developed processing plant. However, this is not extensively investigated due to the scope of the project.

1.3 Aim and Objectives

This project's primary aim is to contribute knowledge to the development of a hydrometallurgical processing plant for Au recovery from WPCBs which utilises a non-toxic and recyclable iodide lixiviant for Au leaching and has the potential to be applied in real-life industrial-scale WPCB recycling operations in a technically and economically feasible manner. The primary aim of this project was achieved through the completion of two research objectives which are herein discussed.

The first research objective of this project was to use findings from literature to develop a conceptual process and theoretical process plant outline for a hydrometallurgical processing plant for Au recovery from WPCBs which utilises a non-toxic and recyclable iodide lixiviant for Au leaching. The following processing circuits collectively constitute the developed processing plant (these are described in greater detail in Chapter 4):

- Circuit 1. Size-reduction of WPCBs to liberate entrained Au which may be encapsulated by non-metallic WPCB Materials.
- Circuit 2. Leaching of BMs from size-reduced WPCBs using a 3-stage BM leaching process comprised of a separate HNO_3, HCl, and H_2SO_4-H_2O_2 leaching stage.
- Circuit 3. Leaching of Au from size-reduced and BM leached WPCBs using a conventional iodide lixiviant (I^--I_2-H_2O_2) to produce a pregnant WPCB iodide leachate/ I^--I_2-Au electrolyte solution.
- Circuit 4. Concentration and recovery of Au from a pregnant WPCB iodide leachate/ I^--I_2-Au electrolyte solution using a novel system comprised of an electrowinning (EW) stage for Au recovery together with a simultaneous solid-liquid extraction (SLE) stage which utilises an Au selective ion-exchange extractant membrane (Au-IEM) for Au concentration. This novel system is herein referred to as the IEM-SLE and EW process.

The second research objective of this project was to determine the early stage technical and economic feasibility of the processing plant, and thereafter determine whether or not the developed processing plant justifies further research and development (i.e., process optimisation, detailed techno-economic feasibility assessment and life-cycle assessment, etc.) for future application in real-life industrial-scale WPCB recycling operations.

The processing plant's early-stage technical feasibility assessment was supported by a laboratory experiment which studied circuit 4 of the processing plant to determine if it is technically feasible/ possible. Discussed in greater detail in Chapter 3, this laboratory experiment investigated the concentration and recovery of Au from an I^--I_2-Au electrolyte solution using the novel IEM-SLE and EW process. It is important to note that circuits 1 to 3 of the processing plant were not extensively included in the early-stage technical feasibility assessment, since previous work has already shown that it is technically feasible/ possible to employ the size-reduction and leaching processes used in these circuits (Mecucci and Scott, 2002; Jha et al., 2012; Behnamfard et al., 2013; Ficeriova et al., 2011; Yang et al., 2011; Nekouei et al., 2018; Dias et al., 2019)

Done in parallel with the previously described technical feasibility assessment, the processing plant's early-stage economic feasibility assessment was supported by a discounted cash flow and profitability (DCFP) assessment. After this assessment, a sensitivity analysis was performed to determine the sensitivity of the DCFP assessment results (i.e., to determine the sensitivity of the processing plant's economic feasibility) in response to changes in key assumptions used. It is important to note that the development and design of the processing plant was done in parallel with its technical and economic feasibility assessment.

1.4 Limitations

The primary limitation of this dissertation is that there is a degree of uncertainty in the findings presented for the following reasons:

- There is a lack of prior research on the use of the IEM-SLE and EW process for the simultaneous concentration and recovery of Au from pregnant WPCB iodide electrolyte solutions/ leachates (due to the novelty of this technology). This may hinder the credibility of the project's findings since there is very little published data available for comparison. However, to improve the credibility of the project's findings and to verify repeatability, critical stages of the IEM-SLE and EW process were tested experimentally in 3 sets, with set averages reported and their repeatability evaluated through standard deviation.
- There may be measurement uncertainty in the project's laboratory experimental data/results due to the inaccuracy or imprecision of measurement instruments. Hence, there may be a degree of uncertainty in the findings presented in this work, since the project's laboratory experimental data/results were used to assess the processing plant's technical feasibility, and thereafter used in the processing plant's economic feasibility assessment. To minimize measurement uncertainty, only high-quality, reliable, and properly calibrated measurement instruments were used in this work, under controlled

conditions. Measurement uncertainty in the project's experimental data was quantified through standard measurement uncertainty calculated after taking 3 repeated experimental measurements.

- Assumptions used in the processing plant's early-stage economic feasibility assessment are based on an ideal economic model, and an ideal processing plant condition designed and developed using experimental findings obtained under ideal conditions. The sensitivity of the processing plant's economic feasibility in response to changes in key assumptions (i.e., deviations from the ideal conditions or model) used is investigated through a sensitivity analysis (Chapter 5).

1.5 Structure of Dissertation

The work in the remaining chapters of this dissertation is structured as follows:

- Chapter 2: Literature Review – Presents findings from previous work investigating BM leaching from WPCBs, Au leaching from WPCBs, Au concentration by LLE, Au Concentration by SLE, Au recovery by EW, simultaneous Au concentration and recovery by IEM-SLE and EW, and IEMs and IEM Separation.
- Chapter 3: Technical Feasibility – Presents and discusses the materials, apparatus, method, and results of a laboratory experiment (whose results were used to assess the processing plant's technical feasibility) investigating the concentration and recovery of Au from a WPCB iodide leachate/ I^--I_2-Au electrolyte solution using the novel IEM-SLE and EW technique.
- Chapter 4: Process Development and Process Plant Design – Presents a detailed process description and theoretical process plant outline (communicating key technical bases, variables, and assumptions) for the processing plant.
- Chapter 5: Economic Feasibility – Presents and discusses the methodology and results of the processing plant's economic feasibility assessment, which was done through a

discounted cash flow and profitability assessment. Thereafter a sensitivity analysis of the processing plant's economic feasibility is presented and discussed.

- Chapter 6: Conclusion and Recommendation – Presents the conclusions drawn from the design and development of the processing plant, and the results of the processing plant's technical and economic feasibility assessment. Thereafter, provides recommendations on how to improve the design and development of the processing plant, and the results of the processing plant's technical and economic feasibility assessment. Finally, concludes on whether or not the developed processing plant justifies further research and development for future application in actual industrial-scale WPCB recycling operations.

Chapter 2
Literature Review

Traditional hydrometallurgical processes for Au recovery from WPCBs (all of which have been exploratory) typically commence with the size-reduction of WPCBs to liberate entrained Au which may be encapsulated by non-metallic WPCB Materials (Dalrymple et al., 2007). Thereafter, BMs such as Cu, Zn, Fe, Al, Ni, Pb, and Sn are leached from WPCBs using mineral acids such as HNO_3, HCl, or H_2SO_4 (together with various oxidants such as H_2O_2). This leaching process eliminates BM impurities which can inhibit the extent of Au leaching. After BM leaching is complete, the generated leachate is separated from the WPCB solid residue by filtration. Au is subsequently leached from the WPCB solid residue using a suitable lixiviant, which is commonly either a cyanide, thiosulphate, thiourea, or halide based lixiviant. The resulting Au bearing leachate is then separated from the WPCB solid residue by filtration. Finally, Au is concentrated and recovered from the pregnant leachate using liquid-liquid extraction (LLE) or solid-liquid extraction (SLE) together with electrowinning (EW). (Galva, 2023; Kasper et al., 2018; Zheng et al., 2006; Deschenes et al., 1987; Xie et al., 2014; Mahandra et al., 2021; Raiguel et al., 2020)

The remainder of this chapter firstly presents a literature review on Au and BM leaching from WPCBs, Au concentration using LLE or SLE, Au recovery using EW, and Au concentration and recovery using EW and ion-exchange extractant membrane (IEM) SLE. Thereafter, a literature review on IEMs and IEM separation is presented.

The findings from the literature reviews presented in this chapter were used in Chapter 4 to achieve the first research objective of this project, which was to develop a conceptual process and theoretical process plant outline for a hydrometallurgical processing plant for Au recovery from WPCBs.

2.1 Base Metal Leaching from WPCBs

A review of the literature has shown that efficient BM leaching from WPCBs can be achieved by a 3-stage leaching process comprised of a separate HNO_3, HCl, and H_2SO_4-H_2O_2 leaching stage. A 3-stage BM leaching process is recommended due to the complex chemical composition of WPCBs (Mecucci and Scott, 2002; Jha et al., 2012; Behnamfard et al., 2013; Ficeriova et al., 2011; Yang et al., 2011).

Mecucci and Scott (2002) used a 2-6 M HNO_3 lixiviant to study the leaching of Pb, and Sn from size-reduced WPCBs with a particle size <2.5 mm, for 6 h, at a 23 °C temperature, and 333.3 g/L solid to liquid (S/L) ratio. Under these conditions, Pb and Sn were leached with efficiencies of 99 %, and 65 % respectively. The lower Sn leaching yield was attributed to the formation of an insoluble metastannic acid oxide layer (H_2SnO_3) over the Sn surface. Findings from Mecucci and Scott (2002) have been substantiated by Jha et al. (2012) who reported that Pb and Sn could be leached from the solder of crushed WPCBs (with a <7 mm particle size) by a two-stage leaching process. In the first stage, 97 % of Pb was leached by a 0.2 M HNO_3 lixiviant, after leaching for 45 min, at a S/L ratio of 100 g/L, and 90 °C temperature. In the second stage, 98.74 % of Sn was leached using a 3.5 M HCl lixiviant, after leaching for 120 min, at a S/L ratio of 200 g/L, and a temperature of 90 °C.

Ficeriova et al.(2011) used a 2 M H_2SO4 and 2 M H_2O_2 lixiviant to study the leaching of Cu, Zn, Fe, Al, and Ni from size-reduced WPCBs with a particle size <0.8 mm. In this study, WPCBs were leached for 8 h, at a temperature of 80 °C, S/L ratio of 100 g/L, and agitation rate of 500 rpm. Under these conditions, Cu, Zn, Fe, Al, and Ni were leached with efficiencies of 85 %, 76 %, 82 %, 77 %, and 70 %. In a similar study by Behnamfard et al. (2013), size-reduced WPCBs with a particle size <0.3 mm were leached using a 2 M H_2SO4 and 35 wt. % H_2O_2 lixiviant, for 3 h, at a temperature of 25 °C, S/L ratio of 100 g/L, and agitation rate of 200 rpm. Under these conditions, Cu was leached with a 99.75 % yield. The findings from Behnamfard et al. (2013) and Ficeriova et al. (2011) have been substantiated by Yang et al. (2011) who reported that Cu leaching yield increases with an

increase in H_2SO_4 or H_2O_2 concentration, an increase in time, decrease in S/L ratio, and decrease in particle size.

In addition to the previously described studies, several other authors have successfully leached BMs from WPCBs using HNO_3, HCl, and H_2SO_4-H_2O_2 lixiviants (Le et al., 2011; Vijayaram et al., 2013; Bas et al.,2014; Birloaga et al., 2013; Jadhav and Hocheng, 2015; Kumari et al., 2016; Deveci et al, 2010; Oh et al, 2003). These studies are summarised in Table 2.1.1.

Table 2.1.1 Summary table of previous studies investigating the leaching of BMs from WPCBs ((a) Le et al., 2011, b) Vijayaram et al., 2013, c) Bas et al.,2014, d) Birloaga et al., 2013, e) Jadhav and Hocheng, 2015, f) Kumari et al., 2016, g) Deveci et al, 2010, h) Oh et al, 2003))

Source	Lixiviant	Particle Size (mm)	Temperature (°C)	Solid-liquid ratio (g/L)	Agitation rate (rpm)	Time (hrs)	Optimum recovery yield
a	7M HNO_3	≤ 1	60	20 -160	300	1	Cu: 99.99
b	3 M HCl + 1 M HNO_3	≤ 0.2	60	100	-	2	Cu: 92.7, Sn: 93.3
c	5 M HNO_3	< 3.35	30-70	6	-	2	Cu: 99.9, Ag: 85
d	2 M H_2SO_4 + 0.1M H_2O_2	< 2	90	10	600	3	Cu: 46.3, Sn: 21.1, Zn: 51.1
e	1 M HCl	40	120		150	22	Cu: 99.99, Zn:99.99, Sn: 99.99, Ni: 99.99, Pb: 99.99, Fe: 99.99, Al: 99.99
f	2.4 M H_2SO_4	< 2	150	100	20	1.5	Cu: 99, Ni: 99, Fe: 99
g	1.6 M H_2SO_4 + 0.8 M H_2O_2	< 3.35	68	15	140	4	Cu: 98.2
h	2M H_2SO_4 + 0.2 M H_2O_2	< 1	85	10	150	48	Cu: 95, Fe: 95, Zn: 95, Ni: 95, Al: 95

2.2 Au Leaching from WPCBs

It has been reported in the literature that conventional cyanide, thiosulphate, thiourea, and halide based lixiviants are suitable lixiviants for high-yield leaching of Au from WPCBs as complexed Au(I) or Au(III) ions (Li et al., 2018).

2.2.1 Cyanide Lixiviants

Conventional cyanide lixiviants are aqueous solutions containing a cyanide (CN^-) complexing agent such as calcium cyanide ($Ca(CN)_2$), sodium cyanide (NaCN), or potassium cyanide (KCN) together with an oxygen (O_2) oxidising agent. Such lixiviants leach Au as $[Au(CN)_2]^-$ at alkaline pH> 10 according to equation 1 (Eq.1). (Kasper et al., 2018)

$$4Au + 8CN^- + O_2 + 2H_2O = 4Au(CN)_2^- + 4OH^- \quad \text{(Eq.1)}$$

In terms of Au leaching from WPCBs, cyanide lixiviants offer advantages such as high yield, rapid kinetics, and low reagent cost. However, cyanide lixiviants are corrosive, highly toxic, and difficult to recycle (and thus result in the generation of copious amounts of waste requiring costly treatment). (Galva, 2023; Kasper et al., 2018)

Kasper et al. (2018) investigated the direct leaching of Au from WPCBs of mobile phones using a commercial cyanide lixiviant. In this instance, Au was leached with an 88 % yield after a 2 h leaching time, at a temperature of 25 ± 2 ^oC, pH of 12.5, and S/L ratio of 1/25. The results from Kasper et al. (2018) are slightly substantiated by the findings presented in an earlier study by Petter et al. (2014), who used a 6 - 8% KCN lixiviant to leach Au from WPCBs of mobile phones. In this instance, Au was leached with a 70 % yield after a 2 h leaching time, at a temperature of 25 ^oC, pH of 12.5, and 1/20 S/L ratio. The difference between the yields obtained by Petter et al. (2014) and Kasper et al. (2018) can be attributed to the difference in S/L ratios applied, or due to discrepancies in the concentration of cyanide lixiviants used.

2.2.2 Thiosulphate Lixiviants

Conventional thiosulphate lixiviants are aqueous solutions containing a thiosulphate ($S_2O_3^{2-}$) complexing agent such as ammonia thiosulphate ($(NH_4)_2S_2O_3$) or sodium thiosulphate ($Na_2S_2O_3$), together with a Cu^{II}, ammonia (NH_3), and O_2 oxidising agent. Such lixiviants leach Au as $[Au(S_2O_3)_2]^{3-}$ at alkaline pH (9-10.5) according to Eq.2 (Konyratbekova et al., 2015).

$$Au + 5S_2O_3^{2-} + Cu(NH_3)_4^{2+} = Au(S_2O_3)_2^{3-} + 4NH_3 + Cu(S_2O_3)_3^{5-} \quad \text{(Eq.2)}$$

In terms of Au leaching from WPCBs, thiosulfate lixiviants offer advantages such as low toxicity and non-corrosivity (Petter et al., 2014). However, thiosulphate lixiviants suffer from slow leaching kinetics and high reagent consumption due to thiosulphate decomposition to sulphur (Zhang et al., 2012).

Ficeriová et al. (2011) investigated the direct leaching of Au from size-reduced WPCBs of mobile phones using a thiosulphate lixiviant comprised of 0.5 M $(NH_4)_2S_2O_3$ together with 0.2 M Cu^{II} sulphate ($CuSO_4$) and 1M NH_3, at a pH of 9, 40 °C temperature, 500 rpm stirring rate, and 1/11 S/L ratio. According to Ficeriová et al.(2011), the thiosulphate lixiviant was able to leach Au with a yield of 98 % after 48 hrs. Oh et al.(2003) and Ha et al.(2014) have also achieved similar results to Ficeriová et al.(2011). Oh et al.(2003) reported a high Au leaching yield of 95 % (after 48 h) using a thiosulphate lixiviant comprised of 0.2 M $(NH_4)_2S_2O_3$ together with 0.02 M Cu^{II} sulphate and 0.4 M NH_4OH, at a 40 °C temperature, 150 rpm stirring rate, and 5 g/L S/L ratio. While Ha et al.(2014) reported a high Au leaching yield of 90 % (after 10 hrs) using a thiosulphate lixiviant comprised of 0.06 M $N_2S_2O_3$ together with 0.01 M Cu^{II} sulphate, 0.2 M NH_4Cl and 0.26 NH_3, at pH of 10, 50 °C temperature, and 400 rpm stirring rate.

2.2.3 Thiourea Lixiviants

Conventional thiourea lixiviants are aqueous solutions containing a thiourea ($CS(NH_2)_2$) complexing agent together with a ferric ion (Fe^{3+}) oxidising agent. Such lixiviants leach Au as $[Au(CS(NH_2)_2]^{2+}$ at acidic pH (1-2) according to Eq.3. (Zheng et al., 2006)

$$2Au + 4CS(NH_2)_2 + 2Fe^{3+} = 2Au(CS(NH_2)_2)^{+} + 2Fe^{2+} \quad \text{(Eq.3)}$$

In terms of Au leaching from WPCBs, thiourea lixiviants offer advantages such as high yield and low toxicity. However, thiourea lixiviants suffer from high reagent consumption due to the oxidation and decomposition of thiourea to sulphur, cyanamide, or $[FeSO_4CS(NH_2)_2]^{+}$. (Zheng et al., 2006)

Wu et al. (2011) studied the leaching of Au from size-reduced WPCBs using a thiourea lixiviant comprised of 12 g/L thiourea together with 0.8 % Fe^{3+}, for 1 hr, at a S/L ratio of 1/10, 300 rpm stirring rate, 20 – 25 ^{o}C temperature, and 1.5 pH. Under these conditions, Au was leached with a 91.4 % yield. Ficeriová et al. (2008) and Li et al. (2012) have also achieved similar results to Wu et al. (2011). Ficeriová et al. (2008) reported a high Au leaching yield (97 %) from WPCBs after 1.5 hrs using a thiourea lixiviant comprised of 10 g/L $CS(HN_2)_2$, 5 g/L Fe^{3+} and 10 g/L H_2SO_4, at a 20 ^{o}C temperature, and 125 g/L S/L ratio. While Li et al. (2012) reported a high Au leaching yield of 90 % from 154 µm particle size WPCBs after 2 hrs using a thiourea lixiviant comprised of 24 g/L $CS(HN_2)_2$, 0.6 % Fe^{3+} and 0.5 M H_2SO_4, at a 20 ^{o}C temperature.

2.2.4 Halide Lixiviants

Conventional chloride, bromide, and iodide lixiviants are the primary halide lixiviants which have been used to leach Au from WPCBs. Conventional bromide lixiviants used for Au leaching are typically aqueous solutions containing a bromine (Br_2) or copper bromide (CuBr) oxidising agent together with a bromide (Br^{-}) complexing agent such as sodium bromide (NaBr) or potassium bromide (KBr). In most instances, conventional bromide lixiviants leach Au at mild pH (5-8) as $AuBr_4^{-}$ according to Eq.4 (Cui et al., 2020). Conventional chloride lixiviants used for Au leaching

are typically aqueous solutions containing a chlorine (Cl_2), nitric acid (HNO_3), hydrogen peroxide (H_2O_2), hypochlorous acid (HOCl), or copper chloride ($CuCl_2$) oxidising agent, together with a chloride (Cl^-) complexing agent such as hydrochloric acid (HCl), sodium chloride (NaCl), or calcium chloride ($CaCl_2$). Au is usually leached in such lixiviants at acidic pH (<3) as $AuCl_4^-$ according to Eq.5 (Martinez-Ballesteros et al., 2021). Conventional iodide lixiviants used for Au leaching are typically aqueous solutions containing a diiodine (I_2) oxidising agent, iodide (I^-) complexing agent such as potassium iodide (KI) or sodium iodide (NaI), and a hydrogen peroxide (H_2O_2) auxiliary oxidising agent. Au is typically leached in such lixiviants as AuI_2^- at acidic pH (2-7) according to Eq.6 (Xu et al., 2010; Sahin et al., 2015; Batnasan et al., 2019).

$$2Au + 3Br_2 + 2Br^- = 2(AuBr_4)^- \quad \text{(Eq.4)}$$

$$2Au + 3Cl_2 + 2Cl^- = 2(AuCl_4)^- \quad \text{(Eq.5)}$$

$$2Au_{(s)} + I^-_{(aq)} + I_3^-{}_{(aq)} \rightarrow 2AuI_2^-{}_{(aq)} \quad \text{(Eq.6)}$$

In terms of Au leaching from WPCBs, halide lixiviants offer advantages such as high yield, rapid kinetics, recyclability (in case of iodide and bromide lixiviants), and low toxicity. However, chloride and bromide lixiviants are highly corrosive, iodide and bromide lixiviants have high reagent costs, and chloride lixiviants are difficult to recycle.

Au leaching from WPCBs in bromide lixiviants has been studied in works by Cui et al. (2020). In the investigation by Cui et al. (2020), a bromide lixiviant in the form of an aqueous solution containing 1.17 M NaBr, 0.77 M Br_2, and 2 M HCl was used at a S/L ratio of 50 g/L to leach Au from size-reduced WPCBs, for 10 hrs, at a 23.5 ^oC temperature, and 400 rpm agitation speed. Under these conditions, >95 % of Au was leached.

The use of chloride lixiviants for Au leaching from WPCBs has been studied by Martinez-Ballesteros et al. (2021). In the study by Martinez-Ballesteros et al. (2021), a chloride lixiviant in the form of an aqueous solution containing 4 M HCl, 0.067 M NaClO, and 0.017 M NaCl, was used to leach Au from size-reduced WPCBs with a particle size of 177 µm, for 2 hrs, at a 600 rpm agitation speed,

1/5 S/L ratio, 40 °C temperature, and 0.34 Mpa pressure. Under these conditions, Au was leached with a >95 % yield.

Au leaching from WPCBs in iodide lixiviants has been studied in works by Xu et al. (2010) and Sahin et al. (2015). In the investigation by Xu et al. (2010), an iodide lixiviant in the form of an aqueous solution containing 1-2 % H_2O_2 and 1.0-1.2 % I_2 and I^- (with a 1/8 I^-/I_2 mole ratio) was used at a S/L ratio of 1/10 to leach Au from size-reduced WPCBs with a <2 mm particle size. Xu et al. (2010) reported that Au could be leached with a high yield of >95 %, in a short leaching time of 4 hrs, at ambient temperature of 25 °C, with a slow agitation speed of <200 rpm, without the emission of toxic fumes, and under non-corrosive conditions/at a mild pH of 2-7. Sahin et al. (2015) achieved similar results to Xu et al. (2010) when using an iodide lixiviant in the form of an aqueous solution containing 1 % H_2O_2 together with 3 % I_2 and I^- (with a 1/10 mole ratio of I^-/I_2) at a S/L ratio of 3/20 to leach Au from size-reduced WPCBs with a <2 mm particle size. The high Au leaching yield and short Au leaching time observed by Xu et al. (2010) and Sahin et al.(2015) was attributed to the low potential for Au oxidation in aqueous iodide solutions (with this low potential perhaps attributable to the observation that Au is a soft acid and thus has a high affinity for soft bases with a high polarization degree such as iodine).

In addition to the studies by Xu et al. (2010) and Sahin et al. (2015), Au leaching from WPCBs in iodide lixiviants has also been investigated by Batnasan et al.(2019) who further suggested that such leaching processes are affordable despite the high cost for I_2 (~ 0.710 US$/kg in May 2021), since >80% of I^- ions produced after Au leaching can be oxidised/regenerated back to I_2 which can then be recycled in subsequent process cycles (unfortunately, the loss of iodine due to imperfect regeneration results in a negative economic impact since some iodine replenishment is required). Batnasan et al. (2019) reported that in slightly acidic conditions, I^- ions can be oxidised to I_2 following the addition of a strong acid such as HNO_3, or H_2O_2 (Eq.7). While Xu et al. (2010) reported that I^- ions can be oxidised to I_2 following the application of a 10-14 V cell voltage.

$$2I^-_{(aq)} + H_2O_{2(aq)} + 2H^+_{(aq)} \rightarrow I_{2(aq)} + 2H_2O_{(aq)} \qquad E = 1.143\ V \qquad \text{(Eq.7)}$$

2.3 Au Concentration by Liquid-Liquid Extraction (LLE)

Solid-liquid extraction (SLE) and liquid-liquid extraction (LLE) are the two most common separation techniques employed for Au concentration from pregnant cyanide, thiosulphate, thiourea, or halide leachates.

In the LLE technique, the pregnant leachate containing dissolved Au ions is firstly pumped into a reactor where it is mixed with an immiscible non-polar hydrophobic liquid reagent (referred to as a solvent extractant), which selectively reacts with the dissolved Au ions, forming charge-neutral Au complexes which are loaded and concentrated into the solvent extractant (examples of such a reaction are shown in Eq.8 and Eq.9). The resulting mixture is allowed to settle and separate into an aqueous layer (comprised of the dense Au barren leachate) with an immiscible overlying solvent extractant layer (now containing dissolved Au). After settling has been completed, the aqueous layer is carefully pumped or funnelled out of the reactor. Thereafter, the solvent extractant is mixed with an immiscible aqueous electrolyte solution, which strips the dissolved Au, forming an Au concentrated electrolyte solution, which is subsequently allowed to settle and separate from the lower-density solvent extractant. The Au concentrated electrolyte solution is then carefully pumped or funnelled out of the LLE reactor, and thereafter transported to a separate facility for the recovery of metallic Au, while the solvent extractant is then recycled/ used in subsequent processing cycles. It is important to note that the previously described loading and stripping operations are often repeated in order to increase the Au concentration in the final electrolyte solution.

The selection of a suitable extractant for Au concentration is dependent on leachate characteristics. For example, in order for a solvent extractant to fully settle and separate physically from leachate, the solvent extractant should have a low solubility in the leachate, in addition to having a significant density difference with the leachate, and a low viscosity. Furthermore, since Au extraction is typically dependent on complex formation between the extractant and Au counter anions in a leaching reagent, the co-ordination chemistry of Au in a leaching reagent may affect the choice of

extractant. The pH of a leaching reagent also affects the choice of extractant since most extractants have a specific pH range in which they are effective (e.g., extractant solubility is pH dependent).

Au selective solvent extractants are typically basic or neutral extractants. Basic solvent extractants which have been used for the LLE of Au from cyanide, thiosulphate, thiourea, or halide leachates include salts of protonated amines such as tridecylamine, trioctylamine, Primene JMT, Amberlite LA2, Hostarex A327, N-di-n-octylacetamide (DOAA), and N,N-di-n-octylauramide (DOLA), or phosphorus compounds such as tributyl phosphate (TBP), 2-ethyl hexyl phosphonic acid mono-2-ethylhexyl ester (PC-88A), tributyl phosphine oxide (TBPO), and Di-2-ethylhexyl phosphoric acid (D2EHPA). Eq.8 illustrates the reaction mechanism for the solvent extraction of $AuCl_4^-$ using a basic solvent extractant in the form of a chloride amine salt ($R_3NH^+Cl^-$).

$$AuCl_4^- + R_3NH^+Cl^- \rightleftharpoons [(R_3NH^+)(AuCl_4^-)] + Cl^- \quad \text{(Eq.8)}$$

Neutral solvent extractants which have been used for the LLE of Au from cyanide, thiosulphate, thiourea, or halide leachates include ethers such as dibutyl carbitol (DBC) or diethylene glycol dibutyl ether (DEGBE), and ketones such as methyl isobutyl ketone (MIBK) and di-isobutyl ketone (DIBK). Eq.9 illustrates the reaction mechanism for the solvent extraction of $AuCl_4^-$ using a neutral extractant in the form of DBC.

$$_aH^+ + AuCl_4^- + {}_b[DBC] + H_2O \rightleftharpoons [{}_aH^+ \cdot {}_bDBC \cdot H_2O \cdot AuCl_4^-]^- \quad \text{(Eq.9)}$$

The yield of Au LLE is measured in terms of the percentage of Au which is successfully loaded into a solvent extractant and stripped into an electrolyte solution. Compared to SLE, LLE offers higher selectivity, rapid kinetics, large Au loading capacity and a wider range of available extractants. However, many of the solvent extractants used in the LLE of Au are dangerous and present mass balance issues. For example, MIBK (one of the most widely available commercial solvent extractants used for Au LLE) is a highly flammable substance with a low flash point of 14°C, that can form explosive peroxides on exposure to air (Caravaca, 1994; Nicol et al., 1987), while the use of DBC (a readily available Au selective solvent extractant) can result in the loss of dissolved Au due to DBC

volatilization, which is highly probable considering DBC's low vapour pressure of 0.04 mbar at 20 °C (Mironov, 2012).

The LLE of Au from pregnant cyanide, thiosulphate, thiourea, and halide leachates has been investigated in works by Deschenes et al. (1987), Xie et al. (2014), Mahandra et al. (2021), and Raiguel et al. (2020).

Deschenes et al. (1987) used a 40 % Di-(2-ethylhexyl)phosphoric acid (D2EHPA) and 10 % TBP phosphorous compound solvent extractant in 50 % Varsol with H_2SO_4 to investigate the LLE of Au from a thiourea leachate with an 8 g/L $SC(NH_2)_2$ concentration and 102 mg/L Au concentration, at a pH of 1, contact time of 2 min, solvent extractant/leachate ratio of 1, and with stripping using 10% HCl. Under these conditions, Au was concentrated with a >85 % yield.

Xie et al. (2014), used an amine solvent extractant LIX 7950 (at a 0.5 % concentration) together with 5g/L 1-dodecanol in n-dodecane and H_2SO_4 (50 % v=v) or NaOH (2 mol/L) to study the LLE of Au from an alkaline cyanide leachate with an initial Au concentration of 53.5 mg/L at a pH of around 9.5, contact time of 10 min, solvent extractant/leachate ratio of 2, and with stripping using 0.1 mol/L NaOH. Under these conditions, Au was concentrated with a >95 % yield.

Mahandra et al. (2021) used a phosphorous compound solvent extractant Cyphos IL 101 (at a 3.5 mmol/L concentration) in toluene, NaOH and H_2O to study the LLE of Au from a thiosulphate leachate with a 0.2 mol/L $Na_2S_2O_3$ concentration and 10 mg/L Au concentration, at a pH of 9, contact time of 10 min, solvent extractant/leachate ratio of 10, and with stripping using 2 M NaCl. Under these conditions, Au was concentrated with a >96 % yield.

Raiguel et al. (2020) compared the use of a pure ether solvent extractant DBC to a pure ketone solvent extractant MIBK for the LLE of Au from a halide leachate with a chloride (Cl^-) concentration of 10 mol/L and 0.1 g/L Au concentration, at a pH of 1.5, contact time of 30 min, solvent extractant/leachate ratio of 1, and with stripping for 60 min using 1 mol/L $SC(NH_2)_2$. Under these conditions, Au was concentrated with a >95 % yield for both DBC and MIBK.

2.4 Au Concentration by Solid-Liquid Extraction (SLE)

The principles of the SLE technique are similar to those of the LLE technique. However, in this instance, the pregnant leachate containing dissolved Au ions is mixed or passed through an immiscible non-polar hydrophobic solid reagent, referred to as a solid extractant. Like the solvent extractant in the LLE technique, the solid extractant in the SLE technique selectively reacts with dissolved Au ions, forming charge-neutral Au complexes. In this occurrence, the charge-neutral Au complexes are loaded/concentrated onto the surface of the solid extractant particles through adsorption. Once loaded with Au, the solid extractant is separated from the leachate through filtration. Thereafter, the solid extractant is mixed with an immiscible aqueous electrolyte solution which strips the dissolved Au and forms an Au concentrated electrolyte solution which is subsequently separated from the solid extractant through filtration. (Bolinsky and Shirley, 1996; Villaescusa et al., 1996; Fleming et al., 2003)

The yield of Au SLE is measured in terms of the percentage of Au which is successfully adsorbed (loaded/concentrated) onto the solid extractant and stripped/eluted into the electrolyte solution. Compared to LLE, SLE offers advantages such as simpler equipment, less reagent loss, no phase disengagement, and easy phase separation. However, SLE suffers from slower mass transfer rates and thus longer process time. (Rovira, 1998)

Many solid extractants used in the SLE of Au from cyanide, thiosulphate, thiourea, or halide leachates are Au selective ion-exchange (Au-IX) extractants. Au-IX extractants are typically used as resin beads (in column, solution, or pulp) or membranes, and are comprised of either polymeric materials containing charged ionic functional groups fixed to their polymeric matrix, or polymeric materials hosting a carrier liquid with ionic functional groups fixed within their network or pores (Gomes et al., 2001). Loading of Au on Au-IX extractants during SLE occurs when dissolved Au ions in solution interact with ionic functional groups in the Au-IX extractant (Marston and Gisch, 2010).

A number of Au-IX extractants are available on the market. These can be grouped roughly according to their functionality as strong-base anion (SBA) and medium-base anion (MBA) extractants (Kotze, 2010; Marston et al., 2010). Au-IX SBA extractants typically contain quaternary ammonium functional groups with fixed positive charges. Examples include the Purolite A193 and Dowex-Minix extractant. These extractants are not pH-sensitive and operate effectively across the entire pH range. The loading of Au as $Au(CN)_2^-$ onto an SBA extractant is depicted in Eq.10 below. (Marston and Gisch, 2010)

$$P—NR_3 + SO_4^- + Au(CN)_2^- \rightarrow P—NR_3 + Au(CN)_2^- + 1/2SO_4^{2-} \quad \text{(Eq.10)}$$

where P represents the polymer matrix and R an alkyl chain

In the case of Au SLE from pregnant cyanide leachates using Au-IX SBA extractant, stripping is commonly performed with a $CS(NH_2)_2/H_2SO_4$ mixture (Eq.11). This is particularly due to the strong affinity of Au-IX SBA extractants for complexed Au ions. (Marston and Gisch, 2010)

$$P—NR_3 + Au(CN)_2^- + 2CS(NH_2)_2 + 2H_2SO_4 \rightarrow P—NR_3 + H_SO_4^- + Au(CS(NH_2)_2)^{2+}HSO_4^- + 2HCN \quad \text{(Eq.11)}$$

Au-IX MBA extractants contain a mixture of quaternary, tertiary, secondary and primary amine groups. Examples include the Purolite S992* [currently Purogold MTA9920] and Henkel's Aurix (with guanidine functionality) extractant. The functional groups on Au-IX MBA extractants must be protonated for interactions with Au ions to occur (Eq.12 and Eq.13). (Van Deventer et al., 2012)

$$\text{Protonation: } P—NR_2 + H^+ \rightarrow P—NR_2H^+ \quad \text{(Eq.12)}$$

$$\text{Adsorption: } P—NR_2 + H^+Cl^- + Au(CN)_2^- \rightarrow P—NR_2H^+Au(CN)_2^- + Cl^- \quad \text{(Eq.13)}$$

The extent of amine protonation at a specific pH is determined by the basicity, or pKa value, of the functional group on the Au-IX MBA extractant. Stripping of Au from Au-IX MBA extractants is typically performed using an alkali such as sodium hydroxide. (Van Deventer et al., 2012)

Although activated carbon can also be used as a solid extractant in the SLE of Au, Au-IX extractants can be preferred since they often offer improved Au loading selectivity over BMs. Van Deventer et al. (2012) compared the loading performance of the Au-IX MBA extractant Purogold S992 relative to activated carbon. Metal loading tests were performed at a pH of 10.5 using a synthetic cyanide leachate containing 150 ppm of CN^- and 9, 13.6, 1.0, and 10.4 mg/L of dissolved Au, Cu, Zn, and Ni. Metal loading test results (Table 2.3.1) show that Purogold S992 is able to load Au without any Cu, while activated carbon results in the co-loading of 105 mg/kg of Cu. The high Au loading selectivity of Purogold S992 is one of the primary reasons why it was selected as the extractant carrier in the Au-IEM employed in this work.

Table 2.4.1 Metal loading performance onto Purogold S992 and activated carbon (Van Deventer et al., 2012)

Metal	Metal concentration in solution, mg/L	Adsorbent loading, mg/kg	
		Purogold S992	Activated carbon
Au	9	4183	16450
Cu	13.6	Not detected	105
Zn	1.0	96	233
Ni	10.4	128	129

The use of Au-IX extractants for the SLE of Au from pregnant cyanide, thiosulphate, thiourea, and halide leachates, has been investigated in works by Suratman (2008), Msumange (2021), Mensah-Biney (2016), and Zhang et al. (2012).

Suratman (2008) used columns of Au-IX SBA extractants Amberjet-4200 and IRA-400 to study the SLE of Au from a thiosulphate leachate with a 0.1 M $(NH_4)_2S_2O_3$ concentration and 10 mg/L Au concentration, at a pH of 11, contact time of 10 min, and with stripping/elution for 4 hrs using 0.2 M thiocyanate (at a flow rate of 100 ml/min and pH of 2). Under these conditions, Au was concentrated with a >99 % yield.

Msumange (2021) used beads of Au-IX MBA extractant Purogold S992 to study the SLE of Au from a cyanide leachate with a 1.5 g/L NaCN concentration and 28.2 mg/L Au concentration, at a pH of 10.5, contact time of 24 hrs, extractant/ leachate ratio of 3 g/L, 650 rpm stirring rate, and with

stripping for 8hrs using a mixture of 20 g/L NaCN and 5 g/L NaOH at a temperature of 60 °C and pH of 10.5. Under these conditions, Au was concentrated with a 94.3 % yield.

Mensah-Biney (2016) used resin beads of Au-IX extractant Amberlite 252 as solid extractants in studies investigating the SLE of Au from a thiourea leachate with a 0.025 M $SC(NH_2)_2$ concentration, 0.55 g/L ferric sulphate concentration, 0.45 g/L cysteine concentration and 100 mg/L Au concentration, at a pH of 1.5 and contact time of 144 hrs. Mensah-Biney (2016) reported that stripping could be achieved using 0.3M $SC(NH_2)_2$ at a temperature of 120 °C. Under these conditions, Au was concentrated with a yield of >85 %.

In a study by Zhang et al. (2012), Purolite A500/2788 (an SBA extractant) was used in its chloride form as a fixed bed solid extractant in the SLE of Au from halide leachates with a 0.1 M I^- concentration, 0.005 M I_2 concentration and 600–700 ppm Au concentration. The flow rate for loading was 10-bed volumes per hour (BV h^{-1}), while for stripping it was 2 BV h^{-1}. Kinetic tests showed that loading equilibrium was reached within 5 h. All experiments were performed at ambient temperature (22 °C) and stripping was done using a 2 M NaCl and 0.3 M Na_2S electrolyte solution. Under these conditions and in the absence of excess triiodide (I_3^-), Au was concentrated with a high yield of >90 %. Zhang et al. (2012) reported a decrease in Au SLE yield when excess I_3^- was present in the leachate. Towards this end, it was found that the loading of excess I_3^- on the A500/2788 extractant was strong due to the dissociation of the loaded I_3^- to I^- and I_2, the latter being deposited on the A500/2788 extractant by physisorption, thereby fouling the extractant surface and reducing SLE yield.

2.5 Au Recovery by Electrowinning (EW)

Electrochemical reduction or electrowinning (EW) is the conventional technique used for Au recovery from electrolyte solutions (including pregnant leachates). Although it is possible to recover Au using chemical reduction techniques, EW is preferred since it is more environmentally friendly and produces Au with greater purity. (Roslan et al., 2017)

2.5.1 Au EW Fundamentals

Au EW commences with the supply of an Au concentrated electrolyte solution into an EW cell containing an anode and cathode attached to a direct-current power supply. A cell potential is then generated after an electric current (from the power supply) is applied to the electrodes. This electric current creates a potential energy difference between the electrodes and results in the transfer of Au ions (by migration, diffusion, and convection) to a region near the surface of the cathode called the Helmholtz double layer. At the Helmholtz double layer, Au ions, which are complexed to anionic ligands in the electrolyte, become polarized in the electric field of the cathode. The distribution of the ligands around the Au ions are then distorted and thereafter Au ions diffuse into the Helmholtz double layer. Within the Helmholtz double layer, the anionic ligand is separated from the Au cation, which is subsequently reduced and deposited on the cathode (Eq.14). (Bailey, 1987; Ogura et al., 1971).

$$AuX_n^{Z-ny}(aq) + Ze^- \rightleftharpoons Au^Z(aq) + nX^y(aq) + Ze^- \rightleftharpoons Au(s) + nX^y(aq) \quad \text{(Eq.14)}$$

where Z = oxidation state of Au, n = number of ligand atoms complexed to Au, y = oxidation state of ligand.

At the anode, H_2O in the electrolyte decomposes, evolving O_2 gas, which is released to the atmosphere (Eq.15). (Bailey, 1987; Ogura et al., 1971)

$$2H_2O(l) \rightarrow O_2(g) + 4H^+(aq) + 4e^- \quad \text{(Eq.15)}$$

The yield of Au EW is measured in terms of the percentage of Au which is successfully deposited onto the cathode.

2.5.2 Practical Au EW Considerations

Previous research has shown that the main process parameters affecting the efficiency of Au reduction-deposition during Au EW are cell potential, current density and efficiency, and specific energy consumption. (Bailey, 1987)

Cell Potential

During Au EW, cell potential (E_{cell}) governs the reversible electrochemical reduction-deposition of Au, and at standard conditions is equal to its equilibrium value which follows the Nernst equation shown in Eq.16 (Ogura et al., 1971). In the context of the current study, cell potential provides the energy for Au reduction-deposition, and thus Au concentration and recovery in the developed processing plant IEM-SLE and EW circuit.

$$E_{cell} = E^{eq} = E^0 + RT/nF \cdot \ln \{\exp(a(Au^Z)_{ox}/\ a(Au)_{red})\} \quad \text{(Eq.16)}$$

where F is the Faraday constant (F = 96,485.339 C mol^{-1}), E^{eq} is the equilibrium cell potential, R is the ideal gas constant (R = 8.314 J K^{-1} mol), T is the temperature in Kelvin, $a(Au^Z)_{ox}$ is the chemical activity of oxidized Au atoms, $a(Au)_{red}$ is the chemical activity of reduced Au ions, and E^0 is the standard electrode potential measured as the individual electrode potential of the reversible electrode in standard conditions (concentration of 1 M and temperature of 298 K).

At non-standard conditions, cell potential deviates from its equilibrium value (increases or decreases) due to electrode polarization. As a result, over or under potential energy is needed for Au reduction-deposition to occur. Over potential can be due to concentration overpotential (diffusion), ohmic overpotential (electrical resistance), kinetic overpotential (charge transfer), or adsorption

overpotential. While, under potential arises when the electrodeposited Au has a stronger interaction with the cathode surface than with itself. (Renoware, 2011)

Current Density

Current density during Au EW is the amount of electrical charge per unit area of electrode. It is calculated according to Eq.17 (Free and Moats, 2014).

$$j = I/A \quad \text{(Eq.17)}$$

where j is the current density in ampere/m^2, I is the applied current in ampere, and A is the surface area of electrode in m^2.

It is important to note that current density is an important Au EW parameter/practical consideration which in the present study was used in the scale-up of the processing plant's EW process (IEM-SLE and EW circuit), in order to determine the applied current and electrode size for the full-scale processing plant.

Current Efficiency

Current efficiency during Au EW is the ratio of electrical charge used to deposit Au to the total charge passed. In the context of the current study, current efficiency describes the efficiency with which electrons are transferred in the processing plant's IEM-SLE and EW circuit in order to facilitate the electrochemical reduction-deposition of Au.

Current efficiency (C_E) is usually expressed as the ratio of the actual mass of the deposit (m_{actual}) to the theoretical mass ($m_{theoretical}$) (Eq.18) and can be calculated using Eq.19 (Bailey, 1987).

$$C_E = m_{actual} / m_{theoretical} \quad \text{(Eq.18)}$$

$$C_E = (nFV(C_i - C_f)/ \int_0^t I(t)dt)100(\%) \quad \text{(Eq.19)}$$

Where V is the electrolyte solution volume used, C_i is the initial Au concentration in the electrolyte, C_f is the final gold concentration, F is the Faraday constant (96485 C or $A \cdot s$), n is the number of electrons involved in the Au reduction-deposition reaction, and I the current intensity.

Au reduction-deposition during Au EW is an electrochemical process and is thus governed by Faraday's law, which states that the theoretical mass of a substance deposited at an electrode is proportional to the quantity of electricity passed. Mathematically, Faraday's law is given in Eq.20. (Steyn and Sandenbergh, 2014)

$$m_{theoretical} = MIt/vF = zIt/F = XQ/F \quad \text{(Eq.20)}$$

where $m_{theoretical}$ is the theoretical mass of deposited Au (g/mol), I is current in ampere, t is time in seconds, v is the valency of the deposited Au, F is the Faraday constant, Q is the quantity of current flow (coulomb), and z =M/v is the chemical or electrochemical equivalent.

Specific Energy Consumption

Specific energy consumption (E_s) of Au reduction-deposition during Au EW is the power (in watts or W) required to deposit one kilogram of Au and has the units, kWh/kg. It is mathematically written as in Eq.21 and can be calculated using Eq.22 (Bailey, 1987).

$$E_s = EIt/m \quad \text{(Eq.21)}$$

$$E_s = E\ (nF/(3600MC_E) \quad \text{(Eq.22)}$$

where E is the average cell voltage in volts, I is the applied current in ampere, m is the mass of Au deposited at time t in hours, M is the atomic weight of Au, n is the number of electrons involved in Au-reduction deposition, F is the Faraday constant, and C_E the current efficiency.

In the context of the present work, the specific energy consumption of Au reduction-deposition is an important Au EW parameter which is used to compare the power requirement/ energy usage of the

developed processing plant's EW process (IEM-SLE and EW process) to that of similar processes which have previously been developed.

2.5.3 Previous Investigations into Au EW

Au EW has been investigated in works by Yap and Mohamed (2008), Roslan et al. (2017), Lekka et al. (2015), Kasper et al. (2016), and Meng et al. (2019).

Yap and Mohamed (2008) studied Au EW from cyanide electrolyte solutions using an electro-generative flow-through EW cell comprised of an electrolyte solution tank hosting an activated reticulated vitreous carbon cathode (80 pores per inch and 2.0 cm × 5.5 cm × 0.4 cm) and an electrolyte solution tank hosting a 99 % pure zinc anode (2 cm × 5.5 cm × 0.06 cm). Electrolyte solution tanks were sandwiched between stainless steel and Teflon endplates, separated by a Neosepta® CM-01 cation exchange membrane with rubber gaskets to prevent leakage, and mounted between two flow frames consisting of mesh turbulence promoters (with an inlet and an outlet to allow electrolyte solutions to flow through the frames). Electrodes were attached to a stainless-steel current collector plate (with conductive carbon adhesive), which was connected by an external conducting wire. Galvanic components were sandwiched together with eight bolts and nuts. Electrolyte solutions were pumped into the cell through an inlet opening at the bottom of the cell by a peristaltic pump and flowed out of the cell from an outlet at the top of the cell (these electrolyte solutions flowed separately in a closed circuit). In the Au EW tests, 250 mL of Au bearing cyanide electrolyte solution (prepared from $KAu(CN)_2$ salts with 100 mg L^{-1} Au(I) concentrations in 0.2 % (w/v) of sodium cyanide) was pumped into the electrolyte solution tank hosting the cathode. While 250 mL of 0.5 % (w/v) sodium cyanide electrolyte solution was pumped into the electrolyte solution tank hosting the anode. Electrolyte solutions were maintained at a pH of 11.0 ± 0.1. Yap and Mohamed (2008) reported that >99 % of Au was recovered within 4 hrs of operation for 100 mg/L of initial $KAu(CN)_2$ concentration. This high Au recovery was attributed to the cathode's large porous surface area, high void volume, rigid structure, low resistance to fluid flow, and the purging

of the EW cell with nitrogen gas to remove any dissolved oxygen which would have inhibited the deposition of Au.

Roslan et al (2017) studied Au EW from chloride electrolyte solutions using an EW cell similar to that used by Yap and Mohamed (2008). However, in this instance, electrolyte solution tanks were separated by a Neosepta® AM-01 anion exchange membrane. In the Au EW tests, 250 mL of Au bearing chloride electrolyte solution (100 mg/L Au(III) in 0.2 M NaCl solution) was pumped into the electrolyte solution tank hosting the cathode. While 250 mL of 0.1 M NaCl electrolyte solution was pumped into the electrolyte solution tank hosting the anode. Roslan et al (2017) reported that $>$ 99 % of Au was recovered within 1 hrs of operation for 100 mg/L of initial Au (III) concentration.

Lekka et al. (2015) investigated the EW of Au from aqua regia electrolyte solutions at a 0.55 V cell potential (vs. Ag/AgCl/KCl_3M). Lekka et al. (2015) reported the selective recovery of >99 % of Au over Cu^{2+} which was reduced to soluble $CuCl_2^-$. In a similar study, Kasper et al. (2016) reported that 99 % of Au could be selectively recovered (over Cu) by EW from ammoniacal thiosulphate electrolyte solutions by controlling cell potential in a range between −400 and −500 mV (vs Ag/AgCl).

Meng et al. (2019) studied the EW of Au from iodide electrolyte solutions using an EW cell (Figure 2.5.1) comprised of an electrolyte solution tank hosting a titanium plate cathode and an electrolyte solution tank hosting a graphite plate anode. Electrolyte solution tanks were separated by a generic commercial IEM which allowed the transport of anions while rejecting cations (this type of membrane is referred to as an anion-exchange membrane or AEM). In the Au EW tests, an iodide electrolyte solution containing 20 mg/L of dissolved Au as AuI_2^- ions was pumped into the electrolyte solution tank hosting the cathode, while an iodide electrolyte solution with a 0.59% I_2 mass fraction and 1:7.5 I_2 to I^- mole ratio was pumped into the electrolyte solution tank hosting the anode. Au EW tests were done at a 12.9 V cell potential for 2 hrs. Meng et al. (2019) reported that the application of a cell potential resulted in the transport of dissolved AuI_2^- ions to the surface of the cathode where they underwent a reduction reaction (Eq.23) which produced I^- and solid Au (which was deposited

on the surface of the cathode). It was also reported that the application of a cell potential resulted in the transfer of I^- ions (through the AEM) to the surface of the anode where they were oxidized to I_2 (Eq.24), and the simultaneous electrolysis of H_2O at the anode surface to O_2 and H^+ (Eq.25).

$$AuI_2^-{}_{(aq)} + e \rightarrow Au_{(s)} + 2I^-{}_{(aq)} \qquad E_1 = 0.561 + 0.0592\lg[a(AuI_2^-)/a^2(I^-)] \qquad \text{(Eq.23)}$$

$$2I^-{}_{(aq)} - 2e \rightarrow I_{2\,(aq)} \qquad E_3 = 0.544 + 0.0592\lg a(I^-) \qquad \text{(Eq.24)}$$

$$2H_2O_{(aq)} - 4e \rightarrow O_{2(g)} + 4H^+{}_{(aq)} \qquad E_4 = 1.229 + 0.0592\lg a(H^+) \qquad \text{(Eq.25)}$$

The AEM used by Meng et al. (2019) was presumably for the inhibition of H^+ leakage and concentration into the catholyte tank. In theory, the inhibition of H^+ into the catholyte tank of the EW cell improves Au recovery because an increase in H^+ concentration decreases the reduction potential of AuI_2^-. In other words, AEMs are beneficial for improving proton transport efficiency. (Bhunia and Dutta, 2018). The main potential advantage of using the EW technique for Au recovery from iodide leachates, is that such a technique allows for the simultaneous recovery of Au and I_2, in a few process steps, and in an environmentally benign manner, without the use of hazardous chemical regents or the production of hazardous waste (Meng et al., 2019). Guo et al. (2020) reported that 83 % of I_2 can be recovered during Au EW and that iodide electrolytes can be recycled efficiently for 4 process cycles before dilution is required.

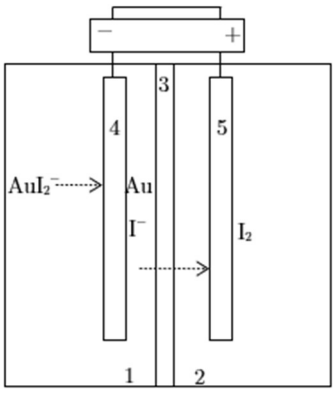

Figure 2.5.1 Schematic illustration of the EW cell used by Meng et al. (2019), where 1 = electrolyte solution tank hosting cathode, 2 = electrolyte solution tank hosting anode, 3 = generic commercial AEM, 4 = cathode, 7 = anode

The previous investigations into Au EW show that EW is an effective and simple processing method for the recovery of high yield (>95%) and high purity (>99%) Au from pregnant leach solutions, including iodide leachates. In the context of the present work, the findings from the aforementioned studies into Au EW suggest that EW is a suitable Au recovery process for use in the developed processing plant's concentration and recovery circuit (IEM-SLE and EW circuit). In addition to high effectiveness and simplicity, another benefit of using an EW process for Au recovery in the developed processing plant includes the simultaneous recovery of iodide solution during the electrochemical reduction-deposition of Au in the processing plant's IEM-SLE and EW circuit.

2.6 Simultaneous Au Concentration and Recovery by Ion-exchange Extractant Membrane (IEM) SLE and EW

Previous investigations have demonstrated that it is possible to simultaneously concentrate and recover Au from pregnant leachates/ electrolyte solutions using ion-exchange extractant membrane solid-liquid extraction (IEM-SLE) and electrowinning (EW).

Sun et al. (2020) performed laboratory experiments to study the simultaneous concentration and recovery of Au using IEM-SLE and EW. Experiments were performed in an IEM-SLE and EW cell (herein referred to as an IX-EW cell) comprised of an electrolyte solution tank hosting a Cu plate cathode and graphite plate anode (each with a 10 cm^2 area and spaced 5.0 cm apart), and an electrolyte solution tank without any electrodes. Electrolyte solution tanks (which had equal volumes) were separated by an Au selective IEM (Au-IEM) with an effective area of 7.07 cm^2. The Au-IEM used was composed of 50 wt.% polyvinylidene fluoride (PVDF) polymer matrix, 10 wt.% 2-nitrophenyl octyl ether (NPOE) plasticiser, and 40 wt.% [A336][SCN] carrier liquid. In the Au concentration and recovery tests, 150 mL of cyanide electrolyte solution (with a 0.20 mol/L NaCl concentration and pH of 10.0) containing 50 mg/L of dissolved Au(I) ions as $Au(CN)_2^-$ was pumped into the electrolyte solution tank without any electrodes (feed tank), while 150 mL of cyanide electrolyte solution (with a 3.0 mol/L KSCN concentration and pH of 10.0) was pumped into the

electrolyte solution tank hosting the cathode and anode. Au concentration and recovery tests were performed at a 1.50 V cell potential for 12 hrs and at 400 rpm agitation speed. Under these conditions, $>$ 95 % of Au was successfully concentrated and recovered as a deposit on the Cu cathode. Results of a stability evaluation experiment showed that the Au-IEM used can be operated stably for 10 cycles on a continuous run mode. A schematic illustration of the IX-EW cell used by Sun et al. (2020) is shown in Figure 2.6.1.

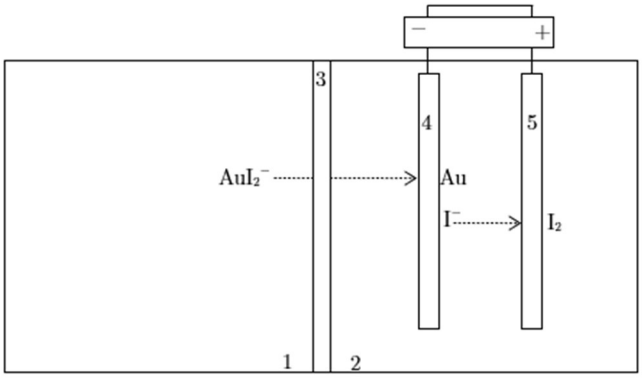

Figure 2.6.1 Schematic illustration of the IX-EW cell used by Sun et al. (2020), where 1 = electrolyte solution tank without any electrodes, 2 = electrolyte solution tank hosting cathode and anode, 3 = Au-IEM, 4 = cathode, 7 = anode

It is important to note, that in the context of the present work, the developed processing plant's Au concentration and recovery circuit utilises an IEM-SLE and EW process. The use of IEM-SLE together with EW offers the advantage of reduced processing steps and improved IEM-SLE efficiency, provided that the electric field of the EW circuit enhances ion mobility. This is because an enhanced ion mobility increases the rate of ion transport/ migration through a solution and increases the rate and efficiency of ion stripping from a membrane (Sun et al., 2020).

2.7 IEMs and IEM Separation

The hydrometallurgical processing plant developed in this project was designed to employ IEMs during the recovery and concentration of Au from pregnant leachates/ electrolyte solutions (using IEM-SLE together with EW). This section gives a brief overview of IEM classification, IEM design principles, IEM production, and IEM separation fundamentals.

2.7.1 IEM Classification

Illustrated in Figure 2.7.1, IEMs may be classified based on functionality as (Asante-Sackey et al., 2021):

- Monopolar – IEM containing only negatively or positively charged ionic functional groups.
- Amphoteric – IEM with both negatively and positively charged ionic functional groups which are randomly distributed.
- Bipolar – IEM composed of alternating layers of negatively and positively charged ionic functional groups.
- Mosaic – IEM composed of macroscopic fixed domains of negatively and positively charged ionic functional groups arranged in parallel.

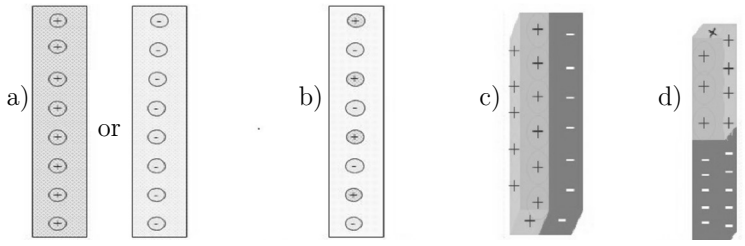

Figure 2.7.1 Categorized IEMs. (a) Positive or negatively charged monopolar IEM, (b) Amphoteric IEM, (c) Bipolar IEM and (d) Mosaic IEM (adapted from Asante-Sackey et al., 2021)

More commonly, however, IEMs are classified as being either homogeneous or heterogeneous. In heterogenous IEMs, charged ionic functional groups are contained within the polymeric matrix of

the IEM, without any chemical bonds. While in a homogenous IEM, charged ionic functional groups are chemically bonded to the polymer matrix of the IEM. In comparison to heterogenous IEMs, homogeneous IEMs typically have a more balanced distribution of ionic functional sites and a higher permselectivity and conductivity. However, homogenous IEMs are more expensive and complicated to manufacture than heterogenous IEMs. Furthermore, homogenous IEMs typically have lower chemical and mechanical stability in comparison to heterogenous IEMs.

In the context of the present study, it is important to note that the Au-IEM which was employed in the developed processing plant (in the IEM-SLE and EW circuit) is in essence a heterogenous IEM comprised of a PVC polymer matrix, hosting a non-chemically bonded Purogold S992 extractant carrier with ionic functional groups.

2.7.2 IEM Design Principles

IEMs used in SLE and/or EW applications are designed to have desirable characteristics such as (Xu, 2005):

- High permselectivity, since IEMs with high permselectivity, are able to separate counterions and co-ions with high efficiency.
- Good ionic conductivity, since IEMs with high ionic conductivity help minimize overpotentials associated with ohmic losses, further reducing losses in voltage efficiency.
- High chemical stability, since IEMs with high chemical stability, are able to operate effectively over a wide pH range and in the presence of oxidizing agents.
- Low electrical resistance, since IEMs with low electrical resistance, are less susceptible to electrolytic short circuits.
- Good mechanical and form stability, since IEMs with good mechanical and form stability have a low degree of swelling or shrinking in transition from dilute to concentrated ionic solutions.

In the context of the present study, it is important to note that the aforementioned design principles were used to design the Au-IEM which was employed in the developed processing plant. For example, PVC was selected for use as the base polymer in the Au-IEM employed since it has a low electrical resistance ($>10^{14}$ Ωat 23 ^{o}C), it is chemically stable, and has good mechanical and form stability (e.g., >50 Mpa ultimate tensile strength). While Purogold S992 was selected for use as the extractant carrier in the Au-IEM employed since it has a high selective permselectivity for Au(I) ions.

2.7.3 IEM Production

Homogeneous IEMs can be produced through the polymerization or polycondensation of monomers that carry anionic or cationic moieties, or through the introduction of anionic or cationic moieties into the structure of a polymer which may be in an appropriate solution or a preformed film. Heterogenous IEMs can be produced through the melting and pressing of a dry IX resin with a granulated polymer such as polyvinylchloride (PVC), or through the dispersion of an IX resin in a polymer solution. (Asante-Sackey et al., 2021; Xu, 2005)

In the context of the present study, it is important to note that the Au-IEM which was employed in the developed processing plant was produced through the dispersion of a Purogold S992 IX resin in a PVC solution. This synthesis procedure is described in greater detail in Chapter 3.

2.7.4 IEM Separation Fundamentals

Current Density

IEMs are used in EW applications such as in the developed processing plant's IEM-SLE and EW circuit, because they allow current transfer and are able to carry current when ions are transported through their surface during EW applications. In the context of the present work, this suggests that a membrane current density is generated in the developed processing plant's IEM-SLE and EW circuit's membranes when Au ions are transported through the Au-IEM and iodide ions are transported through the AEM. According to Faraday's law and shown in Eq.26, the aforementioned

membrane current density is dependent on factors such as applied current, active membrane surface area, ion mass transfer rate (flux), and ion valance. (Strathmann, 2004)

$$i = \mathrm{I/A} = \mathrm{F} \sum_i^n z_i J_i \quad \text{(Eq.26)}$$

where i is the membrane current density, I is the applied current, A is the active membrane surface area, J_i is the ion flux, z_i is the ion valance, and F is the Faraday constant.

Selectivity

IEMs are used in SLE and/or EW applications due to their ability to selectively allow and/or inhibit the mass transport of ions through their surface. In the context of the present work, the Au-IEM used in the IEM-SLE and EW circuit of the developed processing plant selectively allows the mass transport of Au ions through its surface based on the selective interaction between functional groups in the Au-IEM's SS992 extractant carrier and dissolved Au ions over competing BM ions, while the AEM used in the IEM-SLE and EW circuit of the developed processing plant selectively allows the mass transport of iodide anions and the inhibition of hydrogen cations. This is because charged ionic functional groups in the AEM show an electrostatic affinity towards negatively charged iodide ions and repulsive forces against positively charged hydrogen ions. In this instance, the capability of the AEM's ability to discriminate between oppositely charged ions (permselectivity) is expressed mathematically (Eq.27) as the Donnan potential (ϕ_{Don}), which is used to refer to the potential difference between the AEM (ϕ^{m}) and the iodide solution (ϕ^{s}) (Donnan, 1995).

$$\phi_{\mathrm{Don}} = \phi^{\mathrm{m}} - \phi^{\mathrm{s}} = (\mathrm{RT}/\mathrm{Z_jF}) \ln (\mathrm{a^s_j}/\mathrm{a^m_j}) \quad \text{(Eq.27)}$$

where, T is the absolute temperature, R is the universal gas constant, F is Faraday's constant, and $\mathrm{Z_j}$, $\mathrm{a^s_j}$ and $\mathrm{a^m_j}$ are the electrochemical valence, the activity in the solution and in the AEM of the component j, respectively.

Transport Rate (Flux)

The mass transport rate (flux) of ion transfer through the surfaces of the IEMs used in the developed processing plant can be described by the extended Nernst-Planck equation (Eq.28), which suggests that the flux of ions is driven by factors such as ion concentration, electric potential difference, and convection by hydrostatic pressure difference (Krol, 1997).

$$J_i = v\mathrm{C}_i - \mathrm{D}_i(\mathrm{d}\mathrm{C}_i/\mathrm{d}x) - (z_i\mathrm{F}\mathrm{C}_i\mathrm{D}_i/\mathrm{RT})(\mathrm{d}\phi/\mathrm{d}x) \qquad \text{(Eq.28)}$$

where J_i is the flux of the ion i, v is the convective velocity, while $\mathrm{C_i}$, $\mathrm{D_i}$ and z_i are the concentration, the diffusion coefficient, and the valency of the ion i, x is the distance coordinate across the membrane, R is the universal gas constant, T is the absolute temperature, and F is the Faraday constant.

Ion Mobility

The mobility of ions through the surfaces of the IEMs used in the developed processing plant is primarily determined by the size and physical structure of the IEMs. It can be expected that the mobility of iodide ions through the surface of the AEM follows a more direct pathway in comparison to the mobility of Au ions through the surface of the Au-IEM. This is because although the IEMs used are similar in size, the AEM used has a homogeneous IEM physical structure, while the Au-IEM has a heterogeneous IEM physical structure with more disruptive ion pathway channels. Figure 2.7.2 illustrates a typical transport path of ions through a homogenous and heterogeneous IEM. (Asante-Sackey et al., 2021; Xu, 2005)

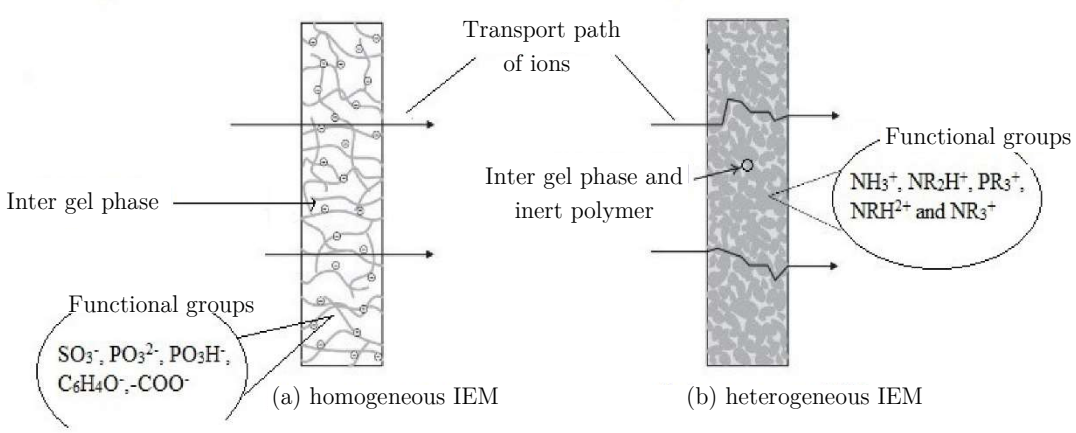

Figure 2.7.2 Ion pathway through a (a) homogeneous IEM and (b) heterogeneous IEM (Asante-Sackey et al., 2021)

Chapter 3
Technical Feasibility

As discussed in Chapter 1, this project's objectives were to develop a conceptual process and theoretical process plant outline for a hydrometallurgical processing plant for Au recovery from WPCBs (herein referred to as the processing plant), and to assess the developed processing plant's early-stage technical and economic feasibility, to determine whether or not it justifies further research and development. Figure 3.1 presents a simplified overall block flow diagram of the processing plant.

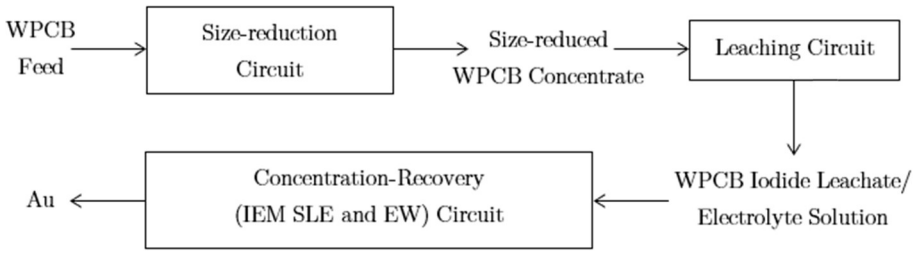

Figure 3.1 Simplified overall block flow diagram of the processing plant

Discussed in greater detail in Chapter 4, the processing plant is comprised of a size-reduction, leaching, and concentration-recovery circuit (IEM-SLE and EW circuit). In the size-reduction circuit, WPCBs are reduced to an ideal product size (2mm/2mm) before being transported to the leaching circuit where they are firstly leached using a 3-stage BM leaching process comprised of an HNO_3, HCl, and H_2SO_4-H_2O_2 leaching stage, and thereafter leached using a conventional iodide lixiviant. The WPCB iodide leachate/ I^--I_2-Au electrolyte solution which is produced in the leaching circuit is thereafter transported to the concentration-recovery circuit where Au is recovered using the IEM-SLE and EW technique/ process.

A 3-stage BM leaching process was selected due to the complex chemical composition of WPCBs and on the basis of the findings from previous work by Mecucci and Scott (2002) and Jha et al. (2012), which suggests that most BMs contained in WPCBs can be leached using a combination of HNO_3, HCl and H_2SO_4-H_2O_2 lixiviants.

A conventional iodide lixiviant (I^--I_2-H_2O_2) was selected for Au leaching because unlike many alternative lixiviants (cyanide, thiosulphate, thiourea, chloride, or bromide lixiviants), conventional iodide lixiviants have been reported to be capable of leaching Au from WPCBs with high leaching efficiencies and kinetics at ambient temperatures, slow agitation speeds, under non-corrosive conditions/ mild pH, and without the emission of toxic fumes, while also being affordable on account of their high (>80 %) recyclability (Xu et al., 2010; Sahin et al., 2015; Batnasan et al., 2019).

The processing plant's concentration and recovery circuit utilises an IEM-SLE and EW technique/ process for Au concentration and recovery. SLE was selected in preference to LLE because it offers the advantage of simpler equipment, less reagent loss, no phase disengagement, and easy phase separation (Rovira, 1998). An Au-IEM was selected in preference to activated carbon on the basis of previous work which reported that Au-IEMs offer an improved Au loading selectivity in the presence of Cu (Van Deventer et al., 2012). It is important to note that the cost of Au-IEMs is typically higher than that of activated carbon, due to the high cost of Au-IX extractants used in Au-IEMs. For example, according to van Deventer et al. (2014), the absorbent unit cost of Purogold S992 Au-IX extractant is $40,630 and for activated carbon, it is $2,200. However, the high cost of Au-IEMs in comparison to activated carbon is balanced by their lower capital outlay, due to the use of less capital-intensive stripping methods. This is because the stripping of activated carbon is typically done in a kiln at high temperatures in excess of 700 ^oC, while Au-IX extractants can be eluted at medium to ambient temperatures, without the need for an expensive kiln (which can cost over $500,000 according to Manjengwa, 2019b).

The remainder of this chapter presents the processing plant's early-stage technical feasibility assessment (materials, apparatus, method, and results), which was done in parallel with its process

development and design (Chapter 4), and early-stage economic feasibility assessment (Chapter 5) – i.e., the results and findings of this project's technical feasibility assessment are integrated with the processing plant's development and design, and early-stage economic feasibility study.

The processing plant's early-stage technical feasibility assessment was supported by a laboratory experiment which studied the concentration and recovery of Au from a WPCB iodide leachate/ I^--I_2-Au electrolyte solution using the novel IEM-SLE and EW technique. It is important to note that the processing plant's size-reduction and leaching circuits were not extensively investigated in its early-stage technical feasibility assessment since previous work has already shown that it is technically feasible/ possible to employ the size-reduction and leaching processes used in these circuits (Mecucci and Scott, 2002; Jha et al., 2012; Behnamfard et al., 2013; Ficeriova et al., 2011; Yang et al., 2011; Nekouei et al., 2018; Dias et al., 2019)

3.1 Materials and Apparatus

3.1.1 WPCB I^--I_2-Au Electrolyte Solution, and I^--I_2 Electrolyte Solution

In terms of apparatus, the aqueous WPCB I^--I_2-Au electrolyte solution/ iodide leachate which was used in the laboratory experiment was prepared in a low-form glass beaker on a heating plate, equipped with a 3D printed system closure, an overhead mechanical agitator, and a thermometer. The previously described leaching set-up is shown in Figure 3.1.1.

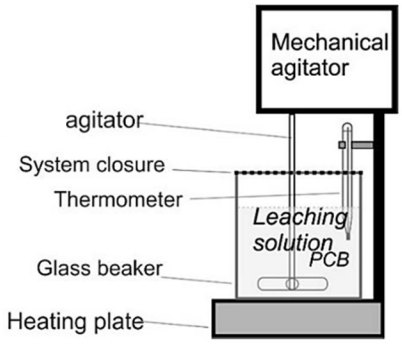

Figure 3.1.1 Scheme of leaching set-up

The I^--I_2 electrolyte solution which was used in the laboratory experiment was an aqueous solution prepared with a 2.5 g/L I_2 (Merck) and 10 g/L KI (Merck) concentration. While, the aqueous WPCB I^--I_2-Au electrolyte solution/ iodide leachate which was used in the laboratory experiment was prepared by leaching pulverised WPCBs (with a 2mm/2mm cm particle size) in 0.2 M HNO_3 lixiviant (for 45 min at 500 g/L S/L, 18 rpm agitation rate, and 90 ^oC temp), 3.5 M HCl lixiviant (for 120 min, at 500 g/L S/L, 18 rpm agitation rate, and 90 ^oC temp), 2M H_2SO4 and 2M H_2O_2 lixiviant (for 3 hrs, at 500 g/L S/L, 18 rpm agitation rate, and 25 ^oC temp), and 2.5 g/L I_2, 10 g/L I^-, and 10 g/L H_2O_2 lixiviant (for 4 hrs at 500 g/L S/L, 18 rpm agitation rate, 25 ^oC temp, and pH 6). The observed metal leaching yields and metal concentrations in the leachates produced after each respective leaching stage are presented in Table 3.3.3 and Table 3.3.2, respectively. These yields and concentrations were determined through the chemical analysis of samples of each leachate produced using ICP-OES.

It is important to note that all leaching stages were performed 3 times under a single set of operating conditions, and the reported metal concentrations are set averages, with their repeatability evaluated through standard deviation.

Images of the WPCBs (prior to pulverisation) which were used in the preparation of the WPCB iodide leachate are shown in Figure 3.1.2. The WPCBs were originally 50 g in mass and 10 cm x 15 cm in size and their metal composition is shown in Table 3.3.1. Metal composition of the WPCBs used was determined by leaching 50 g of pulverised and homogenised WPCBs in aqua regia at a S/L ratio of 25 g/L, for 24 hrs, and then chemically analysing the leachate produced by ICP-OES. It is important to note that the WPCBs used in this study are unpopulated (not covered by a solder) ideal/ model boards which were specifically designed for this project by Trax Interconnect. A detailed description of the ideal/ model boards used in this study is provided in Chirume (2018).

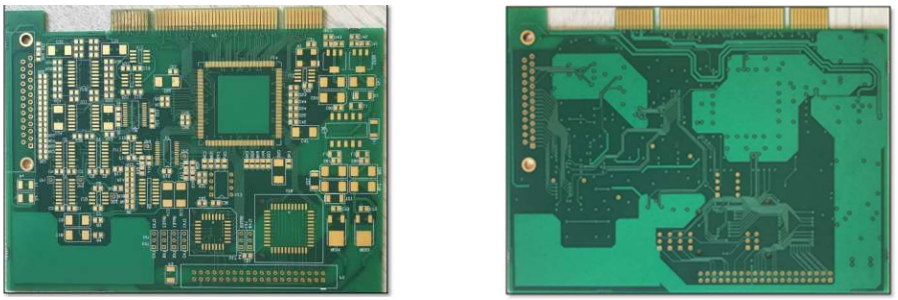

Figure 3.1.2 10 cm x 15 cm WPCB used in the laboratory experiment (left = front, right = back)

3.1.2 Au Selective Ion Exchange Extractant Membrane (Au-IEM)

The Au-IEM which was used in the laboratory experiment was in essence a heterogenous IEM comprised of 40 wt.% poly-vinyl-chloride (PVC) polymer-backbone and 60 wt.% Purogold S992 extractant carrier. This membrane composition was based on data provided by Křivčík et al. (2014) who suggested that extractant membranes with a 40/60 polymer-backbone/ extractant carrier ratio exhibit good selectivity, permselectivity, and conductivity. This is important considering that selectivity determines how well the Au-IEM separates AuI_2^- ions from competing BM impurity ions, permselectivity determines the efficiency (yield) in which the Au-IEM will transport AuI_2^- ions through its body, and conductivity determines the rate at which AuI_2^- ions will be transported through the Au-IEM body. (Křivčík et al., 2014)

The Au-IEM used in this work was synthesised using a similar procedure as that reported by Schow et al. (1996) and Sugiura et al. (1989). This synthesis procedure commenced with the preparation of a casting solution in the form of a 100 % 1.0 L tetrahydrofuran (THF) solution (Merck) containing approximately 20 g of dissolved S5718 PVC (Sasol) and 30 g of undissolved Purogold S992 extractant (Purolite). This casting solution was mixed for 30 min in order to obtain a uniform distribution of PVC-THF solution and S992 extractant. Once prepared, the casting solution was poured into a 150 mm × 15 mm petri dish (sitting on a flat glass plate and covered with filter paper and a watch glass), which was placed in a flat box under inert nitrogen (N_2) atmosphere for 24 hrs to allow for THF to evaporate slowly and have little contact with air humidity, thus, to avoid excessive formation

of pores (which would result in decreased selectivity and permselectivity of AuI_2^-). After complete evaporation of THF, a few droplets of distilled H_2O was added into the petri dish, and thereafter the remaining solid (Au-IEM) was peeled off.

It must be noted that the Purogold S992 extractant carrier was not ground prior to mixing with THF to ensure that the individual resin beads which made up the Purogold S992 extractant carrier retained their mechanical strength and performance. Furthermore, it was observed that the individual resin beads of the Purogold S992 extractant carrier did not disintegrate when mixed with THF as expected. Instead, the PVC acted as a binding agent which joined/ cast the individual resin beads of the S992 extractant carrier together.

The technical specifications of the THF and PVC used to synthesise the Au-IEM employed in the laboratory experiment are shown in Table 3.1.1.

Table 3.1.1 Technical specifications of the PVC and Purogold S992 resin used to synthesise the Au-IEM employed in the laboratory experiment (Sasol, n.d.; Purolite, n.d.)

S5718 PVC properties	K-value	57
	Appearance	White powder
	Particle size > 250 µm	< 5.0 %
	Cold plasticiser adsorption	17 %
	Apparent density	≥ 550 g/L
	Volatile matter	< 0.3 %
Purogold S992 properties	Polymer structure	Macroporous polystyrene crosslinked with divinylbenzene
	Appearance	Light yellow spherical beads
	Functional group	Proprietary mixed amines
	Ionic form	Freebase
	Particle size range	600 – 1300 µm
	Specific gravity	1.05
	Temperature limit	80 °C

PVC was selected for use as the base polymer in the Au-IEM employed in the laboratory experiment for the following reasons (Almeida et al., 2012; Witt and Radzymińska-Lenarcik, 2019):

- PVC is not prone to hydrolysis (owing to its all-carbon backbone), so it is not damaged easily due to changes in pH.
- PVC is an amorphous polymer with a small degree of crystallinity (this is mainly because PVC has relatively polar and non-specific dispersion forces which dominate its intermolecular interactions, owing to C-Cl functional groups present), and as a consequence, has good mechanical properties, so it can withhold its shape once cast.
- PVC is commercially available and has been used successfully in previous studies as a base polymer in extractant membranes.
- PVC is ion-permeable and thus allows for AuI_2^- migration through its surface and interior.

Purogold S992 was selected for use as the extractant carrier in the Au-IEM employed in the laboratory experiment for the following reasons (Fedyukevich et al., 2015; Van Deventer, 2014):

- Purogold S992 is a macroporous-type poly(vinylbenzyl) anion exchange extractant tailored for selective extraction of Au (I) in preference to competing metal impurity ions such as Zn(II), Ag(I), Fe(II), Cu(I) and Ni(II). The high selectivity of Purogold S992 towards Au(I) (and thus presumably AuI_2^-) results from the presence of soft electro-donating nitrogen atoms in the proprietary amine functional group of Purogold S992, which strongly interact with Au(I).
- Purogold S992 is commercially available, has low acute toxicity, and has been used successfully in previous work for the extraction of Au(I).

Purogold S992 has a macroporous structure and a styrenic backbone which is cross-linked with divinylbenzene (DVB). This essentially means that it contains a network of pores within a gel matrix. Light is scattered by the pores, making the Purogold S992 extractant appear opaque. Proprietary functional groups that are attached to the backbone and located throughout the Purogold S992 extractant interact with Au ions in solution. The rate of reaction (kinetics) between Au ions in solution and the Purogold S992 extractant is controlled by the rate of ion diffusion through the thin film of H_2O surrounding each individual bead of the Purogold S992 extractant (film diffusion) and

through each bead of the Purogold S992 extractant itself (particle diffusion). In a dilute solution/ during the adsorption phase, the rate of film diffusion is slower than the rate of particle diffusion. However, during the subsequent stripping/ elution phase, the rate of film diffusion is faster than the rate of particle diffusion (Van Deventer, 2014). It is important to note that in the present study, resin beads of Purogold S992 are suspended within a PVC matrix. Hence, a PVC layer is present over the surface of each individual S992 resin bead in the Au-IEM employed. This PVC layer increases the diffusion path length of ions, and as a result, may interfere with and reduce the rate of ion diffusion, since ions have to travel through the outer PVC later before they can interact with the S992 resin beads and their outer H_2O film. Furthermore, it is possible that when the S992 resin beads were mixed in PVC, their outer H_2O film may have been damaged, thus resulting in further interference and reduction of ion diffusion rate.

THF was selected for use as the solvent during the preparation of the Au-IEM employed in the laboratory experiment for the following reasons (Fontas et al., 2007):

- THF has been reported to be highly effective at dissolving PVC at ambient temperature (25^oC).
- THF has a low acute toxicity and is commercially available.

3.1.3 Anion-Exchange Membrane (AEM)

The AEM used in the laboratory experiment was the AFX membrane (Neosepta and Astom Corporation). The AFX membrane is a homogenous AEM comprised of a poly-styrene-co-divinylbenzene base polymer with positively charged ion-exchange functional groups (which are typically propriety quaternary ammonium bases $–(CH_3)_3N^+$)). The AFX membrane is also reinforced and interpenetrated with PVC. (Zaheri and Davarkhah, 2020)

The AFX membrane was selected for use as the AEM employed in the laboratory experiment for the following reasons (Zaheri and Davarkhah, 2020; Chengyi et al., 2020):

- AFX membrane is commercially available and has a highly selective permeability for anions due to the presence of positively charged IX functional groups, and thus allows for efficient blockage of H^+ transport through its surface and interior.
- AFX membrane has a low electric resistance, which is very important for plant operation costs as it allows for efficient electrical energy usage.
- AFX membrane has a low diffusion coefficient which minimises undesired back diffusion or transfer of H^+.
- AFX membrane has high mechanical strength and dimensional stability (high resistance to swelling and shrinking), so it can maintain its shape with changing temperature, composition, concentration, etc.
- AFX membrane has good chemical stability, so it can withstand harsh pH.

3.1.4 Experimental IX-EW Cell

The laboratory experiment investigating the concentration and recovery of Au from the generated WPCB iodide leachate/ I^--I_2-Au electrolyte solution was performed in a custom-made experimental IEM-SLE and EW cell (herein referred to as an IX-EW cell) comprised of three distinct, hollow, open-top cubic Pyrex tanks (feed tank, electrolyte solution tank hosting a cathode, and electrolyte solution tank hosting an anode) with inner volumes of 2197 mL/ dimension of 13 cm × 13 cm × 13 cm. Each tank was equipped with a 20 cm × 20 cm gasket. A circular hole with a 10 cm diameter was machined into the left and right lateral faces of the electrolyte solution tank hosting the cathode, left lateral face of the electrolyte solution tank hosting the anode, and right lateral face of the feed tank. A square 12 cm × 12 cm Au-IEM was positioned radially between the right lateral face of the feed tank and the left lateral face of the electrolyte solution tank hosting the cathode, while a square 12 cm × 12 cm AEM was positioned between the left lateral face of the electrolyte solution tank hosting the anode and the right lateral face of the electrolyte solution tank hosting the cathode. Eight nut and bolt fasteners were used to join the three tanks of the experimental IX-EW cell

together. These fasteners passed through the gasket of the tanks. A schematic illustration of the experimental IX-EW cell used is shown in Figure 3.1.3

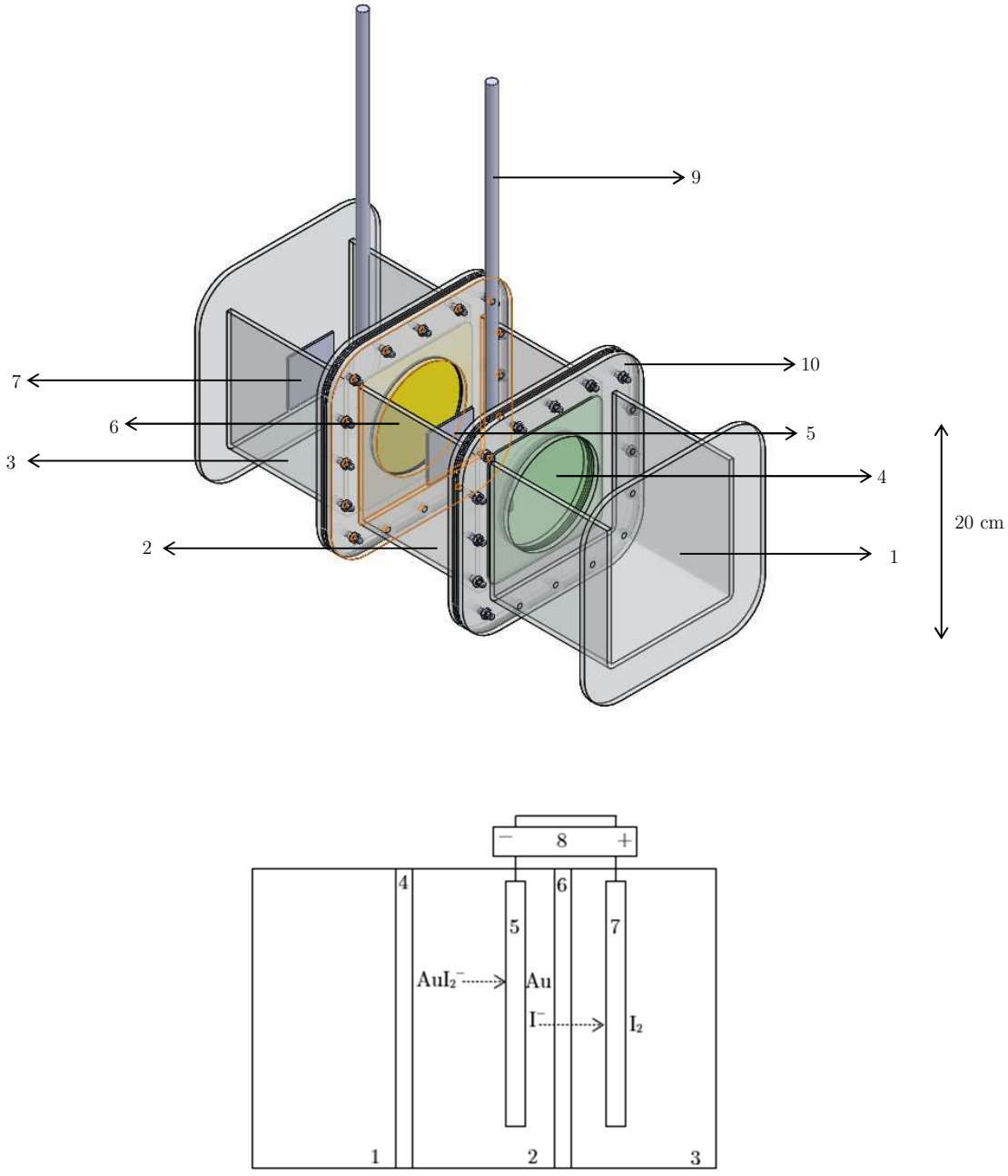

Figure 3.1.3 Schematic illustration of side view (bottom) and isometric view (top) of the experimental cell used; where 1 = feed tank, 2 = electrolyte solution tank hosting cathode, 3 = electrolyte solution tank hosting anode, 4 = Au selective ion-exchange extractant membrane, 5 = cathode, 6 = anion exchange membrane, 7 = anode, 8 = DC power supply,
9 = overhead stirrer, 10 = gasket with nut and bolts

The experimental IX-EW cell utilised a 5 cm × 7 cm × 0.1 cm mesh titanium anode with a 35 cm^2 contact surface area and a 5 cm × 7 cm × 0.1 cm stainless-steel plate cathode with a 35 cm^2 contact surface area. Electrodes were spaced 13 cm apart. The cathode was connected to the negative pole of a DC power supply, while the anode plate was connected to the positive pole of the same DC power supply.

A titanium anode and stainless-steel cathode were selected for use as electrodes in the IX-EW cell since they:

- are highly corrosion resistant, insoluble in acidic and alkaline solutions, and stable over a wide range of current densities (i.e., they are durable electrodes which would survive if applied at an industrial scale),
- have good current distributions and electrical conductivities (i.e., they allow for efficient transfer of electrical energy/ cell voltage application), and
- have been used successfully in the past in the electrowinning of Au^+.

The DC power supply used in this project had a maximum voltage >24 V, was capable of operating under constant current or voltage mode and had the capability to be power factor corrected. To control agitation speed, each tank of the electrochemical cell used in this project was equipped with an overhead stirrer.

3.2 Method

In summary, the laboratory experiment investigating the concentration and recovery of Au from the generated WPCB iodide leachate/ I^--I_2-Au electrolyte solution using the IEM-SLE and EW process (herein referred to as the experiment) commenced by loading 2.0 L of WPCB iodide leachate/ I^--I_2-Au electrolyte solution into the feed tank of the experimental IX-EW cell, and loading 2.0 L of KI^--I_2 electrolyte solution into the electrolyte solution tanks of the IX-EW cell hosting the cathode and anode. Thereafter, electrical power was provided to the DC power supply connected to the electrodes

in the IX-EW cell for 6.0 hrs, at a constant cell voltage of 12.9 V, temperature of 25 ^{o}C, 250 rpm agitation speed, and average current of 5 A, and 1429 A/m^2 equivalent current density.

Once electrical power had been provided for the specified time (6.0 hrs), the DC power supply was switched off and the cathode was removed from the IX-EW cell. Thereafter, Au which had deposited on the cathode as a dark brown powder was gently scrapped off, weighed, and placed in a 100 mL container for storage. Using a syringe, a 25 mL sample electrolyte solution was collected from the feed tank and electrolyte solution tank hosting the cathode after 2 hrs, 4 hrs, and 6 hrs. These sample solutions were placed in 50 mL containers for storage.

The Au and BM concentration of the deposited Au and sample electrolyte solutions from the feed tank and electrolyte solution tank hosting the cathode was determined through chemical analysis by ICP-OES. Au concentration and recovery yield was then determined using Eq.29:

$$Y = (C_2/C_1) \times 100(\%) \quad \text{(Eq.29)}$$

where Y is the Au concentration and recovery yield, C_1 is the amount of Au (in mg) in the WPCB iodide leachate/ I^--I_2-Au electrolyte solution before cell voltage is applied, and C_2 is the amount of Au (in mg) deposited on the cathode.

Finally, a 50 mL sample solution was collected from the electrolyte solution tank hosting the anode after 6 hrs, and the I_2 and I^- concentration of this solution was determined through chemical analysis using UV-Vis spectroscopy.

The aforementioned chemical analysis results were used to understand the technical feasibility of Au concentration and recovery using the IEM-SLE and EW technique. It is important to note that all experiments were done in 3 sets under a single set of operating conditions and all concentrations reported are set averages, with repeatability evaluated through standard deviation.

3.3 Results and Discussion

3.3.1 Au and BM Concentrations in WPCBs

Chemical analysis results in Table 3.3.1 show that each 50 g of WPCB used in the preparation of WPCB iodide leachate contained 0.054 ± 0.001 g of Au, 27.8 ± 0.048 g of Cu, 3.50 ± 0.059 g of Al, 0.802 ± 0.002 g of Ni, and 1.65 ± 0.044 g of Fe (i.e., each WPCB was comprised of 0.11 wt.% Au, 55.7 wt.% Cu, 7.00 wt.% Al, 1.60 wt.% Ni, and 3.31 wt.% Fe). These metal concentrations are similar to the chemical analysis results reported by Chirume (2018) who also analysed the composition of similar WPCBs. The chemical analysis results in Table 3.3.1 suggest that a total of 1.09 ± 0.034 g of Au, 557 ± 0.964 g of Cu, 70.0 ± 1.19 g of Al, 16.0 ± 0.049 g of Ni, and 33.1 ± 0.873 g of Fe was initially contained in each 1.0 kg of WPCB used to prepare 2.0 L of WPCB iodide leachate/ I^--I_2-Au electrolyte solution.

It is important to note that the high Au and Cu concentration of the model/ideal WPCBs used in this study is over 3 times higher than that of typical/ non-ideal WPCBs and that the ideal/ model WPCBs used were unpopulated boards without a solder. The concentration of Au, Cu, and some other metals found in typical WPCBs is shown in Table 1.1.2. Ideal/ model WPCBs were used in this study in preference to typical WPCBs because the processing plant's early-stage feasibility was assessed assuming ideal conditions in most instances. As stated in Section 1.4, this is one of the primary limitations of the present study, however, the sensitivity of the processing plant's feasibility was assessed (in Section 5.2.5) in response to deviations from the base-case condition developed assuming an ideal model/conditions (e.g., analysis of the processing plant's economic feasibility sensitivity in response to change in estimated and assumed revenue due to a decrease in Au concentration in feed WPCBs). Ideal/ model WPCBs were also used in this study since they were readily available, and their use allowed for the simple preparation of relatively homogenous WPCB feed particulate (since the ideal WPCBs had similar compositions). The use of ideal homogenous WPCB feeds with high Au and Cu concentrations was beneficial since it allowed for simple mass balancing of Au and Cu during the respective leaching stages and during concentration and recovery

by IEM-SLE and EW. Effective mass balancing of Au and Cu is important since these metals hold most of the economic value of WPCBs and they are the only metals which report into the processing plant's WPCB iodide leachate in appreciable concentrations (this is discussed in more detail in Section 3.3.2). The use of typical/ non-ideal WPCBs was not extensively investigated in this study due to scope constraints, and because the use of typical WPCBs may have resulted in a decreased statistical significance of results, due to increased variability/imprecision between test results. This is because the use of typical WPCBs is expected to result in a more inconsistent/variable WPCB feed composition between the various leaching trials (due to the complex and variable chemistry of typical/ non-ideal WPCBs), and as a result increase the variability of the laboratory experiment results and thus decrease statistical significance of the projects findings.

Table 3.3.1 Au and BM concentrations in WPCBs

	Au	**Cu**	**Al**	**Ni**	**Fe**
Metal concentration (g) in 50 g WPCB	0.054 ± 0.001	27.8 ± 0.048	3.50 ± 0.059	0.802 ± 0.002	1.65 ± 0.044
Metal wt.%	0.11	55.7	7.00	1.60	3.31

3.3.2 Au and BM Concentrations in Leachates and Leaching Yields

Chemical analysis results of the Au and BM (Cu, Al, Ni, and Fe) concentrations in the leachates produced after each sequential leaching stage during the preparation of WPCB iodide leachate are presented in Table 3.3.2.

Table 3.3.2 Au and BM concentrations in leachates

		Leachate			
		HNO_3	HCl	H_2SO_4-H_2O_2	I_2-I^--H_2O_2
Metal concentration (g) in 2.0 L leachate	Au	0.00	0.00	0.00	1.07 ± 0.009
	Cu	185 ± 0.742	95.1 ± 0.753	156 ± 1.25	0.121 ± 0.001
	Al	31.4 ± 1.07	15.9 ± 0.310	2.21 ± 0.118	0.00
	Ni	6.56 ± 0.438	1.66 ± 0.044	1.23 ± 0.027	0.00
	Fe	20.7 ± 0.295	1.86 ± 0.224	1.55 ± 0.20	0.00

Results in Table 3.3.2 show that after the final iodide leaching stage, 1.07 ± 0.009 g of Au was reported into 2.0 L of WPCB iodide leachate, with Cu the only BM impurity which was reported into in the WPCB iodide leachate (present in a concentration of 0.121 ± 0.001 g).

Chemical analysis results of Au and BM leaching yields after each respective leaching stage are summarised in Table 3.3.3. These results show that the total Au leaching yield obtained after the preparation of the WPCB iodide leachate was 97.78 %. The high Au leaching yield observed following the preparation of the WPCB iodide leachate is comparable to the Au leaching yield observed by Batnasan et al. (2016) who used a similar conventional iodide lixiviant to leach Au from WPCBs at a >95 % yield.

Table 3.3.3 Au and BM leaching yields

		Leachate				
		HNO_3	HCl	H_2SO_4-H_2O_2	I_2-I^--H_2O_2	Cumulative
Metal leaching yield (%)	Au	0.00	0.00	0.00	97.78	97.78
	Cu	33.20	17.06	28.28	0.02	78.56
	Al	43.99	22.64	3.08	0.00	69.70
	Ni	39.11	10.32	7.58	0.00	57.02
	Fe	63.11	5.62	4.32	0.00	73.04

Results in Table 3.3.3 also show that the BM (Cu, Al, Ni, and Fe) leaching yields observed during the preparation of the WPCB iodide leachate (with cumulative yields ranging between 57.02 % to 78.56 %) are significantly lower than the WPCB BM leaching yields reported by Mecucci and Scott (2002), Jha et al. (2012), Behnamfard et al. (2013), Ficeriova et al. (2011), and Yang et al. (2011) who used either HNO_3, HCl, or H_2SO_4-H_2O_2 lixiviants to leach BMs from WPCBs with >95 % yields. The lower BM leaching yields observed can be attributed to the high 500 g/L S/L ratio employed, which is significantly greater than the 100 g/L to 333 g/L S/L ratio employed by Mecucci and Scott (2002), Jha et al. (2012), Behnamfard et al. (2013), Ficeriova et al. (2011), and Yang et al. (2011). The high 500 g/L S/L ratio employed may have decreased BM leaching yields due to increased lixiviant reagent consumption.

The high 500 g/L S/L ratio employed in this work is supported by Yannopoulos (1991) who reported that Au is effectively leached at high S/L ratios between 350 g/L to 500 g/L in industrial operations. A higher S/L ratio can be beneficial since it results in a smaller leaching reactor size requirement and thus reduced cost. A 500 g/L S/L ratio is also deemed as being feasible for use in the processing plant's leaching circuit since the leaching results obtained prior to the laboratory experiment show that a high Au leaching yield is obtained at the high 500 g/L S/L ratio employed. This implies that the high 500 g/L S/L ratio employed in this work is feasible for Au leaching from WPCBs, and thus feasible for use in the processing plant's leaching circuit. Although the high 500 g/L S/L ratio employed resulted in less feasible BM leaching yields, BM recovery is not a primary concern of the processing plant. In other words, it can be argued that the processing plant's 3-stage BM leaching process is feasible for its intended application despite the use of a high 500 g/L S/L ratio, since BMs did not readily report into the WPCB iodide leachate, and BMs did not interfere with Au leaching yield.

It is important to mention that the leaching results presented were achieved from unpopulated WPCBs without solder. A desoldering step was not included in the processing plant since it was developed primarily for Au recovery and based on the assumption that all Au recovered would be derived from connectors and contacts without solder. The aforementioned assumption is supported by Goodman (2002) who reported that the majority of Au contained in WPCBs is located on connectors and contacts which are not covered by solder.

3.3.3 Au Concentration and Recovery by IEM-SLE and EW

Chemical analysis results of the sample electrolyte solutions collected from the IX-EW cell feed tank and electrolyte solution tank hosting the cathode after 2 hrs, 4 hrs, and 6 hrs (Table 3.3.4), show that there was no Au concentrated in the feed tank after 2 hrs. However, after 2 hrs, there was still 0.498 ± 0.021 g of Au (~47 wt.% of initial Au) which was still concentrated in the electrolyte solution tank hosting the cathode, thus indicating that Au concentration and recovery as a deposit on the cathode was incomplete. Similarly, it was observed that after 4 hrs, Au concentration and recovery

as a deposit on the cathode was still incomplete, since 0.174 ± 0.015 g of Au (~16.4 wt.% of initial Au) was found to be concentrated in the electrolyte solution tank hosting the cathode. However, after 6 hrs it was found that no Au was concentrated in the electrolyte solution tank hosting the cathode, thus indicating that Au concentration and recovery as a deposit on the cathode was complete after 6 hrs. Chemical analysis results of sample solutions also found that no BMs reported into the electrolyte solution tank hosting the cathode, thus confirming that Au was selectively transported through the Au-IEM and into the electrolyte solution tank hosting the cathode. However, it is important to note that the chemical analysis results of the Au-IEM found that 0.03 ± 0.004 g of Cu was adsorbed onto the Au-IEM after the laboratory experiment together with 0.051 ± 0.004 g of residual Au. However, this adsorbed Cu was not stripped and transported into the electrolyte solution hosting the cathode.

Table 3.3.4 Metal concentrations in 2.0 L electrolyte solutions in IX-EW cell

		Time			
		0 hrs	**2 hrs**	**4 hrs**	**6 hrs**
Metal concentration (g) in feed tank[a]	Au concentration (g)	1.07 ± 0.009	0.00	0.00	0.00
	Cu concentration (g)	0.121 ± 0.001	0.118 ± 0.001	0.091 ± 0.002	0.089 ± 0.002
Metal concentration (g) in the electrolyte solution tank hosting the cathode[b]	Au concentration (g)	0.00	0.498 ± 0.021	0.174 ± 0.015	0.00
	Cu concentration (mg)	0.00	0.00	0.00	0.00

[a]Containing 2.0 L WPCB iodide leachate/electrolyte solution, [b]Containing 2.0 L iodide electrolyte solution

Chemical analysis results of the 1.02 ± 0.006 g deposit obtained after the laboratory experiment showed that Au was the only metal, which was quantitatively detected in the deposit, constituting >99%. Hence, the total Au concentration and recovery yield observed after the laboratory experiment was 95.50 %. The high Au concentration and recovery yield observed after the laboratory experiment is comparable to, but slightly lower than the 98.75 % Au recovery yield observed by Meng et al. (2019). The lower Au recovery yield observed can be attributed to the loss of

approximately 4 % of Au to the Au-IEM through incomplete elution/ stripping (this was confirmed by the presence of residual Au on the Au-IEM). In this instance, Au loss could be reduced by increasing the temperature or pH of the electrolyte solution hosting the cathode. However, an increase in temperature and/or pH may have resulted in the degradation of the Au-IEM, due to a loss of mechanical strength in response to temperature changes, or osmotic shock in response to changes in pH. (Van Deventer, 2014). In addition to the loss of Au to the Au-IEM, other drawbacks/ limitations of the IEM-SLE and EW process used in the laboratory experiment, include the high cell voltage employed and the long IEM-SLE and EW time. The high 12.9 V cell voltage employed in the present work is significantly higher than the 2.1 – 5 V cell voltage applied in many industrial Au EW processes (however it must be noted that these industrial EW processes are rarely focused on Au recovery from leachates with dilute Au concentrations as in the present work). The long 6 hr EW time required to achieve a maximum 95.50 % Au concentration and recovery yield in the present work is triple the amount of time that was required by Meng et al. (2020) who used a similar EW process to concentrate and recover Au from an iodide leachate with a maximum yield of 96% after 2 hrs.

The developed and experimentally investigated IEM-SLE and EW process could be improved by overcoming the aforementioned limitations/ drawbacks through process and configuration optimization. Process and configuration optimization could be achieved by conducting additional experiments investigating how Au concentration and recovery yield are affected by changes in operating conditions (e.g., cell voltage, temperature, etc.) or IX-EW cell configuration (e.g., electrode spacing, membrane contact surface area, etc.). Findings from these additional experiments could be used to design a more improved IEM-SLE and EW process which is able to concentrate and recover Au with a greater yield (>95.50 %), using a lower cell voltage (< 12.9 V), and in a shorter time (< 4 hrs). However, it must be noted that the aforementioned additional experiments for process and configuration optimization of the developed IEM-SLE and EW process were not attempted in the present study since this fell beyond the scope of the present work which aimed to confirm the in-principal feasibility of the process.

As stated in Section 2.5.1, one of the key advantages of using EW techniques for Au recovery from iodide leachates, is that such techniques allow for the simultaneous recovery of Au and I_2, in a few process steps, and in an environmentally benign manner, without the use of hazardous chemical regents or the production of hazardous waste (Meng et al., 2019). Recovered I_2 can then be re-used in subsequent process cycles to reduce costs. In the present work, approximately 2.0 L of iodide (I_2 and I^-) solution was recovered after the laboratory experiment from the electrolyte solution tank hosting the anode, as a dark purple liquid. Chemical analysis results found that the recovered iodide solution had a 6.11 ± 0.85 g/L I_2 concentration and 26.77 ± 3.73 g/L I^- concentration. This implies that approximately 82 % of initial iodine and 89 % of initial I^- was recovered in the iodide solution from the electrolyte solution tank hosting the anode (this finding is comparable to the 83 % I_2 recovery yield obtained by Meng et al., 2021). In addition to the recovered iodide solution, 2.0 L of clear aqueous solution/ water with a Cu (as Cu^{2+}) concentration of 89.07 ± 1.79 mg was recovered from the feed tank, while 2.0 L of clear di-ionised water was recovered from the electrolyte solution tank hosting the cathode.

The lab results of this project revealed that the IEM-SLE and EW technique was able to concentrate and recover a maximum of 1.02 g of Au from 2.0 L of WPCB iodide leachate after 6.0 hrs, as a deposit on the stainless-steel cathode in the IX-EW cell. Consequently, the average flux of Au ions through the 12 cm × 12 cm Au-IEM was determined to be 3.27 mg/m^2.s or 8.4 × 10^{-6} mol/m^2.s. This flux is comparable to the 5.5 × 10^{-6} to 14.8 × 10^{-6} mol/m^2.s Au flux reported by Sun et al., 2020, who studied the flux of Au ions through an IEM comprised of a polyvinylidene fluoride back bone and [A336][SCN] carrier, during the recovery of Au in cyanide solution using a technique similar to the investigated IEM-SLE and EW process (As discussed in the Chapter 2, the process applied by Sun et al., 2020 is primarily differentiated by the absence of an AEM, and by the use of only a single electrolyte solution tank which hosted both the anode and cathode).

Since the full-scale processing plant was designed to operate at an Au concentration equal to that of the Au concentration in the feed WPCB iodide leachate used in the laboratory experiment, it was

assumed that the flux in the full-scale processing plant is equal to the flux in the laboratory experiment (i.e., 3.27 $mg/m^2.s$ or 8.4×10^{-6} $mol/m^2.s$.)

A summary of the key results is presented in Table 3.3.5. As previously stated in sections 3.2 and 3.1, all leaching, and experiments were performed in 3 sets using a single set of operating conditions, and all chemical analysis results reported are set averages, with repeatability evaluated through standard deviation.

Table 3.3.5 Summary of key results

Description	Result
Au leaching yield	97.78 %.
Au concentration and recovery yield	95.50 %
I_2 yield in recovered iodide solution	82 %
I^- yield in recovered iodide solution	89 %
Au flux	3.27 $mg/m^2.s$ or 8.4 × 10-6 $mol/m^2.s$

The obtained laboratory experiment results provide some evidence that the developed processing plant has the potential to be technically feasible if employed in a real-life industrial-scale WPCB recycling operation. This is primarily because Au was recovered with a high yield (95.50 %) following the laboratory experiment investigating the concentration and recovery of Au from a WPCB iodide leachate/ I^--I_2-Au electrolyte solution using the novel IEM-SLE and EW technique. In other words, the results of the laboratory experiment show that the processing plant's key process circuit (concentration-recovery circuit) is technically feasible under the investigated conditions. However, due to the previously described limitations/ drawbacks of the IEM-SLE and EW process employed in the processing plant's concentration-recovery circuit, it is evident that more research and development is required to further improve the developed IEM-SLE and EW process before it can be employed in a real-life industrial-scale WPCB recycling operation in a technically feasible manner. This future research and development should be done in parallel with an economic feasibility study, so as to ensure that the developed processing plant is designed holistically in terms of both technical and economic feasibility.

Chapter 4
Process Development and Process Plant Design

This chapter presents a detailed process description and theoretical process plant outline for a hydrometallurgical processing plant for Au recovery from WPCBs (herein referred to as the processing plant). It is important to note that the development and design of the processing plant was done in parallel with its early-stage technical and economic feasibility assessment (Chapter 3 and 5). An overview of the processing plant's daily mass and energy flows is shown in Figure 4.1.

It must be emphasised that the developed processing plant operates entirely as a batch operation. A batch operation was selected in preference to a continuous operation so that some equipment could be used in multiple steps – e.g., one leaching reactor could be used for all 3-BM leaching stages, one filter press could be used for all solid-liquid separation steps, etc.

4.1 Plant Capacity, Availability, and Operation

Findings from de Waal (2018) and Ghodrat et al. (2016) have illustrated that it could be techno-economically feasible to recover Au from WPCBs when processing plants are operated at a WPCB recycling capacity of 30 kt per annum (ktpa). Based on these findings it was assumed that the processing plant would operate at a WPCB recycling capacity of 30 ktpa. Furthermore, based on international metallurgical industry standards, it was assumed that the processing plant would operate for 340 days per annum, with an 88 % availability (i.e., 300 days for production processing and 40 days for auxiliary processing and maintenance).

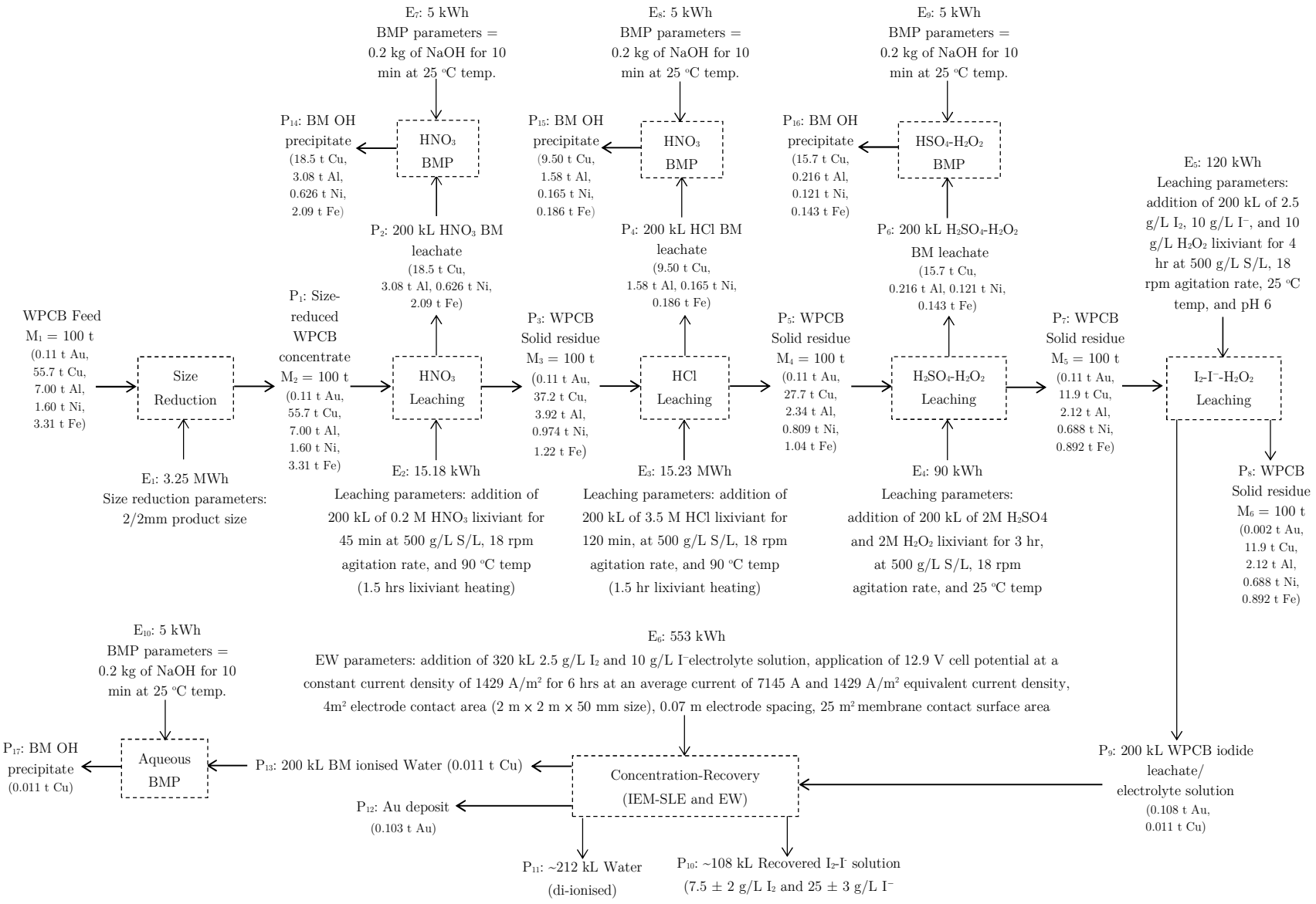

Figure 4.1 Overview of the processing plant's daily mass and energy flow (where BMP = base metal precipitation, E = energy requirement, P = product, and M = mass)

4.2 Feed Composition

It was assumed that the processing plant's WPCB feed composition is equal to the ideal WPCB composition observed prior to the laboratory experiment/ technical feasibility assessment (see Table 3.3.1, Chapter 3). In other words, it was assumed that each 100 t of WPCB feed processed in the processing plant per day is comprised of 0.11 wt.% Au, 55.67 wt.% Cu, 7.00 wt.% Al, 1.60 wt.% Ni, and 3.31 wt.% Fe, as illustrated in Table 4.2.1.

Table 4.2.1 Processing plant's WPCB feed composition

	Au	**Cu**	**Al**	**Ni**	**Fe**
Metal wt.%	0.11	55.67	7.00	1.60	3.31

4.3 Size-Reduction Circuit

Previous studies have provided evidence that successful WPCB size reduction occurs when WPCBs are reduced to an ideal particle size of 2 mm × 2mm (Nekouei et al., 2018; Dias et al., 2019). This evidence was used to design the size-reduction circuit of the processing plant which is herein described and illustrated in Figure 4.3.1.

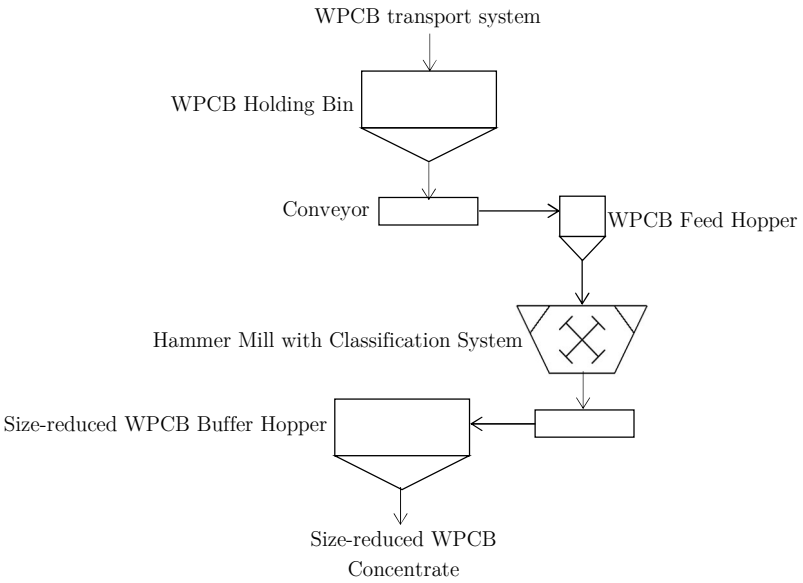

Figure 4.3.1 Processing plant's size-reduction circuit flowsheet

The processing plant's size-reduction circuit was assumed to commence with the introduction of transported WPCBs into a holding bin where they would be stockpiled and thereafter transported into a WPCB feeder hopper via an elevator conveyor belt. WPCBs from the feeder hopper would subsequently be transferred into a hammer mill (with a classification system) where they would be size reduced to the ideal product size of 2 mm/2 mm, without any loss of mass. Finally, the size-reduced WPCB concentrate from the hammer mill would be discharged and directed into a size-reduced WPCB buffer hopper via a conveyor belt.

It was assumed that the processing plant's size-reduction circuit would utilise a hammer mill for 2 hours at a production throughput of 50 t/h to process the required 100 t of WPCB per day.

Tumuluru and Heikkila (2019) studied the size-reduction of bio-composite materials with similar physical characteristics to WPCBs and reported that the energy consumption for hammer milling ranges between 5 and 60 kWh/t. Based on these reported values it was assumed that the processing plant's hammer mill would have an energy demand of 32.5 kWh/t of WPCB. It was also assumed that all energy associated with ancillary equipment such as conveyors is negligible. This is because the energy associated with a hammer mill vastly outweighs that of its associated ancillary equipment.

It has been reported in the literature that WPCB size reduction may result in localised heating and oxidation of volatile organic compounds, which may be released into the environment as a toxic-off gas/ dust. To prevent air pollution from occurring, it was assumed that size-reduction in the processing plant would be executed using an automatic, computer-controlled water injection system, with atomized compressed air to suppress dust and cool volatile organic compounds, so that less hazardous emissions are generated. In this instance, compressed air is injected with water to generate "Cold Steam" which greatly multiplies the water spray surface area. It was assumed that when the hammer mill is at "idle" there would be no wasted water flow. In addition to environmental benefits, the attenuation of toxic off-gas dust formation during WPCB size reduction is beneficial since it prevents Au loss to the environment.

4.4 Leaching Circuit

Investigations by Mecucci and Scott (2002), Jha et al. (2012), Xu et al. (2010), Sahin et al. (2015), Ficeriova et al. (2011), and Batnasan et al. (2019) have provided evidence of high- yield BM and/or Au leaching from WPCBs. This evidence was used to design the processing plant's leaching circuit which is herein described and illustrated in Figure 4.4.1.

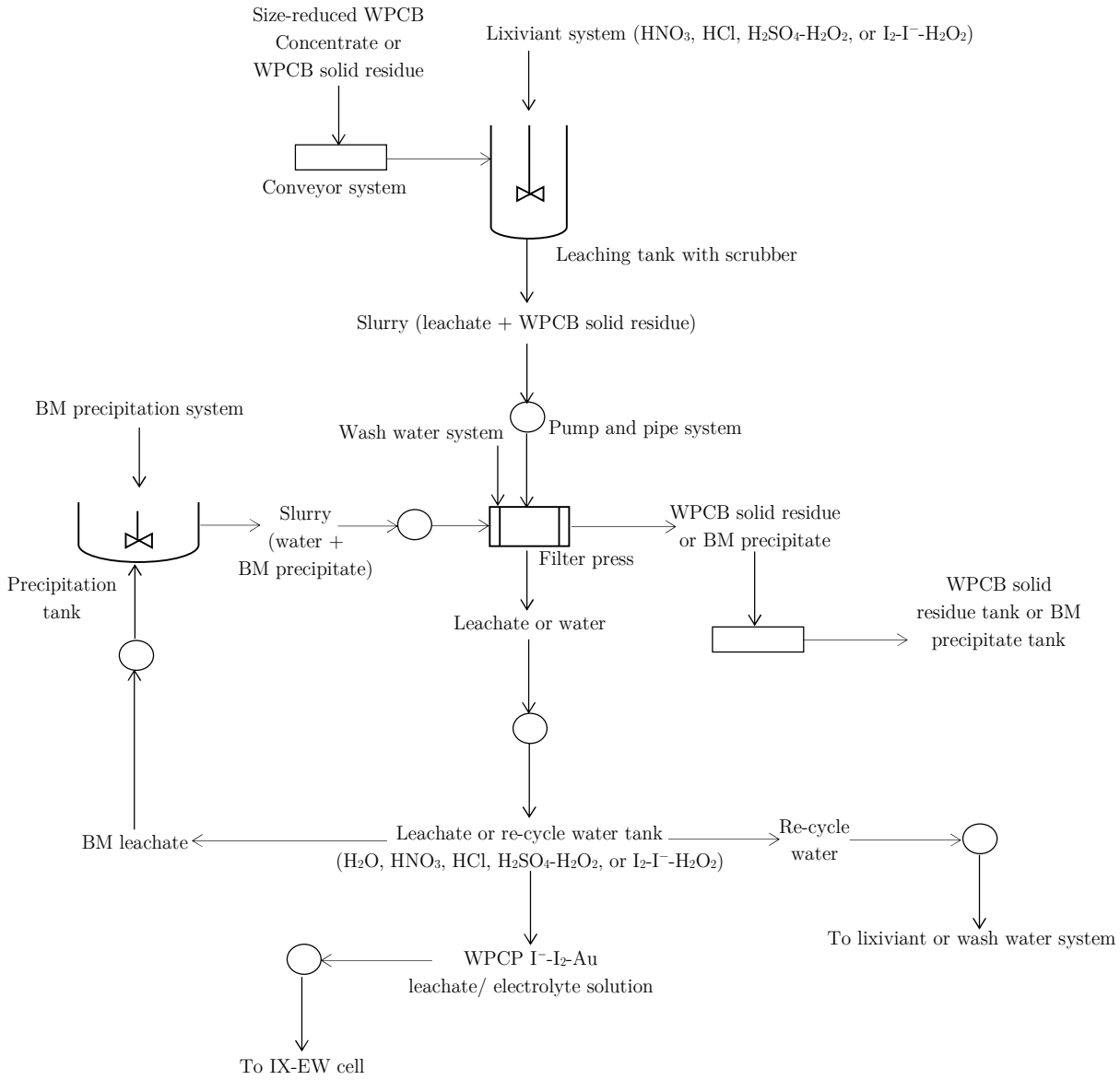

Figure 4.4.1 Processing plant's leaching circuit flowsheet

The processing plant's leaching circuit commences with the use of a conveyor system to transport the size-reduced WPCB concentrate from the buffer hopper (in the size-reduction circuit) to a leaching tank where it is agitated leached using a 0.2 M HNO_3 lixiviant, for 45 minutes, at a S/L ratio of 500 g/L, 18 rpm agitation speed, and 90 ^oC temperature. This HNO_3 leaching stage produces a slurry/pulp comprised of a mixture of NO_3^--BM leachate and size-reduced WPCB solid residue, together with a gas stream consisting of hydrogen and nitrous oxide (NOx) components which are captured by a fume scrubber attached to the leaching tank. The generated NO_3^--BM leachate and size-reduced WPCB solid residue slurry are subsequently pumped into a filter press which separates the WPCB solid residue from the NO_3^--BM leachate. Thereafter, the filtered NO_3^--BM leachate is pumped into an HNO_3 by-product tank, the filtered WPCB solid residue is washed with water to remove excess HNO_3 lixiviant, and the wash water is pumped into an HNO_3 wash water tank where it is stored for use in subsequent HNO_3 leaching cycles. The WPCB solid residue is subsequently conveyed back into the leaching reactor where it is agitated leached using a 3.5 M HCl lixiviant, for 120 min, at a S/L ratio of 500 g/L, 18 rpm agitation speed, and 90 ^oC temperature. This HCl leaching stage produces a slurry comprised of a mixture of Cl^--BM leachate and size-reduced WPCB solid residue, in addition to an HCl gas stream which is captured by the fume scrubber attached to the leaching tank. The produced Cl^--BM leachate and size-reduced WPCB solid residue slurry are subsequently pumped into the filter press which separates the WPCB solid residue from the Cl^--BM leachate. The filtered Cl^--BM leachate is then pumped into an HCl by-product tank, the filtered WPCB solid residue is washed with water to remove excess HCl lixiviant, and the wash water is pumped into an HCl wash water tank where it is stored for use in subsequent HCl leaching cycles. The WPCB solid residue is subsequently conveyed into the leaching reactor where it is agitated leached using a 2M H_2SO_4 and 2M H_2O_2 lixiviant, for 3 hrs, at a S/L ratio of 500 g/L, 18 rpm agitation rate, and 25 ^oC temperature. This H_2SO_4-H_2O_2 leaching stage produces a slurry comprised of a mixture of SO_4^{2-}-BM leachate and size-reduced WPCB solid residue, together with an H_2SO_4-SO_2 gas stream which is captured by the fume scrubber attached to the H_2SO_4-H_2O_2 leaching tank. The SO_4^{2-}-BM leachate and size-reduced WPCB solid residue slurry are thereafter pumped into the

filter press which separates the WPCB solid residue from the SO_4^{2-}-BM leachate. The filtered SO_4^{2-}-BM leachate is thereafter pumped into an H_2SO_4 by-product tank, the filtered WPCB solid residue is washed with water to remove excess H_2SO_4-H_2O_2 lixiviant, and the wash water is pumped into an H_2SO_4 wash water tank where it is stored for use in subsequent H_2SO_4-H_2O_2 leaching cycles. The WPCB solid residue is subsequently conveyed back into the leaching reactor where it is agitated leached using a 2.5 g/L I_2, 10 g/L I^- (in the form of KI), and 10 g/L H_2O_2 lixiviant, for 4 hrs, at a S/L ratio of 500 g/L, 18 rpm agitation rate, 25 °C temperature, and pH of 6. This I^--I_2-H_2O_2 leaching stage produces a slurry comprised of I^--I_2-Au leachate and a size-reduced WPCB solid residue. The I^--I_2-Au leachate and size-reduced WPCB solid residue slurry are then pumped into the filter press which separates the WPCB solid residue from the WPCB I^--I_2-Au leachate. The filtered WPCB I^--I_2-Au leachate is then pumped into a holding tank, the filtered WPCB solid residue is washed with water to remove excess iodide lixiviant, and the wash water is pumped into an iodide wash water tank where it is stored for use in subsequent I^--I_2-H_2O_2 leaching cycles. Finally, the WPCB solid residue is conveyed to a solid residue tank.

It was assumed that subsequent to all 3-BM leaching stages, the BM leachates in the HNO_3, HCl, and H_2SO_4 by-product tanks would be pumped (sequentially) into a precipitation reactor where dissolved BM ions would be precipitated as OH-BM precipitates following the addition of sodium hydroxide (NaOH) which is mixed with the BM leachate for 10 min at a temperature of 25 °C and agitation speed of 18 rpm. In this instance, it was calculated and assumed that the addition of 0.2 kg of NaOH would increase the pH of all solutions from around 3 to >9.5 and thus result in the precipitation of BM impurities contained in the leachates with 100 % yield. Eq.30-34 show the reactions between BM ions and sodium hydroxide to form OH-BM precipitates:

$$Cu^{2+}_{(aq)} + 2OH^-_{(aq)} \rightarrow Cu(OH)_{2(s)} \quad \text{(Eq.30)}$$

$$Fe^{2+}_{(aq)} + 2OH^-_{(aq)} \rightarrow Fe(OH)_{2(s)} \quad \text{(Eq.31)}$$

$$Fe^{3+}_{(aq)} + 3OH^-_{(aq)} \rightarrow Fe(OH)_{3(s)} \quad \text{(Eq.32)}$$

$$Al^{3+}_{(aq)} + 3OH^-_{(aq)} \rightarrow Al(OH)_{3(s)} \quad \text{(Eq.33)}$$

$$Ni^{2+}_{(aq)} + 2OH^-_{(aq)} \rightarrow Ni(OH)_{2(s)} \quad \text{(Eq.34)}$$

It was also assumed that the BM precipitates would be separated from the residual di-ionised water with 100 % efficiency through solid-liquid separation using the filter press. Thereafter, the BM precipitate would be conveyed to a BM solid residue storage tank, while the di-ionised water would be transferred to a storage water tank for use in subsequent process cycles.

Since the processing plant operates as a batch process, a single leaching reactor and scrubber, precipitation reactor, and filter press are used for the relevant processes of its leaching circuit which operate sequentially. It was assumed that the processing plant's filter press and scrubber operate with 100 % efficiency.

Illustrated in Table 4.4.1, the yield/ extent of leaching of Au and BMs (namely Cu, Al, Ni, and Fe) in the respective leaching stages of the full-scale processing plant is assumed to be the same as the metal leaching yields observed during the leachate preparations in the laboratory experiment/ technical feasibility assessment (see Table 3.3.3, Chapter 3).

Table 4.4.1 Processing plant's daily leachate metal compositions

			200 kL leachate metal composition			
		100 t WPCB	HNO_3	HCl	H_2SO_4-H_2O_2	I_2-I^--H_2O_2
Daily leaching metal mass flows (t)	Au	0.11	0.00	0.00	0.00	0.108
	Cu	55.7	18.5	9.50	15.7	0.011
	Al	7.00	3.08	1.58	0.216	0.00
	Ni	1.60	0.626	0.165	0.121	0.00
	Fe	3.31	2.09	0.186	0.143	0.00

Table 4.4.1 assumes that any given 200 kL of WPCB I^--I_2-Au leachate produced in the processing plant per day, would have an Au concentration of 537.8 mg/L (would contain 0.108 t of Au) and Cu concentration of 55.7 mg/L (would contain 0.011 t of Cu).

From the previously described leaching process description, it is evident that to leach 100 t of WPCB per day in the processing plant (as required) at a S/L ratio of 500 g/L, a leaching reactor with a volume > 200 kL is required. Similarly, a precipitation reactor with a >200 kL volume is required to precipitate BMs from ~200 kL leachates. Hence, it was assumed that the processing plant would

utilise a 400 kL Xinhai Minerals Processing EPC SJ8.5x9.0 agitation tank with a scrubber and heating utility as its leaching reactor, and a separate 400 kL Xinhai Minerals Processing EPC SJ8.5x9.0 agitation tank as its precipitation reactor.

An SJ8.5x9.0 tank has an 8.50 m diameter and 9.00 m length, 480 m^3 tank size, 30 kW motor, 3.3 m impeller diameter, and 18.5 rpm impeller speed. Illustrated in Figure 4.4.2, the SJ8.5x9 tank is a double impeller leaching tank including a motor, cycloidal planetary gear speed reducer, bearing block and agitating shaft, and the agitating shaft equipped with a double impeller, from the top view the impeller rotating clockwise, each impeller composed of 4 blades (lined with rubber to prevent corrosion), and the angle of the top blade and the below one is 45 degree.

Figure 4.4.2 SJ8.5x9.0 Tank (Xinhai, n.d.)

A standard leaching reactor like the SJ8.5x9.0 tank has a specified power of 30 kW. Based on this power specification, it was calculated and assumed that the energy demand for leaching and precipitation in the processing plant (assuming a 100 % motor efficiency) would be 313 kWh or 3.13 kWh/t WPCB.

It was assumed that the processing plant's leaching reactor would contain stainless steel immersion heaters with thermocouples for heating lixiviants, during the HNO_3 and HCl BM leaching stages.

Assuming that HNO_3 and HCl lixiviants behave like H_2O (similar weight, heat capacities, etc.), it was determined that 15.2 MWh of energy would be required to heat 200 kL of HNO_3 lixiviant and 15.2 MWh of energy would be required to heat 200 kL of HCl lixiviant. In other words, the processing plant's leaching circuit would have an additional energy demand of 30.3 MWh or 0.303 MWh/t of WPCB for the heating utilities used. Hence, the total energy demand for the processing plant's leaching circuit, including the heating utility used is 30.6 MWh or 0.306 MWh/t of WPCB.

To heat 200 kL of HNO_3 lixiviant and 200 kL HCl lixiviant in the processing plant, 1.5 hrs prior to leaching, it was determined that 10 megawatts (MW) of heating energy should be provided to the lixiviants by the heating utilities/ immersion heaters in the processing plant's leaching reactor (assuming no efficiency loss). It was assumed that the aforementioned heating energy would be provided by 4 separate Sinus Jevi Type D-8800, W 3161-30 immersion heaters, which each supply 2.5 MW of heating energy. An image of a Sinus Jevi Type D-8800, W 3161-30 immersion heater is shown in Figure 4.4.3.

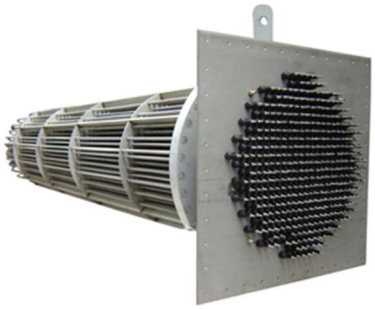

Figure 4.4.3 Sinus Jevi Type D-8800, W 3161-30 immersion heater (sinusjevi, n.d.)

It was assumed that all solid liquid filtration in the processing plant would be performed in an Ishigaki Lasta MC filter press machine (image shown in Figure 4.4.4) which is capable of processing 100 t of solid materials per hour (i.e., since such an Ishigaki Lasta MC filter press would be able to process the required 100 t of WPCB material per day). According to Suez (n.d.), the energy demand for an industrial filter press machine is approximately 25 to 35 kWh/t of suspended solids. Hence, it

was assumed that the use of an Ishigaki Lasta MC filter press in the processing plant would require 30 kWh of power per t of WPCB.

Figure 4.4.4 Ishigaki Lasta MC filter press (Ishigaki, n.d.)

4.5 Concentration-Recovery Circuit

The processing plant's concentration-recovery circuit (which is herein also referred to as the IEM-SLE and EW circuit) utilises a novel process consisting of an IEM-SLE stage for Au concentration, together with a simultaneous EW stage for Au recovery. The integration of an IEM-SLE stage for Au concentration with an EW stage for Au recovery has the potential benefits of Au electroelution from the Au-IEM in the SLE stage. Au electroelution is beneficial since it improves Au ion migration and enhances the breakage of chemical bonds between the functional groups of an Au-IEM and Au ions adsorbed onto the extractant. (Pinto and Martins, 2001)

To design the processing plant's IEM-SLE and EW circuit which is illustrated in Figure 4.5.1 and herein described/outlined, findings from previous work by Free and Moats (2014), van Deventer et al. (2012), Meng et al. (2019), and Batnasan et al. (2019) were used together with the findings from this project's early-stage technical feasibility assessment (i.e., the laboratory experiment results presented in Chapter 3). The project's early-stage technical feasibility assessment revealed that the required flux of Au ions through the Au-IEM in the full-scale processing plant is 3.27 mg/m^2.s or 8.4 $\times$ 10^{-6} mol/m^2.s. As stated in Chapter 3, this flux is comparable to the 5.5 $\times$ 10^{-6} to 14.8 $\times$ 10^{-6} mol/m^2.s Au flux reported by Sun et al. (2020).

Based on the assumption that the processing plant's IEM-SLE and EW circuit was designed to process 1 batch of 200 kL WPCB iodide leachate over a 6-hr plating program per day (with an additional 4 hrs for filling and discharging), it was determined that 2880 m^2 of Au-IEM surface area would be needed to handle the 200 kL of feed WPCB iodide leachate at the required flux. For this reason, it was assumed that Au concentration and recovery in the full-scale processing plant's IEM-SLE and EW circuit would be executed in an IX-EW cell in the form of a modular cell house comprised of 58 repeating units of 1 feed tank (0.14 m internal width and 5 m internal height and length), 2 electrolyte solution tanks hosting a 304 stainless-steel cathode (each with 0.07 m internal width and 5 m internal height and length), and 1 electrolyte solution tank hosting a titanium anode (0.07 m internal width and 5 m internal height and length). It was assumed that the IX-EW cell's tanks would be lined with polypropylene for electrical insulation (Dabbak et al., 2018). 304 stainless steel was the material of choice for most of the IX-EW cell's structural components (e.g., tanks, gaskets, etc.). 304 stainless steel was selected in preference to polymeric materials (e.g., tempered borosilicate glass such as Pyrex) because it is more durable and less at risk of catastrophic fire. (Sander et al., 2020). A titanium basket was selected in preference to a titanium mesh sheet as the anode material for the IX-EW cell since it has a larger surface area available for I_2 recovery. (Hedin and Rohde-Nielsen, 2018).

It was assumed that the IX-EW cell would be completed at both its terminal ends by an electrolyte solution tank hosting a cathode and an electrolyte solution tank hosting an anode. Since the processing plant's IEM-SLE and EW circuit was designed to process 200 kL of WPCB iodide leachate per day, it was assumed that ~ 3.5 m^3 of WPCB iodide leachate would be loaded into each feed tank compartment of the IX-EW cell, while ~1.8 m^3 of I_2-I^- electrolyte solution would be added into each of the electrode hosting compartments. Figure 4.5.3 schematically illustrates the processing plant's IX-EW cell (note that the 3 dotted lines signify repeating units). It was assumed that a Au-IEM with a 25 m^2 contact surface area separates the feed tanks of the IX-EW cell from the other compartments, while an AEM with a 25 m^2 contact surface area separates the electrolyte solution tanks hosting the cathode from the electrolyte solution tanks hosting the anode (akin to the EW cell

used by Meng et al., 2019). The primary difference between the processing plant's IX-EW cell and the EW cell used in Meng et al. (2019) is the presence of a feed tank which is used for Au concentration by IEM-SLE.

The IX-EW cell was designed to utilise an Au-IEM for Au concentration and recovery, and a generic commercial AEM to inhibit H^+ leakage. An Au-IEM was selected in preference to Au-IX extractant resin beads since it offers the advantages of faster ion transport, wider effective pH range, no phase change, and high resistance to osmotic pressure degradation (Fernandes and Warren, 1995). Purogold S992 (produced by Purolite) was selected for use as the IX-EW cell's Au-IEM since it has shown a high resistance to osmotic and thermal shock, good resistance to fouling, high gold loading capacity, and excellent gold loading selectivity. (van Deventer et al., 2012)

It was assumed that each individual tank of the IX-EW cell would be positioned on a stainless-steel pallet installed on a movable pallet track system. This arrangement would allow for easy handling/ separation of these tanks as required for system maintenance (e.g., repairs, membrane replacements, etc.). It was also assumed that the IX-EW cell's cathodes would be attached to a lifting rack connected to an overhead crane for easy handling and transportation (the IX-EW cell's anodes are assumed to undergo cleaning only once a year so connection to the lifting rack is not required).

It has been reported that deformities and misalignment associated with hanger bars could result in the distortion of the IX-EW cell's anode and cathode spacing (Mirza et al., 2016). This could lead to the short-circuiting and reduced service life of the IX-EW cell's electrodes. However, it was assumed that no short circuits are experienced in the processing plant's IX-EW circuit since each electrode is in its own compartment. Based on the EW cell design guidelines provided by Forner et al. (2018), it was assumed that after every 7^{th} process cycle (after 7 days) of Au recovery-deposition in the processing plant's IEM-SLE and EW circuit, the stainless-steel cathodes in the IX-EW cell would be removed using the crane system, and the Au would be manually stripped to recover the deposited Au before the cathodes would be reused in the subsequent process cycles.

The full-scale processing plant's IX-EW cell was designed with the specifications presented in Table 4.5.1 and partially illustrated in Figure 4.5.3. These specifications were carefully selected to ensure that the IX-EW circuit would meet the required daily production capacity (i.e., process 200 kL of WPCB I^--I_2-Au leachate/ electrolyte solution per day). From the specifications presented in Table 4.5.1, it is evident that a 30 m × 30 m floor space would satisfy the processing plant's IX-EW cell's floor space requirements.

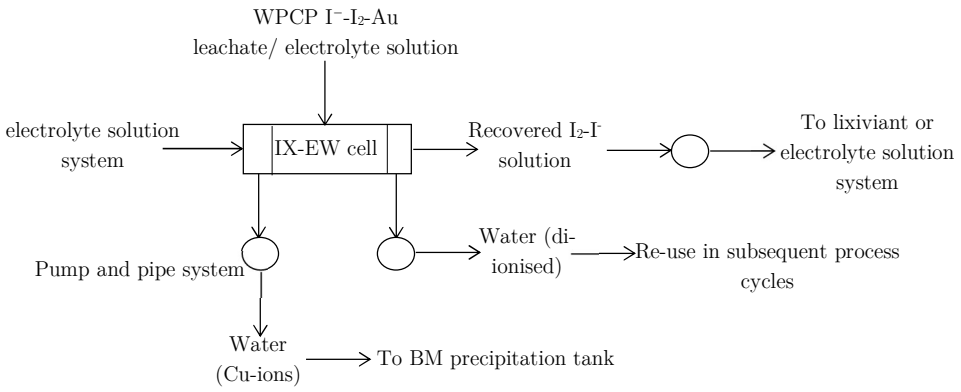

Figure 4.5.1 IEM-SLE and EW circuit flowsheet

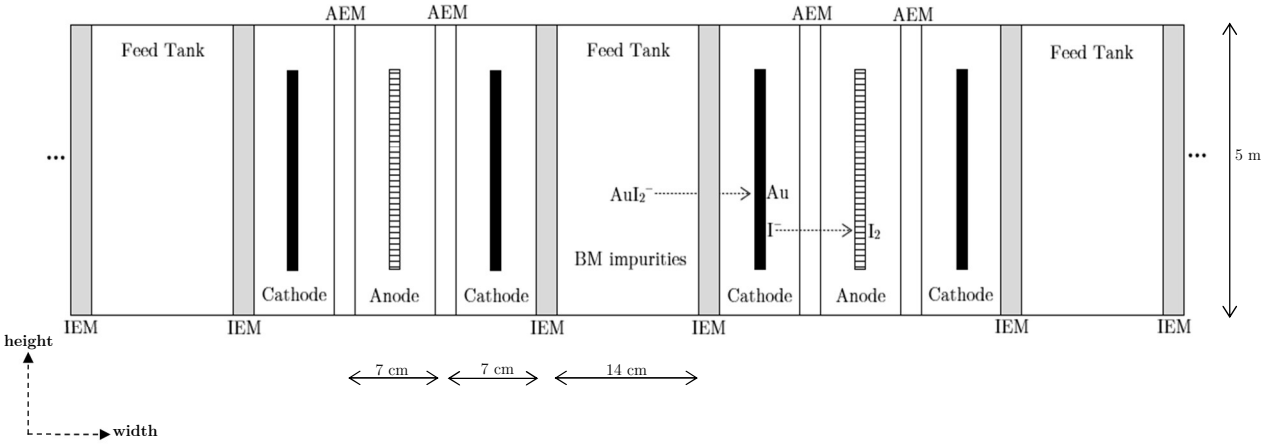

Figure 4.5.2 Schematic illustration of the IX-EW cell

Table 4.5.1 Processing plant's IX-EW cell specifications

	Specification
Tanks	▪ 58 modular feed tanks, each with a 0.14 m internal width and 5 m internal height and length. ▪ 60 modular electrolyte solution tanks hosting an anode, each with a 0.07 m internal width and 5 m internal height and length. ▪ 118 modular electrolyte solution tanks hosting a cathode, each with a 0.07 m internal width and 5 m internal height and length. ▪ ≈ 21 m total internal width for the whole set-up. ▪ Modular tanks are joined together through gaskets welded to the outside of the tanks. Gaskets have a 8 m outside height and length, and a 5 m inside height and length. Gaskets are joined using 8 nut and bolt fasteners (each with a 0.5 m diameter body, 1.5 m length, and 0.6 m diameter head). ▪ Modular tanks have a 5 m × 5 m hole machined through both lateral faces, except the two terminal electrolyte solution tanks hosting an anode, which have a 5 m × 5 m hole machined through a single lateral face.
Electrodes	▪ 4m^2 area (2 m × 2 m × 50 mm) Ti basket anode fabricated from titanium sheets and mesh. ▪ 4m^2 area (2 m × 2 m × 50 mm) stainless-steel plate cathode. ▪ 0.07 m electrode spacing.
Membranes	▪ 116 Au-IEM, each with a 25 m^2 contact surface area. ▪ 118 AEM, each with a 25 m^2 contact surface area.
Solutions	▪ ≈ 3.5 kL (3.5 m^3) of WPCB iodide leachate/ electrolyte solution in each feed tank (≈ 200 kL in total) ▪ ≈ 1.8 kL (1.8 m^3) of I_2-I^- electrolyte solution in each tank hosting a cathode or anode (≈ 320 kL in total). ▪ Solutions are pumped into tanks through an opening located at the top and are discharged through an opening located at the bottom.

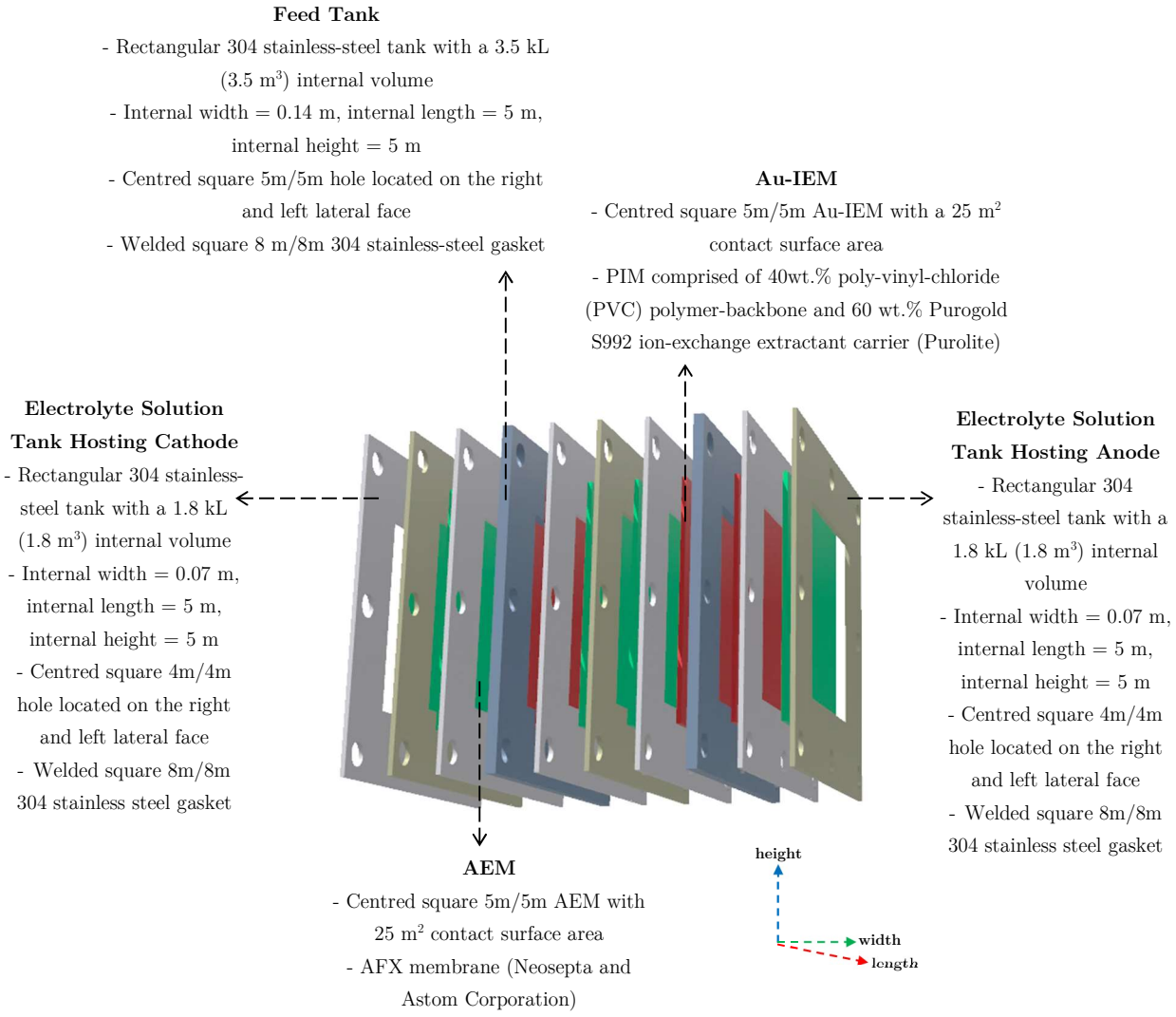

Figure 4.5.3 Visual illustration of the IX-EW cell showing specifications

Au concentration and recovery in the processing plant's IEM-SLE and EW circuit was assumed to commence with the pumping of 200 kL of WPCB I^--I_2-Au leachate/ electrolyte solution from the leaching circuit into the feed tanks of the IX-EW cell. Thereafter, approximately 320 kL of I^--I_2 electrolyte solution with an assumed constant concentration of 2.5 g/L I_2 and 10 g/L I^- would be pumped into each of the electrolyte solution tanks in the IX-EW cell hosting a cathode or anode. Thereafter, through electrical energy supplied to the cathodes and anodes, a constant cell potential

of 12.9 V would be applied to the IX-EW cell for 6 hours at an average current of 7145 A and 1429 A/m^2 equivalent current density (current density was calculated in the laboratory experiment/ technical feasibility assessment in Chapter 3). Hence, it was estimated that the processing plant's IX-EW circuit has an energy demand of 553 kWh or 5.53 kWh/t WPCB or 5.38 kWh/kg Au produced (assuming no loss in efficiency). This Au production energy demand is within the 5 to 15 kWh/kg Au production energy range reported by Kasper et al. (2018) who investigated Au EW from WPCB thiosulphate leachates.

In Section 2.5, it was discussed that the application of an excessively large overpotential during the recovery of Au from electrolyte solutions using the EW technique results in the generation of hydrogen and the formation of hydroxyl ions at the cathode, thus resulting in retarded Au deposition and recovery. It was assumed that excessive overpotentials would be avoided in the IX-EW circuit. It was also assumed that there would be no excess I_3^- in the IX-EW cell feed tank electrolyte solution which may deleteriously impact Au extraction through the Au-IEM. (Zhang et al., 2012)

Based on the results of the processing plant's technical feasibility assessment (Chapter 3), it was assumed that Au would be concentrated and recovered in the IX-EW circuit with a 95.5 % yield. Hence, for a 200 kL WPCB I^--I_2-Au leachate/ electrolyte solution with an assumed Au concentration of 538 mg/L, it was determined that 0.103 t of Au would be recovered.

Illustrated in Figure 4.5.2, it was assumed that BM impurities (which are primarily present in solution as BM cations and BM-I^- anion complexes) are not extracted through the Au-IEM, and as a result, Au is concentrated and recovered in the IX-EW circuit with a >99% purity. The aforementioned assumption is supported by the findings of the technical feasibility assessment/ laboratory experiment results in Chapter 3.

It was assumed that after Au concentration and recovery in the IX-EW circuit, the ~200 kL solution/water in the feed tanks of the IX-EW cell would contain all initial BM ions which were present in the feed WPCB iodide solution (i.e., 0.011 t of Cu). Although the aforementioned

assumption is not strongly supported by the results of the laboratory experiment (which suggests that ~0.004 t of Cu would be adsorbed onto the Au-IEM), the results presented by Van Deventer et al.(2012) suggest that if properly designed and utilised, the processing plant's Au-IEM can avoid Cu adsorption onto its S992 extractant carrier. It was assumed that after Au concentration and recovery in the IX-EW circuit, the ~ 200 kL BM ionised water in the feed tanks would be pumped into the precipitation reactor where it would be mixed with 0.2 kg of sodium hydroxide (NaOH) for 10 min at a temperature of 25 ^{o}C and agitation speed of 18 rpm. It was assumed that the addition of NaOH increases pH from 6 to 9.3 and thus results in the precipitation of the BM impurities contained in the solution with 100 % yield (i.e., precipitation and recovery of 0.011 t of Cu as a hydroxide precipitate). It was also assumed that this BM precipitate would be separated from the feed tank solution with 100 % yield through solid-liquid separation using the filter press. Thereafter, the BM precipitate would be conveyed to the BM solid residue storage tank. While the ~ 200 kL of di-ionised water recovered after BM precipitation and the 212 kL of the di-ionised water recovered from the processing plant's IX-EW cell's electrolyte solution tanks hosting cathode would be used in subsequent process cycles (e.g., for lixiviant or electrolyte solution preparation). Similarly, the ~ 108 kL of recovered iodide solution containing 82 % of initial I_2 and 89 % of initial I^- (i.e., 9.87 g/L I_2 and 42.85 g/L I^- concentration) would also be used in subsequent process cycles, following the addition of I_2, KI, and H_2O for electrolyte solution preparations and following the addition of I_2, KI, H_2O_2, and H_2O for lixiviant preparations.

Chapter 5
Economic Feasibility

This chapter presents and discusses the methodology and results of the processing plant's early-stage economic feasibility assessment (done in terms of a discounted cash flow and profitability (DCFP) assessment) and associated sensitivity analysis.

5.1 Methodology

A key objective of this project (discussed in the aim and objective section in Chapter 1) was to determine the early-stage economic feasibility of the developed processing plant through a DCFP assessment and thereafter determine the sensitivity of the processing plant's DCFP assessment in response to changes in key assumptions used (i.e., determine the sensitivity of the processing plant's economic feasibility in response to changes in key assumptions used in the design and development, and economic feasibility assessment). Though it is fairly simple to appraise the potential economic feasibility of a processing plant in terms of revenue versus cost, it is imperative to consider the time value of money and the influence that substantial up-front capital costs may have (Hitch and Dipple, 2012). For this reason, this project's early-stage economic feasibility assessment was supported by a DCFP assessment over a 10-year project life. This DCFP assessment was done within a South African context, albeit values were reported in US$, at an exchange rate of 15.86 South African Rand to the US$. Values were primarily reported in US$ for ease of comparison when analysing the potential economic feasibility of the processing plant in relation to similar operational processing plants. Furthermore, the US$ is considered the primary reserve currency for the global economy, and as a result, its value in comparison to the South African Rand is presumably better understood by a wider audience. (Kumar, 2014)

This project's DCFP assessment was performed after estimating the costs and benefits associated with the processing plant. The DCFP parameters calculated in this thesis were net present value (NPV), internal rate of return (IRR), profitability indices, and payback period (PBP).

Although DCFP parameters can be used to determine the potential economic feasibility of a processing plant, DCFP parameters will invariably change (with design conditions, economic circumstances, advances in research and development, etc.). Henceforth, all DCFP parameters calculated in this project were subject to a sensitivity analysis which allowed for the examination of deviations from the base case to assess the impact of various input parameters. The sensitivity of each of these input parameters allows for a more accurate appraisal of project value and return, as determined through the calculation of DCFP parameters. (Duening et al., 2015)

The remainder of this section provides the methodology for the DCFP parameters calculated in this project and their key market considerations. Thereafter, the methodology used to estimate the costs and benefits associated with the processing plant is discussed.

5.1.1 Net Present Value (NPV)

Calculated by solving Eq.35, net present value (NPV) is a financial metric which expresses a project's profitability in absolute terms by measuring the difference between the project's total capital investment and net cash flows over a specified duration. (Belli et al., 1996)

$$\text{NPV} = \sum_{t=1}^{N} \frac{C_t}{(1+D)^t} - \text{TCI} \qquad \text{(Eq.35)}$$

where: C_t = net cash flow at time t, t = time of cash flow, N = duration, i = discount rate, and TCI = total capital investment

A positive NPV signifies that a project is potentially economically feasible as it is expected to generate a profit over the specified duration, while a negative NPV indicates that a project is

potentially economically unfeasible as it is expected to result in a loss of profit over the specified duration. (Belli et al., 1996)

5.1.2 Profitability Indices and Pay Back Period (PBP)

Profitability indices are financial metrics which express a project's profitability as a ratio. Profitability indices can be communicated in terms of return on investment (ROI), net margin, or ebitda margin, which are calculated by solving Eq.36, Eq.37, and Eq.38, respectively. (Brigham and Houston, 2012; Lesakova, 2007; Luckham, 1982)

$$\text{ROI} = \left(\left(\frac{\sum_{t=1}^{N}\frac{C_t}{(1+D)^t} - \text{TCI}}{TCI}\right)^{\frac{1}{N}} - 1\right) \times 100 \quad \text{(Eq.36)}$$

$$\text{Net Margin} = \left(\left(\sum_{t=1}^{N}\frac{\frac{C_t}{(1+D)^t}}{R_t}\right)/N\right) \times 100 \quad \text{(Eq.37)}$$

$$\text{Ebitda Margin} = \left(\left(\sum_{t=1}^{N}\frac{\frac{C_t}{(1+D)^t} + \text{I} + \text{T} + \text{D} + \text{A})}{R_t}\right)/\text{N}\right) \times 100 \quad \text{(Eq.38)}$$

where: C_t = net cash flow at time t, t = time of cash flow, N = duration, i = discount rate, TCI = Total capital investment, R_t = annual revenue at time t, I = interest payable, T = taxes payable, D = depreciation, and A = amortization

A project can be considered as potentially economically feasible if its ROI, net margin, and ebitda margin are significantly positive and greater or comparable to that of similar projects in the same industry, as the project is expected to operate efficiently leading to an increase in the likelihood of gaining a sustainable competitive advantage and protecting profits over the long term. However, if a project's ROI, net margin, and ebitda margin are significantly negative or significantly lower than that of similar projects in the same industry, then the project is classified as potentially economically unfeasible and an unfruitful investment, as the project may operate inefficiently and be non-competitive. (Brigham and Houston, 2012; Lesakova, 2007; Luckham, 1982)

The payback period (PBP) is a financial metric which measures the amount of time it takes for an investment to produce cash flows equal to the original investment cost. Projects with short PBPs have a greater potential to be economically feasible and yield a profit for invested capital, while projects with longer PBPs are not only riskier than shorter ones but are also more uncertain. This is because the longer it takes for an investment to earn cash inflows, the more likely it is that the investment will not break even or make a profit. Since most capital expansions and investments are based on estimates and future projections, there is no real certainty as to what will happen to the income in the future. (Brigham and Houston, 2012; Lesakova, 2007; Luckham, 1982)

5.1.3 Financial Considerations

DCFP assessment parameters are directly affected by dynamic market forces, and in particular tax, depreciation, cost of capital, discount rate, and amortisation. This section provides an overview of how these dynamic market forces influenced the calculated DCFP assessment parameters.

Cost of Capital, Discount Rate, and Amortisation

To account for the time value of money when calculating NPV or profitability indices, cash flows used in calculations were discounted at a specific rate which is proportional to the project's cost of capital. The cost of capital for a project is a measure of the minimum return required for that project to justify its capital expenditure and is calculated by summing the project's risk-free rate of return and equity risk premium (Eq.39). The risk-free rate of return for a project refers to the theoretical rate of return for investing in a project with zero risk, while the equity risk premium is the excess return earned by when investing in a project at a return rate over the risk-free rate of return. (Towler and Sinnott, 2012)

$$\text{Cost of Capital} = \text{Risk-Free Rate} + \text{Equity Risk Premium} \tag{Eq.39}$$

In this project, it was assumed that the processing plant has no gearing and would be financed through a debt investment or security, with a 9 % interest rate (0.75 % over the prime South African lending rate as of June 2022), payable annually over a 5-year amortisation period.

As of the end of April 2022, the cost of capital in South Africa for an ungeared company was 17.86 % due to the reported Risk-Free Rate of 9.96 % and Equity Risk Premium of 7.9 % (IEA, n.d.). Hence, this project assumed a cost of capital of 17.86 %, which was used as the base case discount rate.

Tax

As of 1 June 2022, the corporate tax rate in South Africa was a flat rate of 28 %. However, for a company operating in a South African Special Economic Zone (SEZ), there is a reduced corporate tax rate of 15 %. The SEZ tax incentive was introduced into the South African Income Tax Act to promote investment, growth, and job creation in the South African manufacturing industry in the development of designated regions (PWC, n.d.). The qualifying criteria for a company or project to receive SEZ tax incentives in South Africa are as follows (Sars, n.d.):

- company/project must carry out its business in a SEZ that is designated by the Minister of Trade and Industry and approved by the Minister of Finance in consultation with the Minister of Trade and Industry,
- company/project must be incorporated or effectively managed in South Africa,
- company/project must be carrying on business from a fixed place of business within a SEZ,
- at least 90 % of the income of the company or project must be derived from the carrying on of business or provision of services within that SEZ, and
- no more than 20 % of the deductible expenses incurred or 20 % of the income received by or accrued to the company or project are from transactions with connected persons that are residents or with non-residents and those transactions are attributable to a permanent establishment in the Republic of South Africa.

This project assumed that the processing plant would be established in a South African SEZ and would satisfy all of the previously described qualifying criteria – i.e., this project assumed a tax rate of 15 % for the processing plant.

According to the South African Revenue Services, the following charges can be deducted from taxable income as allowable business expenses (Sars, n.d.):

- Business expenses: all outgoings incurred as part of running the business. This includes material and equipment costs, employee costs, administration costs, business rental costs, office supplies, travel, uniforms, wholesale purchase costs for goods resold, financial charges, utilities, legal fees, marketing, and promotion.
- Capital expenses: such as capital equipment, machinery, and renovation costs.
- Start-up expenses: expenditure incurred for business purposes in the period before the commencement of the first year of trade, provided these are expenses that would have qualified as deductible business expenses within the general operation of the business.
- Net operating losses: any losses carried forward from previous years.

Depreciation

Calculated by solving Eq.40, depreciation, in the colloquial sense, is the loss of value of an item. As it pertains to the chemical process industry, depreciation is the loss of value due to the "wear and tear" of the components and facilities of the plant (Turton et al., 2018). It is important to note that this does not include working capital or land. This project used the double declining balance (DDB) depreciation method to estimate the processing plant's depreciation allowance.

The DDB depreciation method is an example of accelerated depreciation schemes which are more economically favourable. This is because, under this depreciation scheme, the earlier years of a plant's life have the greatest cash flow which is worth more than later cash flows due to the time value of money (Ruhmer, 1996).

$$D = 2 \times d \times ABV \quad \text{(Eq.40)}$$

where: D = depreciation allowance, C_d = depreciation rate, and ABV = asset book value

Depreciation decreases tax according to Eq.41 (Ruhmer, 1996).

$$T = (P-D)*t \quad \text{(Eq.41)}$$

where: T = taxes due, P = gross profit, D = depreciation allowance, and t = tax rate

In South Africa, the maximum time frame allowed for the depreciation of new and unused machinery used in a process of manufacture is 4.0 years and the depreciation rate allocated is 40 % in the first year of use and 20 % in the three following years (PWC, n.d.; Sars, n.d.).

5.1.4 Financial Cost Estimations

In order to conduct a DCFP assessment for the processing plant, it was imperative to first determine the processing plant's financial costs and benefits – i.e., annual revenue, total capital investment, and annual production cost.

The processing plant's annual revenue was calculated by estimating the monetary value obtained from selling recovered Au and its associated BM by-products.

The processing plant's total capital investment was calculated using a modified percentage of the delivered equipment cost method (Peter and Timmerhaus, 2003). This method used the processing plant's estimated land cost and building cost together with the total cost of the processing plant's main equipment and ratio factors for a solid-fluid processing plant to estimate direct costs, indirect costs, fixed capital investment, working capital investment, and total capital investment (Table 5.1.1).

The cost of the processing plant's main equipment was obtained from vendor prices and data from literature. Outdated data from literature was updated to the present value using the chemical engineering plant cost index (CEPCI) and Eq.42. Where necessary, the costs of the processing plant's main equipment were adjusted for the required production capacity through Eq.43, using a typical exponent of 0.6 (six-tenths-factor rule). The expected error in the estimation of factored costs is around 10 – 30 %. (Peter and Timmerhaus, 2003)

Cost Item (Present) = Cost Item (Outdated) x CEPCI (Present)/CEPCI(Outdated) (Eq.42)

Cost New Capacity = Cost Old Capacity x (New Capacity/Old Capacity)^0.6 (Eq.43)

Table 5.1.1 Ratio factors for estimating capital investment items of solid-fluid processing plants based on delivered-equipment cost (Peter and Timmerhaus, 2003)

A	**Fixed Capital Investment**	**A1+A2**
A1	**Total Direct Plant Costs**	**1 to 9**
1	Delivered main equipment	C_{ME}
2	Purchased-equipment installation	0.39 C_{ME}
3	Instrumentation & Automation Controls (installed)	0.26 C_{ME}
4	Piping (installed)	0.31 C_{ME}
5	Electrical (Installed)	0.1 C_{ME}
6	Service facilities (installed)	0.55 C_{ME}
7	Land (purchase)	C_L
8	Building (including services*)	C_B
9	Yard improvements	0.12 C_{ME}
A2	**Total Indirect Costs**	**10 to 14**
10	Design, Engineering and Supervision	0.32 C_{ME}
11	Construction Expenses	0.34 C_{ME}
12	Legal Expenses	0.04 C_{ME}
13	Contractors Fee	0.19 C_{ME}
14	Contingency	0.37 C_{ME}
B	**Working Capital**	**0.15TCI**
	Total Capital Investment (TCI)	**A + B**

* Services refer to: Water supply, cooling and pumping, water treatment, water distribution, electric substation, electric distribution, gas supply and distribution, air compression and distribution, refrigeration including distribution, process waste disposal, sanitary waste disposal, communications, raw-material storage, finished-product storage, fire-protection system, and safety installations.

The processing plant's annual production cost was estimated using the guidelines provided by Peter and Timmerhaus (2003). This involved summing together the processing plant's annual:

- direct production cost – total cost of raw materials, waste treatment, utilities, operating labour, direct supervision and clerical labour, maintenance and repairs, operating supplies, patents and royalties, and laboratory charges,
- fixed production cost – total cost of taxes, depreciation, overheads, and

- general production expense – total cost of distribution and sales, administration, and research and development.

Table 5.1.2 Ratio factors for estimating direct production cost, fixed production cost, and general production cost of solid-fluid processing plants (Peter and Timmerhaus, 2003)

C	**Total Direct Production Cost**	**1 to 8**
1	Raw materials and process consumables	$C_{RM\&PC}$
2	Electricity, utility, and by-product management	C_E
3	Operating labour	C_{OL}
4	Direct supervisory and clerical labour	0.18 C_{OL}
5	Maintenance and repairs	0.06 FCI
6	Operating supplies (including fuel)	0.15 (0.06 FCI)
7	Laboratory charges	0.15 C_{OL}
8	Patents and royalties	0.04 ($C_{RM\&PC}$) + C_E + C_{OL} +0.06 FCI +0.15 (0.06 FCI) + 0.15 C_{OL})
D	**Total Fixed Production Costs**	**9 to 10**
9	Insurance	0.029 FCI
10	Plant overhead costs	0.60 (C_{OL} + 0.18 C_{OL} + 0.06 FCI)
E	**Total General Production Costs**	**11 to 12**
11	Administrative costs	0.15 (C_{OL} + 0.18 C_{OL} +0.06 FCI)
12	Product distribution and selling costs	0.13 APC
	Total Annual Production Costs	**C+D+E**

The cost of raw materials and process consumables was obtained from vendors on the basis of the usages and specifications provided in Chapter 4. Operating labour cost was calculated using Eq.44 (Verrett et al., 2020).

Operating labour cost = Number of operating labours x Operating labour salary (Eq.44)

It was assumed that the processing plant is a batch operation with automatic controls. The number of operating labours per process section in a batch operation chemical processing plant with automatic controls is shown in Table 5.1.3 (Seider et al., 2019).

Table 5.1.3 Number of operating labours per process section in a batch operation chemical processing plant with automatic controls (Seider et al., 2019)

Type of process section	Number of operating labours per process section
Fluids processing section	2
Solids-fluids processing	3
Solids processing	4

In addition to being utilised for the calculation of total fixed production cost and general production expense, ratio factors for a solid-fluid processing plant (Table 5.1.2) were used to calculate the cost of direct supervision and clerical labour, maintenance and repairs, operating supplies, patents and royalties, and laboratory charges.

5.2 Results and Discussion

5.2.1 Capital Investment

The estimated start-up cost for the processing plant's equipment is shown in Table 5.2.1. The total start-up cost of equipment (including auxiliary equipment cost, which was assumed to equal 10-20 % of the main equipment cost) was estimated to be $2,839,000. This cost was assumed to account for the cost of fabrication and delivery.

By using the processing plant's total start-up equipment and reagent cost as the delivered main equipment and 100 % value, the total capital investment for the processing plant was estimated to be $20,390,000 as shown in Table 5.2.2. In this sense, the total fixed-capital investment for the processing plant reached a value of $17,330,000 and a working capital value of $3,058,000. The processing plant's calculated total capital investment, working capital, and fixed capital investment cost may be underestimated since the pricing from vendors may have contained some degree of error. This error is expected to be around ± 75 % (Couper et al., 2010).

Table 5.2.1 Processing plant's start-up equipment costs (note, cap. = capacity, ea.= each)

Circuit	Equipment	Cost
Size-reduction circuit main equipment	Elevator conveyor (carbon steel), 200 t/hr cap. (Hebei Taizhe Machinery Equipment Trading)	$8,000
	Hammer mill (with screen), 100 t/hr cap. (Mt. Baker Mining and Metals)	$43,430
	Belt conveyor, 500 t/hr cap. (Henan Baichy Machinery Equipment)	$12,000
	Dust collection and cooling units (Shandong Huayu Metal Materials)	$24,000
Size-reduction circuit auxiliary equipment	Miscellaneous (rails, pipes, etc.)	$8,743
	Holding bin	
	Buffer hopper	
	Feeder hopper	
Leaching circuit main equipment	SJ8.5x9 Leaching tanks × 2 (including backup), 480 m^3 cap. ea. (XinhaiMineral Processing EPC)	$146,800
	SJ8.5x9 Precipitation tanks × 2 (including back up), 480 m^3 cap. ea. (XinhaiMineral Processing EPC)	$146,800
	D-8800 Immersion heaters × 8 (including back up), 2.5 MW cap. ea.(Sinusjevi)	$92,650
	Ishigaki MC Laster filter press, 100 t/hr cap. Ea. (Ishigaki)	$468,800
Leaching circuit auxiliary equipment	Leaching tank scrubbers and miscellaneous equipment (pumps, pipes, etc.)	$171,000
	Leachate and wash water storage tanks	
	Conveyor system	
	Lixiviant, BM precipitation, and wash water systems (preparation tanks, reagent storage units, etc.)	
Recovery circuit main equipment	304 SS assembled IX-EW cell, 520 m^3 total cap. (Inquip Mineral Industry Equipment)	$1,200,000
	Anode (titanium basket, ASTM B265) × 60, 2m/2m/50mm (Hangzhou King Titanium)	$51,600
	Cathode (316 SS sheet) × 118, 2m/2m/50mm (Tongling Huierpu Technology Co., Ltd.)	$70,210
	AEM (AFX) × 116, 5m/5m contact surface area (RisingSun Membrane Technology)	$89,320
	IEM (2709g PVC, 4063g Purogold S992, 135L THF) × 118, 5m/5m contact surface area (Chemanalyst.com, Sunresin New Materials)	$9,440
	DC power supply (30V/10kA) (Guangdong Yibenyuan Power Supply Equipment)	$10,500
Recovery circuit auxiliary equipment	Au melting furnace and miscellaneous equipment (pumps, pipes, etc.)	$286,200
	Electrolyte solution systems (preparation tanks, reagent storage units, etc.)	
	Structural equipment (stainless-steel pallets and track system, lifting rack, overhead crane, nuts, and bolts)	
Total start-up equipment cost = $2,839,000		

Table 5.2.2 Processing plant's total capital investment

	Cost
Total direct costs	**$13,750,000**
Start-up equipment	$2,839,000
Purchased-equipment installation	$1,107,000
Instrumentation & controls (installed)	$738,100
Piping (installed)	$880,100
Electrical (installed)	$283,900
Service facilities[a] (installed)	$1,561,000
100,000 m^2 Land (purchase) [b]	$1,500,000
50,000 m^2 Building,[c] (including services)	$4,500,000
Yard improvements	$340,700
Total indirect costs	**$3,577,000**
Design, engineering, and supervision	$908,500
Construction expenses	$965,300
Legal expenses	$113,600
Contractor's fee	$539,400
Contingency	$1,050,000
Total capital investment (TCI)	**$20,390,000**
Working capital	**$3,058,000**
Fixed capital investment (FCI)	**$17,330,000**

[a]Service facilities required for the processing plant include utility facilities (for water, power, fuel, waste disposal, etc.) and general non-process facilities such as laboratories, offices, food facilities, health and safety facilities, automotive facilities, material loading and handling facilities, etc.

[b], [c]According to the German Federal Ministry for Economic Cooperation and Developments guidelines for environmentally sound WEEE recycling (Dwivedi et al., 2022), a WEEE recycler of capacity of 1 t/day shall require a minimum of 500 m^2 total ground size. On the basis of these guidelines and considering that the processing plant was designed to recycle 100 t/day of WEEE in the form of WPCBs, it was assumed that a total ground size of 50,000 m^2 would satisfy the total ground/ building size requirement for the processing plant and that the processing plant's building would be situated on 100,000 m^2 land. South African property data shows that a $1,500,000 industrial land cost and $4,500,000 industrial building cost is a realistic estimation (anvil property, n.d; allied steel buildings, n.d.)

In terms of cost per t of WPCB, the processing plant's total capital investment was estimated to be $680/t WPCB. This capital investment cost is significantly lower than the $8,741/t WPCB total capital investment reported by Manjengwa (2019b), and the $2,570/t WPCB capital investment reported by Lam et al. (2021), who both investigated the economic feasibility of hydrometallurgical processing plants concerned with Au recovery from WPCBs. It is important to note that costing in

the Lam et al. (2021) processing plant was done in CA$, with conversion to $ (US$) calculated at the average 2021 exchange rate of 1$ = 1.25 CA$.

Some reasons for the lower capital investment of the developed processing plant in comparison to those considered by Manjengwa (2019b) and Lam et al. (2021), include:

- The use of a batch-operation configuration in the developed processing plant, which in comparison to the continuous-operation configuration used in the Manjengwa (2019b) and Lam et al. (2021) processing plants, has a lower equipment cost and thus lower capital investment. In this instance, a batch operation configuration has a lower capital cost since processing equipment can be used in successive processing stages. For example, the developed processing plant uses one leaching reactor for all leaching stages, while the Manjengwa (2019b) and Lam et al. (2021) processing plants require separate leaching reactors for multiple leaching stages.
- The use of capital-intensive physical separation techniques (namely electrostatic and magnetic separation) in the Lam et al. (2021) processing plant, which are not utilised in the developed processing plant. For example, the application of an electrostatic separator in a 100 t/day WPCB processing plant can result in an additional equipment cost of $1,949,000 (cost of 50 t/h electrostatic separator according to Ganzhou Li Ang Machinery Co., Ltd).
- The use of a capital-intensive activated carbon adsorption Au recovery process in the Manjengwa (2019b) processing plant, which was not utilised in the developed processing plant (Au recovery in the developed processing plant is achieved through an IEM-SLE and EW process). The high capital expense of the Manjengwa (2019b) processing plant activated carbon adsorption process can be attributed to the use of a $510,400 ($1,276/ t WPCB) rotary kiln for activated carbon desorption.
- The use of a capital-intensive solvent extraction and electrowinning (SX-EW) process for selective Cu recovery in the Manjengwa (2019b) processing plant, which was not utilised in the developed processing plant (Cu and BM recovery in the developed processing plant is

achieved through a low-cost non-selective hydroxide precipitation process). The SX-EW process used in the Manjengwa (2019b) processing plant has a high capital expense of $915,400 ($2,289/t WPCB), which is primarily driven by the use of an expensive automated Cu cathode stripping machine which costs ~$362,300.

5.2.2 Revenue

In Chapter 4 it was stated that for every 100 t of WPCB treated in the processing plant per day, 0.103 t of Au would be recovered with a >99 % purity. On the consideration that the processing plant was designed to treat 30 kt of WPCB per annum, it was anticipated that 30.8 t of Au would be recovered from the processing plant on an annual basis. Utilising a fixed Au price of $58,920/kg (spot price on 16/06/2022), it was assumed that the 30.8 t of Au recovered from the processing plant per annum would be sold at 90 % of the fixed price of Au, to generate $1,634,000,000 in annual revenue.

Moreover, it was assumed that the BM's recovered as hydroxide precipitates in the processing plant would be sold to downstream BM refineries to increase revenue. As shown in Table 5.2.3, it was calculated (using the assumptions made in Chapter 4) that the processing plant would recover, per annum, a total of 13.1 t of Cu, 1.46 t of Al, 273 t of Ni, and 745 t of Fe as BM hydroxide precipitates. It was assumed that all BM hydroxide precipitate recovered in the processing plant would be sold at 40% of the fixed price of contained Cu, Al, Ni, and Fe since significant downstream processing would be required to selectively recover individual BMs. Utilising a fixed price of $8.14/kg Cu, $2.25/kg Al, $17.81/kg Ni, and $0.12/kg Fe (spot price on 16/06/2022), it was calculated and assumed that the developed processing plant would generate additional annual revenue of $42,720,000 from Cu, $1,318,000 from Al, $1,949,000 from Ni, and $34,820 from Fe. In summary, it was determined that the processing plant generates $1,680,000,000 in revenue per annum.

Table 5.2.3 Processing plant's annual revenue

Metal	Fixed spot price on 16/06/2022	Price used to determine revenue	Recovered mass	Annual revenue
Au	\$58,92/kg	\$53,03/kg	30.8 t	\$1,634,000,000
Cu	\$8.14/kg	\$3.256/kg	13.1 kt	\$42,720,000
Al	\$2.25/kg	\$0.9/kg	1.46 kt	\$1,318,000
Ni	\$17.81/kg	\$7.12/kg	273 t	\$1,949,000
Fe	\$0.12/kg	\$0.05/kg	725 t	\$34,820
Total annual revenue = \$1,680,000,000				

In terms of revenue per t of WPCB, the processing plant's annual revenue was estimated to be \$56,000/t WPCB. The developed processing plant's annual revenue is significantly greater than the \$9,698/t WPCB annual revenue reported by Manjengwa (2019b) and \$6,528/t WPCB annual revenue reported by Birloaga and Veglió (2017), who investigated the economic feasibility of hydrometallurgical processing plants concerned with Au recovery from WPCBs. It is important to note that costing in the Birloaga and Veglió (2017) processing plant was done in €, with conversion to \$ calculated at the average 2017 exchange rate of 1\$ = 0.88 €.

The high annual revenue for the developed processing plant in comparison to those considered by Manjengwa (2019b) and Birloaga and Veglió (2017), can be attributed to the high 0.11 wt.% Au concentration of the developed processing plant's WPCB feed. This Au concentration is significantly higher than the 0.03 wt.% Au concentration of the Manjengwa (2019b) processing plant WPCB feed and 0.02 wt.% Au concentration of the Birloaga and Veglió (2017) processing plant WPCB feed. It is important to note that the high Au concentration of the developed processing plant's WPCB feed is an ideal concentration based on the composition of the model/ideal WPCBs used in the laboratory experiment (Chapter 3), while the low Au concentration of the Manjengwa (2019b) and Birloaga and Veglió (2017) processing plants WPCB feeds are more realistic concentrations based on the use of typical/ non-ideal WPCBs with low Au. An ideal WPCB feed composition was used since the processing plant was designed and developed assuming ideal conditions in most instances (other reasons for the use of ideal/ model WPCBs in this study are discussed in Section 3.3.1).

Hence, on the consideration that the processing plant's annual revenue is dependent on metal recovery from ideal WPCBs with high Au and Cu concentrations, it is expected that the processing plant's annual revenue will decrease if more typical/ non-ideal WPCBs with low Au and Cu concentrations are used. The sensitivity of the processing plant's economic feasibility in response to a decrease in annual revenue is provided in Section 5.2.5.

5.2.3 Production Cost

The estimated energy demand and usage for the various circuits which collectively constitute the processing plant are shown in Table 5.2.4. Using an average South African electricity tariff of \$0.13/kWh (Nersa, 2022), the annual electricity cost for each of the processing plant's circuits was calculated and the sum of the electricity costs for the processing plant's circuits was estimated to be \$287,400/annum. This cost was marked up by 50 % to \$431,100 in order to account for the cost of other utilities (refuse, internet, etc.) and by-product management (WPCB solid residue disposal and BM precipitate handling, etc.). A high by-product management cost is expected considering that the processing plant was designed to produce ≈ 60 t of hazardous WPCB solid residue per day and ≈ 600 kL of acidic wastewater per day. Table 5.2.4 illustrates how the processing plant's leaching circuit is the main contributor to its annual electricity cost. This is primarily due to the use of the Ishigaki LC Laster hydraulic filter press in the processing plant leaching circuit. An alternative would be to use a less energy-intensive gravity filtration system. However, this would result in reduced productivity and increased production costs due to the inferior applied pressure of gravity filtration techniques (Stickland et al., 2016).

Table 5.2.4 Processing plant's electricity cost

	Energy Demand	**Energy Usage/Annum**	**Electricity Cost/ Annum**
Size-reduction Circuit	32.50 kWh/t WPCB	975 MWh	\$126,800
Leaching Circuit	35.0 kWh/t WPCB	1.07 GWh	\$139,000
Recovery Circuit	5.5 kWh/t WPCB	166 MWh	\$21,570
Other			\$143,700
Total electricity cost = \$431,100/annum			

Table 5.2.5 shows the processing plant's estimated $94,500,000/annum raw material cost. This cost assumes that any given WPCB feed treated in the processing plant has a WPCB cost of $3.15/kg. This WPCB cost is the average price for WPCBs in the South African WEEE recycling market, according to Desco Electronic Recyclers. Table 5.2.5 also shows the processing plant's estimated $34,600,000/annum production consumables cost. It was assumed that the processing plant's production consumable cost is the cost of production reagents (lixiviant, electrolyte, and precipitation reagents) which accounts for cost savings from the use of recovered iodide solution and di-ionised water. In Section 4.5 it was assumed that 412 kL of di-ionised water and 108 kL of iodide solution containing 82 % of initial I_2 and 89 % of initial I^- (i.e., 9.87 g/L I_2 and 42.85 g/L I^- concentration) would be recovered in the processing plant after each complete process cycle (per day) and used in subsequent process cycles. This assumption implies that the processing plant recovers and uses in subsequent process cycles 0.156 GL of water, 320 t of I_2, and 1.39 kt of I^-, which results in a $84,690,000/annum cost saving. In summary, the processing plant's total raw material and process consumables cost was estimated to be $129,100,000/annum.

Table 5.2.5 Processing plant's raw material and process consumable cost

		Cost/Annum	**Source**
A. Lixiviant reagents cost	I_2, 150 t	$8,250,000	indmin.com
	I^-, 600 t	$28,800,000	Proto Chemical Industries
	H_2O_2, 4.08 t	$11,380,000	Worldwide Commodities LLC
	HNO_3, 756 t	$1,369,000	pharmacompass.com
	HCl, 7.66 kt	$1,370,000	chemanalyst.com
	H_2SO_4, 39.2 t	$7,890,000	Proto Chemical Industries
	H_2O, 11.8 GL	$711,000	SA Municipal Tariffs (2022)
B. Electrolyte reagents cost	I_2, 240 t	$13,200,000	indmin.com
	I^-, 960 t	$46,080,000	Proto Chemical Industries
	H_2O, 0.096 GL	$284,100	SA Municipal Tariffs (2022)
C. BM Precipitation reagents cost	NaOH, 0.240 t	$1,649	miningchem.co.za
D. Cost savings (recovered iodide solution and water)	I_2, 320 t	- $17,590,000	indmin.com
	I^-, 1.39 kt	- $66,640,000	Proto Chemical Industries
	H_2O, 0.156 GL	- $461,800	SA Municipal Tariffs (2022)
Process consumables cost (A+B+C+D) = $34,600,000/annum			
Raw material cost (WPCB, 30 kt) = $94,500,000/annum			
Total raw material and process consumable cost = $129,100,000/annum			

The processing plant was designed to operate in 3 process sections, namely, a comminution circuit, a leaching circuit, and an IEM-SLE and EW circuit. The processing plant's comminution circuit is a solids processing section and was therefore assumed to require 4 operating labours per shift, as per the guidelines from Table 5.1.3. The processing plant's leaching circuit and IEM-SLE and EW circuit are solids-fluids processing sections and were therefore assumed to require 3 operating labours each, per shift, as per the guidelines from Table 5.1.3. For this reason, it was estimated that the processing plant would require 10 operating labours per shift. Assuming that each day in the processing plant is separated into 3 eight-hour shifts, it was determined that the processing plant would require 30 operating labourers. According to indeed.com, the average salary of a process plant operator in South Africa is $7,270/annum. Hence, the processing plant's total operating labour cost was determined to be $218,100/annum.

Using the processing plant's estimated annual electricity, utility, and by-product management cost, together with the raw material and process consumable cost, operating labour cost, and fixed capital investment cost, the processing plant's production cost was estimated to be $158,300,000/annum as shown in Table 5.2.6. In this sense, total direct production cost reached a value of $136,300,000/annum, total fixed production cost a value of $1,281,000/annum, and total general production cost a value of $20,780,000/annum.

In terms of cost per t of WPCB, the processing plant's annual production cost was estimated to be $5,276/t WPCB. This annual production cost is higher than that reported by Manjengwa (2019b), Lam et al. (2021) and Birloaga and Veglió (2017) who also investigated the economic feasibility of hydrometallurgical processing plants concerned with Au recovery from WPCBs. The Manjengwa (2019b) processing plant has an $18,408/t WPCB annual production cost, the Lam et al (2021) processing plant has a $3,881/t WPCB annual production cost, while the Birloaga and Veglió (2017) processing plant has a $2,439/t WPCB annual production cost.

Table 5.2.6 Processing plant's production cost

	Cost/Annum
Total direct production cost	**$136,300,000**
Raw materials and production consumables	$129,100,000
Electricity, utility, and by-product management	$431,100
Operating labour	$218,100
Direct supervisory and clerical labour	$39,260
Maintenance and repairs	$1,040,000
Operating supplies (including fuel)	$156,000
Laboratory charges	$32,720
Patents and royalties	$5,241,000
Total fixed production cost	**$1,281,000**
Insurance	$502,600
Plant overhead costs	$778,300
Total general production cost	**$20,780,000**
Administrative costs	$194,574
Product distribution and selling costs	$20,580,00
Total annual production costs	**$158,300,000**

Some reasons for the higher annual production cost of the developed processing plant in comparison to those considered by Manjengwa (2019b), Lam et al. (2021), and Birloaga and Veglió (2017), include:

- Processing plant configuration differences. The use of a two-stage leaching process in the Lam et al. (2021) and Birloaga and Veglió (2017) processing plants (Fe^{3+}-HCl-$FeCl_3$ BM leaching followed by thiosulphate Au leaching in Lam et al., 2021 and H_2SO_4-H_2O_2 BM leaching followed by thiourea Au leaching in Birloaga and Veglió, 2017), which operates with a lower quantity of lixiviant and lower cost lixiviant reagents in comparison to the 4-stage leaching process used in the developed processing plant (HNO_3, HCl, and H_2SO_4-H_2O_2 BM leaching followed by iodide Au leaching). For example, the Lam et al. (2021) processing plant operates with 118.3 L of lixiviant per t WPCB for BM leaching, whereas the developed processing plant uses a total of 6.00 kL L of lixiviant per t WPCB for BM leaching. Furthermore, the lower lixiviant cost of the Lam et al. (2021) and Birloaga and Veglió (2017)

processing plants in comparison to the developed processing plant can be related to the low reagent cost of thiosulphate and thiourea lixiviants in contrast to iodide lixiviants. The use of lower quantities of lixiviant reagents for leaching results in a lower annual production cost due to decreased by-product management cost since less by-product wastewater is generated, while the use of lower-cost lixiviant reagents results in a lower annual production cost due to decreased process consumables cost.

- Inflationary production costs increase over time. The Lam et al. (2021) and Birloaga and Veglió (2017) processing plants were designed in an earlier period in comparison to the developed processing plant. Hence, it is expected that the production cost of the developed processing plant would have increased over-time due to the inflationary increase in the cost of labour, raw materials, process consumables, electricity, utilities, etc.
- Geographical production cost differences. Geographical production cost differences are expected since Lam et al. (2021) and Birloaga and Veglió (2017) processing plants were designed to operate in Canada and Europe respectively, while the developed processing plant was designed to operate in South Africa.
- Higher operating labour cost. The Manjengwa (2019b) processing plant has an operating labour cost of $406,000 or $1,015/t WPCB which is significantly higher than that of the developed processing plant's $218,100 or $7.27/t WPCB operating labour cost.

5.2.4 Discounted Cash Flow and Profitability (DCFP) Assessment

Subsequent to the estimation of total capital investment, annual revenue, and annual production cost, the processing plant's base case NPV, ROI, net margin, ebitda margin, and PBP was estimated as shown in Table 5.2.7.

The processing plant's NPV was estimated to be $5,812,000,000 at a bond interest rate of 9 %, a cash flow discount rate of 17.86 %, and a corporate tax rate of 15 %. While the processing plant's ROI, PBP, net margin, and ebitda margin were estimated to be 76.0 %, 0.03 years, 34.74 % and 48.37 %, respectively.

Table 5.2.7 Processing plant's discounted cash flow and profitability assessment results

Year	**1**	**2**	**3**	**4**	**5**	**6**	**7**	**8**	**9**	**10**
Depreciation rate	0.4	0.2	0.2	0.2	0	0	0	0	0	0
Asset Book Value	$2,839,000	$567,800	$340,700	$204,400	$122,600	$0	$0	$0	$0	$0
Depreciation allowance	$2,271,000	$227,100	$136,300	$81,760	$0	$0	$0	$0	$0	$0
Revenue/ annum	$1,680,000 000	$1,680,000,000	$1,680,000,000	$1,680,000,000	$1,680,000,000	$1,680,000,000	$1,680,000,000	$1,680,000,000	$1,680,000,000	$1,680,000,000
Production cost/annum	$158,300,000	$158,300,000	$158,300,000	$158,300,000	$158,300,000	$158,300,000	$158,300,000	$158,300,000	$158,300,000	$158,300,000
Bond repayments/annum	$5,242,000	$5,242,000	$5,242,000	$5,242,000	$5,242,000	$0	$0	$0	$0	$0
Bond interest/annum	$1,164,000	$1,164,000	$1,164,000	$1,164,000	$1,164,000	$0	$0	$0	$0	$0
Taxable Revenue	$1,518,000,000	$1,520,000,000	$1,520,000,000	$1,520,000,000	$1,521,000,000	$1,522,000,000	$1,522,000,000	$1,522,000,000	$1,522,000,000	$1,522,000,000
Tax rate	15%	15%	15%	15%	15%	15%	15%	15%	15%	15%
Tax Paid	$227,700,000	$228,100,000	$228,100,000	$228,100,000	$228,100,000	$228,300,000	$228,300,000	$228,300,000	$228,300,000	$228,300,000
Net Cash Flow	$1,291,000,000	$1,292,000,000	$1,292,000,000	$1,292,000,000	$1,292,000,000	$1,293,000,000	$1,293,000,000	$1,293,000,000	$1,293,000,000	$1,293,000,000
Discount Rate	17.86%	17.86%	17.86%	17.86%	17.86%	17.86%	17.86%	17.86%	17.86%	17.86%
Discounted Cash Flow	$1,095,000,000	$930,300,000	$789,400,000	$669,800,000	$568,300,000	$482,600,000	$409,400,000	$347,400,000	$294,700,000	$250,100,000
Net Present Value = $5,812,000,000			**Net Margin = 34.74**		**ROI = 76.00**		**PBP = 0.03**		**Ebitda Margin = 48.37**	

In summary, due to the processing plant's short PBP and large positive NPV, ROI, net margin, and ebitda margin, it was inferred that the processing plant has a high economic feasibility potential under the ideal specified plant design conditions.

For comparison, the processing plant's NPV is economically more viable than the Manjengwa (2019b) processing plant's reported -$43,660,000 NPV. This can be attributed to the developed processing plant's higher annual revenue/t WPCB, lower capital investment/t WPCB, and lower annal operating cost/t WPCB.

Illustrated in Table 5.2.8, the processing plant's ROI, net margin, and ebitda margin are more economically viable in comparison to the 5-year average ROI, net margin, and ebitda margin of Umicore, Boliden, and SIMS, the world's largest stakeholders concerned with Au recovery from WPCBs (Inv, n.d.).

Table 5.2.8 Comparison of processing plant's profitability indices with alternative projects (Inv, n.d.)

	This work	Umicore	Boliden	SIMS
ROI	76.00%	8.12%	13.23%	4.24%
Net Margin	34.74%	1.84%	12.77%	1.78%
Ebitda Margin	48.37%	6.51%	19.64%	14.01%

The variance in Table 5.2.8 could be attributed to the observation that Umicore, Boliden, and SIMS utilise pyrochemical processes during Au recovery operations, which require high capital investments and have high operating costs. This is primarily because these pyrochemical processes require high-priced machinery (for example, blister furnaces which can be used for WPCB smelting can cost over 30 million US$), demand excessive amounts of energy (1.39 GJ of energy is required to smelt 1.00 t of WPCBs), and require the use of expensive copper and/or precious metal-rich concentrates (which on average cost around 60 US$/t) (Nekouei et al., 2018; Dias et al., 2019; Gurgul et al., 2017; Park and Fray, 2009; Hall and Williams, 2007; Alvarado et al., 2002). Furthermore, Umicore, Boliden, and SIMS operations are also concerned with less profitable business activities such as WEEE waste

management and are based in North American and European countries which in comparison to South Africa have higher production costs (due to the higher cost of labour, land, etc.).

5.2.5 Sensitivity Analysis

As stated in Section 1.4, a limitation of the present work is that the assumptions used in the processing plant's early-stage economic feasibility assessment are based on an ideal economic model, and an ideal processing plant condition designed and developed using experimental findings obtained under ideal conditions. To reduce the impact of the aforementioned limitation on the findings of this work, the sensitivity of the processing plant's economic feasibility in response to changes in key assumptions used is investigated through a sensitivity analysis.

The processing plant's assumed 15% base case corporate tax rate is based on the assumption that the plant would be located inside a South African SEZ. Hence, the processing plant's corporate tax rate can be expected to increase if the processing plant is commissioned outside a South African SEZ. To evaluate the effect of increasing corporate tax rate on the sensitivity of the processing plant's economic feasibility, the processing plant's assumed 15% base case corporate tax rate was increased to 28 % (current South African corporate tax rate for a company outside a SEZ) in sensitivity analysis condition 1 and 33 % (maximum historical corporate tax rate in South Africa) in sensitivity analysis condition 2.

The processing plant's assumed 17.86 % base case discount rate and assumed 9 % base case bond interest rate are based on the assumption that the processing plant has a cost of capital for an ungeared company in South Africa (as of the end of April 2022). Hence, the processing plant's discount rate can be expected to increase due to a rise in market risk, which may be driven by an increase in the inflation rate or exchange rate, and by a decrease in the Au market price. While the processing plant's bond interest rate can be expected to increase if the national repurchase rate is raised. To evaluate the effect of increasing discount and bond interest rate on the sensitivity of the processing plant's economic feasibility, the processing plant's 17.86% base case discount rate was

increased to 19 % (sensitivity analysis condition 1) and 21 % (sensitivity analysis condition 2), while the assumed 9 % base case bond interest rate was increased by 50 % (sensitivity analysis condition 1) and 100 % (sensitivity analysis condition 2).

The processing plant's assumed $20,390,000 base case total capital investment was estimated using a modified percentage of the delivered equipment cost method (Peter and Timmerhaus, 2003), which used the processing plant's estimated land cost and building cost together with the estimated total cost of equipment. Hence, the processing plant's total capital investment can be expected to increase with a rise in land cost, building cost, and/or equipment cost. Equipment cost increases can occur as a result of an increase in inflation or freight charges and an increase in equipment manufacturing costs (which may be driven by an increase in material prices, labour costs, etc.). While the cost of land and buildings typically increases due to a rise in inflation or increased demand. To evaluate the effect of increasing total capital investment on the sensitivity of the processing plant's economic feasibility, the processing plant's assumed $20,390,000 base case total capital investment was increased by 50 % (sensitivity analysis condition 1) and 100 % (sensitivity analysis condition 2).

The processing plant's assumed $158,300,000 base case annual production cost was estimated using the guidelines provided by Peter and Timmerhaus (2003). As specified in Section 5.1.4, this method involved estimating total annual direct, fixed, and general production costs, by using the processing plant's estimated cost of raw materials and production consumables (lixiviant, electrolyte, and precipitation reagents), cost of electricity, utility, and by-product management, and cost of operating labour. Hence, the processing plant's annual production cost can be expected to increase with an increase in the cost of raw materials and production consumables, cost of electricity, utility, and by-product management, and cost of operating labour. The cost of raw materials and production consumables, and the cost of electricity, utility, and by-product management can increase as a result of increased demand or reduced supply and/or availability. While the cost of operating labour can increase with changes in national policies such as an increase in minimum wage or payroll tax. To evaluate the effect of increasing annual production cost on the sensitivity of the processing plant's

economic feasibility, the processing plant's assumed $158,300,000 base case annual production cost was increased by 50 % (sensitivity analysis condition 1) and 100 % (sensitivity analysis condition 2).

The processing plant's assumed $1,680,000,000 base case annual revenue is primarily comprised of the revenue derived from the sale of recovered Au (this constitutes over 97 % of the processing plant's annual revenue). In this instance, the quantity of Au recovered is thus dependent and based on the assumption that all WPCBs treated in the processing plant contain 0.11 wt.% Au and are leached, concentrated, and recovered with the same yields observed experimentally. According to various researchers, the concentration of Au in typical/ non-ideal WPCBs is between 0.01 wt.% and 0.02 wt.% (Menetti & Tenorio, 1995; Iji & Yokoyama, 1997; Veit et al.,2002; Creamer et al., 2006; Das et al., 2009; Yoo et al., 2009; Guo et al., 2011; Bizzo et al., 2014). Hence the processing plant's annual revenue can be expected to decrease with the use of non-ideal WPCBs, due to a reduced Au concentration resulting in less Au being available for leaching, concentration, and recovery in the processing plant. To evaluate the effect of decreasing annual revenue on the sensitivity of the processing plant's economic feasibility, the processing plant's base case annual revenue was decreased by lowering the estimated and assumed WPCB feed Au concentration to 0.02 wt.% in sensitivity analysis condition 1 and 0.01 wt.% in sensitivity analysis condition 2.

Table 5.2.9 presents the corporate tax rate, bond interest rate, total capital investment, annual production cost, and annual revenue used in the processing plant's sensitivity analysis. For comparison, Table 5.2.10 also presents the processing plant's base-case corporate tax rate, bond interest rate, total capital investment, annual production cost, and annual revenue.

Table 5.2.9 Corporate tax rate, discount rate, bond interest rate, total capital investment, annual production cost, and annual revenue used in the processing plant's sensitivity analysis

	Base case condition	**Sensitivity analysis condition 1**	**Sensitivity analysis condition 2**
Corporate tax rate	15%	28%	33%
Discount rate	17.86%	19%	21%
Bond interest rate	9%	14%	18%
Total capital investment	$20,390,000	$30,585,000	$40,780,000
Annual production cost	$158,300,000	$237,500,000	$316,600,000
Annual revenue	$1,680,000,000	$342,800,000	$194,400,000

Table 5.2.11 shows the results of the processing plant's sensitivity analysis. These results are the processing plant's economic feasibility assessment/ DCFP parameters (NPV, ROI, ebitda margin, net margin, and PBP) obtained using the sensitivity analysis condition 1 or 2, corporate tax rate, bond interest rate, total capital investment, annual production cost, and annual revenue.

Table 5.2.10 Processing plant's sensitivity analysis results

	Base case condition	**Sensitivity analysis condition 1**	**Sensitivity analysis condition 2**
NPV	$5,812,000,000	$290,700,000	-$407,500,000
ROI	76.00%	25.26%	No return
Ebitda Margin	48.37%	18.32%	-38.67%
Net Margin	34.74%	9.37%	-18.86%
PBP	0.03 years	0.95 years	No payback

To determine relative sensitivities and thus establish which key assumption used in the developed processing plant's economic feasibility assessment results in the largest change/sensitivity, the developed processing plant's corporate tax rate, bond interest rate, total capital investment, annual production cost, and annual revenue was varied one factor at a time, by a -90 to 100 percentage change. The resulting change in the processing plant's NPV was plotted vs the percentage change in a variable as shown in Figure 5.2.1.

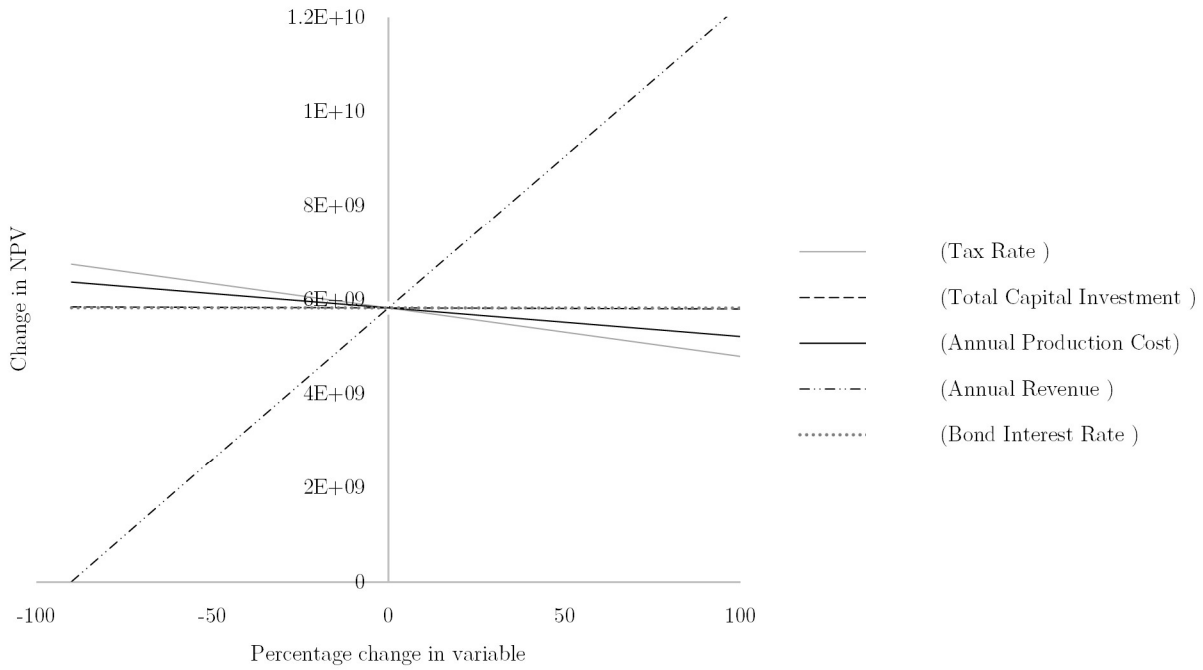

Figure 5.2.1 Change in processing plant's NPV vs percentage change in variable

In terms of the processing plant's early-stage economic feasibility sensitivity analysis, unfavourable outcomes were observed in sensitivity analysis condition 2. This is because, under the aforementioned condition, the processing plant has a negative NPV, ebitda margin, and net margin, while its initial capital investment is not paid back and does not yield a ROI. In contrast, the processing plant remained economically feasible in sensitivity analysis condition 1, however, economic feasibility decreased significantly from the base case condition.

In terms of relative sensitives, the plot of the developed processing plant's NPV vs percentage change in a variable (namely, corporate tax rate, bond interest rate, total capital investment, annual production cost, and annual revenue) shows that key assumptions relating to annual revenue are the most critical (seen by the significantly larger slope compared to that of other variables) towards the processing plant's economic feasibility since they result in the largest change/sensitivity in NPV. Key assumptions relating to annual revenue are also expected to result in the largest change/sensitivity in other DCFP parameters such as ROI, ebitda margin, net margin, and PBP

(since for example a significant increase in NPV implies that a project is more profitable and as a result has an increased ROI, ebitda margin, and net margin).

As previously discussed, the developed processing plant's annual revenue is primarily dependent on WPCB feed Au concentration since this affects how much Au can be recovered and sold to generate most of the processing plant's revenue. Over time, the Au concentration in WPCBs is likely to occur in response to technological advancements in EEE which results in the miniaturisation of contained PCBs and/or micro-plating of Au in these EEE (this results in a reduced Au concentration in the WPCBs produced when these modern-day EEEs have become obsolete). Furthermore, as discussed in Section 5.2.2, the processing plant's annual revenue is primarily based on Au recovery from ideal WPCBs with a high Au and Cu concentration. Therefore, it is expected that the processing plant's annual revenue will decrease if more typical/ non-ideal WPCBs with low Au and Cu concentrations are used. Hence, in a real-life setting, it is expected that the processing plant's annual revenue will decrease with the use of typical/ non-ideal WPCB feeds with low Au and Cu concentration, and/or decrease over time due to reduced WPCB feed Au concentration.

Considering that the sensitivity analysis condition 2 evaluated a more realistic WPCB feed Au concentration of 0.01 wt.%, it can be presumed that the processing plant is likely to be economically unfeasible for industrial-scale application in a real-life setting since the annual revenue obtained from the recovery of Au and BMs from typical/ non-ideal WPCBs is unlikely to result in payback or produce a large positive NPV, ROI, ebitda margin, or net margin.

Based on the results of the sensitivity analysis, it was inferred that the processing plant's economic feasibility is highly sensitive to the key assumptions used in the design and development, and economic feasibility assessment, and in particular assumptions relating to annual revenue. Therefore, any future research and development should carefully review and ensure that any assumptions used are as accurate as possible and that the estimated annual revenue is correctly estimated over the processing plant's life cycle.

Chapter 6
Conclusions and Recommendations

The primary aim of this project was to contribute knowledge to the development of a hydrometallurgical processing plant for Au recovery from WPCBs which utilises a non-toxic and recyclable iodide lixiviant for Au leaching and has the potential to be applied in real-life industrial-scale WPCB recycling operations in a technically and economically feasible manner. Presented in the following chapter are the conclusions and recommendations concerning each of the objectives set to achieve the project aim.

Objective 1 – *Using findings from literature, develop a conceptual process and theoretical process plant outline for a hydrometallurgical processing plant for Au recovery from WPCBs which utilises a non-toxic and recyclable iodide lixiviant for Au leaching.*

Presented in Chapter 4, results from previous literature were used to successfully design a theoretical hydrometallurgical processing plant for Au recovery from WPCBs with utilises a non-toxic and recyclable iodide lixiviant for Au leaching and the novel IEM-SLE and EW technique for Au concentration and recovery. Comprised of a size-reduction, leaching, and concentration-recovery circuit, the developed processing plant was designed to:

- Operate at a capacity of 30 kt WPCB per annum, for 340 days per annum, with an 88 % availability (i.e., 300 days for production processing and 40 days for auxiliary processing and maintenance).
- Recover Au from ideal/ model WPCB feeds with a high 0.11 wt.% Au concentration and high 55.7 wt.% Cu concentration.

- Operate with a size-reduction circuit with a 32.5 KWh/t WPCB energy demand, leaching circuit with a 35.0 KWh/t WPCB energy demand, and concentration-recovery circuit with a 5.5 KWh/t WPCB energy demand.
- Produce WPCB particulate with a final product size of >2mm/2mm using a hammer mill.
- Leach 100 t of WPCB particulate per day at a 500 g/l solid to liquid ratio and 18 rpm agitation speed using a 0.2 M HNO_3 lixiviant at 90 ^oC for 45 min, 3.5 M HCl lixiviant at 90 ^oC for 120 min, 2 M H_2SO_4 and 2 M H_2O_2 lixiviant at 25 ^oC for 3 hrs, and 2.5 g/L I_2, 10 g/L I^-, and 10 g/L H_2O_2 lixiviant for 4 hrs at 25 ^oC temperature and pH of 6.
- Produce 200 kL of WPCB iodide leachate per day with an Au concentration of 0.108 t and a Cu concentration of 0.011 t.
- Produce Au-laden cathodes containing 0.103 t of >99 % Au per day, through the use of the IEM-SLE and EW technique at a 12.9 V cell potential at a constant current density of 1429 A/m^2 for 6hrs at an average current of 7145 A and 1429 A/m^2 equivalent current density, $4m^2$ electrode contact area (2 m × 2 m × 50 mm size), 0.07 m electrode spacing, 25 m^2 membrane contact surface area, and 6 hrs plating time.
- Recycle/ recover iodide solution with an 82 % I_2 recovery yield and 89 % I^- recovery yield.
- Use recycled iodide solution (with 9.87 g/L I_2 and 42.85 g/L I^- concentration) and water in subsequent process cycles.

The designed processing plant has the following limitations:

- ~4 % of Au is lost to the Au-IEM during concentration and recovery in the IEM-SLE and EW circuit. Au loss in a real-life industrial scale setting results in a loss of economic value due to reduced revenue.
- The processing plant's IEM-SLE and EW process uses a high cell voltage (12 V) and has a long EW time (6 hrs). In a real-life industrial-scale setting, applying such a high voltage for such a long duration can cause premature failure of electrical components due to overheating.

- The processing plant is only concerned with the selective recovery of Au and not any other metal. In a real-life industrial-scale setting, this may result in the loss of economic value which could be obtained from the recovery and sale of other economically valuable metals contained in WPCBs.
- The processing plant is designed to process only ideal WPCBs with high Au and Cu concentrations. As evidenced by the results of the sensitivity analysis, the processing plant is likely to be economically unfeasible for industrial-scale application in a real-life setting if non-ideal WPCBs are used.

The designed processing plant can be improved through the:

- Inclusion of additional process operations which are focused on the recovery of economically valuable metals such as Pd, Pt, or rare earth elements, which may be contained in the processing plant's WPCB feed, and/or the inclusion of additional process operations which are focused on the selective recovery of individual BMs. These additional process operations which may utilize various hydrometallurgical techniques such as adsorption, chelation, ion exchange, precipitation, and solvent extraction, could increase the processing plant's revenue through the sale of additionally recovered metals.
- Optimisation of the processing plant's IX-EW cell configuration and key operating conditions in the processing plant's leaching circuit and/or IEM-SLE and EW circuit (e.g., time, temperature, lixiviant concentration, current density, cell voltage, etc.). The optimisation of IX-EW cell configuration and operating parameters may result in a decreased operational cost for the processing plant due to energy savings, reagent savings, etc.
- Investigating the feasibility of using recovered water and iodide solution over multiple process cycles. These investigations will enable a more refined understanding of the processing plant's design and economics.

It is important to note that the aforementioned processing plant improvements were not attempted since this fell beyond the scope of the present work.

Objective 2 - *Determine the early-stage technical and economic feasibility of the processing plant, and thereafter determine whether or not the developed processing plant justifies further research and development for future application in real-life industrial-scale WPCB recycling operations.*

The processing plant's initial or early-stage technical feasibility assessment was supported by a laboratory experiment investigating the recovery of Au from WPCB iodide leachates using the IEM-SLE and EW technique. This experiment was successfully completed, with results presented in Chapter 4. Results of the laboratory experiment demonstrated that the recovery of Au from WPCB iodide leachates using the IEM-SLE and EW technique is technically feasible since it was possible to concentrate and recover Au under the given conditions with a high yield (95.5 %). However, due to the high voltages applied, and due to the loss of Au to the Au-IEM (~4 %), it is evident that more research and development is required to optimise the developed processing plant before it can be subjected to a thorough technical and/or economic feasibility assessment, for application in a real-life industrial-scale WPCB recycling operation, in a technically and economically feasible manner.

Through a discounted cash flow and profitability (DCFP) assessment, the early-stage economic feasibility of the processing plant was successfully determined within a South African context. Presented in Chapter 5, the results of the DCFP assessment showed that the processing plant's NPV was estimated to be $5,812,000,000 at a bond interest rate of 9 %, a cash flow discount rate of 17.86 %, and a corporate tax rate of 15 %. While the processing plant's ROI, PBP, net margin, and ebitda margin were estimated to be 76.00 %, 0.03 years, 34.74 % and 48.37 %, respectively. Due to the processing plant's short PBP and large positive NPV, ROI, net margin, and ebitda margin, it was inferred that the processing plant is economically feasible under the ideal specified plant design conditions. However, the sensitivity analysis of the processing plant's early-stage economic feasibility assessment shows that the developed processing plant is likely to be economically unfeasible for industrial-scale application under non-ideal conditions in a real-life setting since the annual revenue obtained from the recovery of Au from typical/ non-ideal WPCBs is unlikely to result in payback or produce a large positive NPV, ROI, ebitda margin, or net margin. Presented in Chapter 5, the

results of the sensitivity analysis showed that the processing plant's economic feasibility is highly sensitive to the key assumptions used in the design and development, and economic feasibility assessment, and in particular, assumptions relating to annual revenue. Therefore, any future research and development should carefully review and ensure that any assumptions used are as accurate as possible.

The significance of the findings to the processing plant's initial, or early-stage economic feasibility analysis can be improved by conducting a:

- Market assessment to establish if the economic parameters used in the economic feasibility analysis (revenue, capital investment, production cost, tax, etc.) were erroneously estimated.
- Life cycle impact assessment to establish the relationship between feasibility, environmental sustainability, and social responsibility.

Findings - From the findings presented in this thesis, it is evident that the developed processing plant justifies further research and development for future application in real-life industrial-scale WPCB recycling operations. This is because the developed processing plant has the potential to be applied industrially in a technically and economically feasible manner as evidenced by the results of the project's early-stage technical and economic feasibility assessment.

References

Almeida, M.I., Cattrall, R.W., & Kolev, S.D. 2012. Polymer Inclusion Membranes: Concept and Applications. Procedia Engineering. 44.

Alvarado, S., Maldonado, P., Barrios, A., Jaques, I., 2002. Long-term energy-related environmental issues of copper production. Energy 27, 183–196.

Asante-Sackey, D., Rathilal, S., Kweinor Tetteh, E., Ezugbe, E.O., & Pillay, L.V. 2021. Donnan Membrane Process for the Selective Recovery and Removal of Target Metal Ions—A Mini Review. Membranes. 11.

Ashiq, A., Kulkarni, J., & Vithanage, M. 2019. Hydrometallurgical Recovery of Metals from E-waste. Advanced and Emerging Technologies for Resource Recovery from Wastes. Green Chemistry and Sustainable Technology. Springer.

Bailey, D. 1987. Electrolytic Recovery, Theory, Application, Advantages. Presented At The 8th AESF/EPA Conference San Diego.

Bas, A.D., Deveci, H., Yazici, E.Y., 2014. Treatment of manufacturing scrap TV boards by nitric acid leaching. Sep. Purif. Technol. 130.

Batnasan, A., Haga, K., Ariunbolor, N., Kawamura, S., & Shibayama, A. 2016. Leaching and Adsorption of Gold from Waste Printed Circuit Boards Using Iodine-Iodide Solution and Activated Carbon. Engineering Journal. 20.

Batnasan, A., Haga, K., Huang, H., & Shibayama, Atsushi. 2019. Gold Recovery from Waste Printed Circuit Boards by Advanced Hydrometallurgical Processing. Materials Transactions. 60.

Behnamfard, M., Salarirad, M., & Veglio, F. 2013. Process development for recovery of copper and precious metals from waste printed circuit boards with an emphasize on palladium and gold leaching and precipitation. Waste Management. 33.

Belli, P., Anderson, J., Barnum, H., Dixon, J.A., & Tan, J. 1996. Handbook on Economic Analysis of Investment Operations. World Bank Group.

Bhunia, P., & Dutta, K. 2018. Progress and Recent Trends in Microbial Fuel Cells. Elsevier.

Bhunia, S., & Tehranipoor, M. 2019. Hardware Security: A Hands-On Learning Approach (2019), Chapter 4 - Printed Circuit Board (PCB): Design and Test.

Birloaga, I., Michelis, I. De Ferella, F., Buzatu, M., Vegliò, F. 2013. Study on the influence of various factors in the hydrometallurgical processing of waste printed circuit boards for copper and gold recovery. Waste Manag. 33.

Birloaga, I., & Veglió, F. 2017. Simulation and economic analysis of a hydrometallurgical approach developed for the treatment of waste printed circuit boards (WPCB). Global NEST Journal. 20(4).

Biswal, M., Jada, N., & Mohanty, S. 2015. Recovery and utilisation of non-metallic fraction from waste printed circuit boards in polypropylene composites. Plastics, Rubber and Composites. 44.

Bizzo, W.A., Figueiredo, R.A. & De Andrade, V.F. 2014. Characterization of printed circuit boards for metal and energy recovery after milling and mechanical separation. Materials, 7(6).

Branan, C.R. 2005. Rules of Thumb for Chemical Engineers. 4. Elsevier Science.

Brigham, E.F., & Houston, J.F. 2012. Fundamentals of Financial Management. Cengage Learning.

Bruns, H., Eickhoff, M., & Pfeifer, H. 2019. Process model development for pyrolysis of WPCB in microwave-heated lab-scale rotary kiln. 10th European Metallurgical Conference – EMC.

Bolinsky, L., & Shirley, J. 1996. Russian resin-in-pulp technology, current status and recent developments. Randol International.

Caravaca, C. 1994. Gold(I) extraction from cyanide media by the primary amine Primene 81R/iso-decanol system. Hydrometallurgy. 35.

Cesaro, A., Belgiorno, V., & Gorrasi, G. 2019. A relative risk assessment of the open burning of WEEE. Environ Sci Pollut Res. 26.

Chancerel, P., Meskers, C.E., Hagelüken, C., & Rotter, V.S. 2009. Assessment of Precious Metal Flows During Preprocessing of Waste Electrical and Electronic Equipment. Journal of Industrial Ecology. 13.

Chengyi, Z., Zhang, W., & Wang, Y. 2020. Diffusion Dialysis for Acid Recovery from Acidic Waste Solutions: Anion Exchange Membranes and Technology Integration. Membranes. 10 (8).

Chirume, B.M. 2018. Investigation of a Hydrometallurgical Process Route to Recover Metals from Waste Printed Circuit Boards. Faculty of Engineering and the Built Environment, University of Cape Town, South Africa.

Couper, J.R., Penney, W.R., Fair, J.R., & Walas, S.M. 2010. Chemical Process Equipment - Process and Design. Elsevier. 3.

Cowan, D. A., & Brown, J. H. 1959. Effect of Turbulence on Limiting Current in Electrodialysis Cells. Ind. Eng. Chem. 51 (12).

Creamer, N.J., Baxter-Plant, V.S., Henderson, J., Potter, M. & Macaskie, L.E., 2006. Palladium and gold removal and recovery from precious metal solutions and electronic scrap leachates by Desulfovibrio desulfuricans. Biotechnology Letters. 28 (18).

Dabbak, S., Illias, H., Ang, B., Abdul, L., Nurul, A., & Makmud, M. 2018. Electrical Properties of Polyethylene/Polypropylene Compounds for High-Voltage Insulation. Energies.

Danthurebandara, M., Passel, S., Nelen, D., Tielemans, Y., & Van Acker, K. 2013. Environmental and socio-economic impacts of landfills. Proc. of Linnaeus Eco-Tech 2012 International Conference.

Das, A., Vidyadhar, A. & Mehrotra, S.P. 2009. A novel flowsheet for the recovery of metal values from waste printed circuit boards. Resources, Conservation, and Recycling, 53(8).

Deschenes, G. 1987. Investigation on the Potential Techniques to Recover Gold from Thiourea Solution. Proc. of Intl. Symp. on Gold Metallurgy.

Deveci, H., Yazıcı, E., Y, Aydın, U., Yazıcı, R. & Akcil, A. 2010. Extraction of copper from scrap TV boards by sulphuric acid leaching under oxidising conditions. Proceedings of Going Green-Care Innovation 2010 Conference. 45.

Deus, M., Ersin, Y., Oktay, C., & Haci, D. 2021. The Effectiveness of Adsorbents for Selective Recovery of Gold from Copper-Bearing Cyanide Leach Solutions. Bilimsel Madencilik Dergisi. 60.

de Waal, A. 2018. Evaluating the efficiency of metal recycling processes by means of life cycle assessment & exergy analysis. Department of Process Engineering, Stellenbosch University, South Africa.

Dias, J.O., Silva, A.G.P., Holanda, J.N.F., Futuro, A.M., & Pinho, S. 2019. Physical separation applied to WPCB recycling process to optimize copper enrichment. Wastes: Solutions, Treatments and Opportunities III: International Conference. 5.

Donnan, F.G. 1995. Theory of membrane equilibria and membrane potentials in the presence of non-dialysing electrolytes. Journal of Membrane Science. 100.

Duening, T.N., Hirsch, R.D., & Lechter, M.A. 2015. Valuing and Exiting Your Venture, Technology Entrepreneurship. Academic Press. 2.

Dwivedi, S., Gaurav, J.K., Kshirsagar, M., Rathi, V., Davis, N., Bawa, D., Kalia, R., Alam, T., Babbar, A., Balaji, N. 2022. Business Model Toolbox for Setting Up E-waste Recycling Facility in India. Deutsche Gesellschaft für Internationale Zusammenarbeit4 (GIZ) GmbH

Fedyukevich, V., Kubyshkin, S., Blokhin, A., Sukharzhevskii, S., & Vorob'ev-Desyatovskii, N. 2015. Use of ion-exchange resins to deal with the effect of preg-robbing of gold in the course of cyanide leaching. Russian Journal of Applied Chemistry. 88.

Fernandes, M.L.V., & Warren, G.P. 1995. Comparison of resin beads and resin membranes for extracting soil phosphate. Fertilizer Research. 44.

Fleming, C.A., McMullen, J., Thomas, K.G., & Wells, J.A. 2003. Recent advances in the development of an alternative to the cyanidation process: thiosulphate leaching and resin in pulp. Society for Mining, Metallurgy, and Explorations, Inc.

Ficeriova, J., Balaz, P., & Gock, E. 2011. Leaching of gold, silver, and accompanying metals from circuit boards (PCBs) waste. Acta Montanistica Slovaca. 16.

Ficeriová, J., Baláž, P., Dutková, E., & Gock, E. 2008. Leaching of gold and silver from crushed Au–Ag wastes Open Chem. J. 2.

Fontas, C., Tayeb, R., Dhahbi, M., Gaudichet, E., Thominette, E., Roy, P., Steenkeste, K., Fontaine-Aupart, M., Tingry, S., Tronel-Peyroz, E., & Seta, P. 2007. Polymer inclusion membranes: The concept of fixed sites membrane revised. Journal of Membrane Science. 290.

Forner, E.L., Scheepers, J., du Toit, A.J., & Miller, G.M. 2018. Copper electrowinning circuit design: optimized costing as a function of cell arrangement, productivity, rectiformer size, and throughput. Journal of the Southern African Institute of Mining and Metallurgy. 118(11).

Forti, V., Baldé, C.P., Kuehr, R., & Bel, G. 2020. The Global E-waste Monitor: Quantities, flows and the circular economy potential. United Nations University (UNU)/United Nations Institute for Training and Research–co-hosted SCYCLE Programme, International Telecommunication Union (ITU) & International Solid Waste Association (ISWA), Bonn/Geneva/Rotterdam.

Free, M.L., & Moats, M. 2014. Hydrometallurgical Processing, Treatise on Process Metallurgy. Elsevier.

Fujita, T., Ono, H., Dodbiba, G., Yamaguchi, K. 2014. Evaluation of a Recycling Process for Printed Circuit Board by Physical Separation and Heat Treatment. Waste Manag. 34.

Galva, 2023. Galva, Bibliographic References, <http://www.galva.com.br> (accessed on 20.01.23).

Ghalehkhondabi, I., & Ardjmand, E. 2019. Sustainable E-waste supply chain management with price/sustainability sensitive demand and government intervention. Journal of Material Cycles and Waste Management. 22.

Ghosh, B., Ghosh, M. K., Parhi, P., Mukherjee, P. S., & Mishra, B. K. 2015.Waste printed circuit boards recycling: An extensive assessment of current status. J. Clean. Prod. 94.

Gloe, K., Mühl, P., & Knothe, M. 1990. Recovery of Precious Metals from Electronic Scrap, In particular from Waste Products of the Thick-Layer Technique. Hydrometallurgy. 25.

Gomes, C.P., Almeida, M.F., & Loureiro, J.M. 2001. Gold recovery with ion exchange used resins. Sep. Purif. Technol. 24.

Goodman, P. 2002. Current and future uses of gold in electronics. Gold Bulletin. 35.

Gossman, G.I. 1987. The Extractive Metallurgy of Gold. South African Institute of Mining and Metallurgy.7.

Grout, I. 2008. Digital Systems Design with FPGAs and CPLDs, CHAPTER 3 - PCB Design.

Gu, B.J., Wang, J., Wolcott, M.P., & Ganjyal, G.M. 2018. Increased sugar yield from pre-milled Douglas-fir forest residuals with lower energy consumption by using planetary ball milling. Bioresour. Technol. 251.

Guidolin, M.A., Klitzke, W., Alekseev, K., Guidolin, R.H., Avanci, M.A., Pawlowsky, U., Winter, E.J., Mymr, V., & Cataiai, R.E. 2017. Environmentally clean ceramics from printed circuit board sludge, red mud of bauxite treatment and steel slag. Journal of Cleaner Production. 164.

Guo, C., Wang, H., Liang, W., Fu, J. & Yi, X. 2011. Liberation characteristic and physical separation of printed circuit board (PCB). Waste Management. 31.

Guo, X., Qin, H., Tian, Q., & Zhang, L. 2020. The efficacy of a new iodination roasting technology to recover gold and silver from refractory gold tailing. Journal of Cleaner Production. 261.

Gurgul, A., Szczepaniak, W., & Zabłocka-Malicka, M. 2017. Incineration, pyrolysis, and gasification of electronic waste. E3S Web of Conferences. 22.

Ha, V. H., Lee, J., Huynh, T. H., Jeong, J. & Pandey, B. D. 2014. Optimizing the thiosulfate leaching of gold from printed circuit boards of discarded mobile phones, Hydrometallurgy. 149.

Hadiet, P., Xu, M., Lin, C.S.K., Hui, C.W., & McKay, G. 2015. Waste printed circuit board recycling techniques and product utilization. Journal of Hazardous Materials. 283.

Hall, W.J., & Williams, P.T. 2007. Separation and Recovery of Materials from Scrap Printed Circuit Boards, Resour. Conserv. Recycl. 51.

Hagelüken, C. 2006. Recycling of Electronic Scrap at Umicore's Integrated Metals Smelter and Refinery. World of Metallurgy. 59.

Hajime, O., Kazuyo, M., Kenichi, N., Yasushi, K., Shinichiro, N., Yasuhiro, F., & Tetsuya, N. 2017. Optimal Recycling of Steel Scrap and Alloying Elements: Input-Output based Linear Programming Method with Its Application to End-of-Life Vehicles in Japan. Environmental Science & Technology. 51 (22).

Hao, J., Wang, X., Wang, Y., Wu, Y., Guo, F. 2022. Optimizing the Leaching Parameters and Studying the Kinetics of Copper Recovery from Waste Printed Circuit Boards. ACS Omega. 7 (4).

Hazen, G.B. 2009. An extension of the internal rate of return to stochastic cash flows. Management Science. 55(6).

Hedin, E., & Rohde-Nielsen, J. 2018 Metal Recovery by Electro Winning - A Product Concept. KTH Royal Institute of Technology Dissertation.

Hirvikorpi, M., Knuutila, T., Johnsson, M., & Nevalainen, O.S. 2005. A general approach to grouping of PCB assembly jobs, Int. Journal of Computer Integrated Manufacturing. 18(8).

Iji, M. & Yokoyama, S., 1997. Recycling of Printed Wiring Boards with Mounted Electronic Components. Circuit World. 23(3).

Iniaghe, P., & Adie, G.U. 2015. Management practices for end-of-life cathode ray tube glass: Review of advances in recycling and best available technologies. Waste management & research: the journal of the International Solid Wastes and Public Cleansing Association. 33.

Iniaghe, P., & Adie, G.U. 2017. Incorporation of finely ground waste cathode ray tube glass in concrete. Journal of Solid Waste Technology and Management. 43.

Ippolito, N. N., Birloaga, I., Ferella, F., Centofanti, M., & Veglio, F. (2021). Preliminary Study on Gold Recovery from High-Grade E-Waste by Thiourea Leaching and Electrowinning. Minerals. 11.

Iskandar, H., & Rajagopalan, S. 2011. Sequential methodology for integrated optimization of energy and water use during batch process scheduling. Computers & Chemical Engineering. 35(8).
Jadhav, U. & Hocheng, H. 2015. Hydrometallurgical Recovery of Metals from Large Printed Circuit Board Pieces. Scientific reports. 5.

Jalil, M.J., Zaki, H., Azmi, I., Zulkifli, A., Bakar, M., & Rashid, A. 2020. Recovery of Gold from Pregnant Thiourea Leaching Solution by Synergistic Extraction. IOP Conference Series: Materials Science and Engineering. 778.

Jha, M.K. 2012. Leaching of lead from solder material of waste printed circuit boards (PCBs). Hydrometallurgy. 121.

Kamberovi, Ž., Kora, M., Ivši, D., Nikoli, V., & Ranitovi, M. 2009. Hydrometallurgical Process for Extraction of Metals from Electronic Waste-Part I: Material Characterisation and Process Option Selection. MJoM. 15 (4).

Kasper, A., Veit, H., García-Gabaldón, M., & Pérez-Herranz, V. 2017. Electrochemical study of gold recovery from ammoniacal thiosulfate, simulating the PCBs leaching of mobile phones. Electrochimica Acta. 259.

Kim, B.-S., Lee, J.-c., Seo, S.-P., Park, Y.-K. & Sohn, H. Y. (2004) A process for extracting precious metals from spent printed circuit boards and automobile catalysts. JOM, 56(12), 55-58.

Konyratbekova, S., Alya, B., Ussoltseva, G.A., Erust, C., & Akcil, A. 2015. Thermodynamic and kinetic of iodine−iodide leaching in gold hydrometallurgy. Transactions of Nonferrous Metals Society of China. 25.

Kotze, M. 2010. Gold Ion Exchange. In ALTA 2010 Gold Conference. Melbourne, Australia: ALTA Metallurgical Services.

Kotze, M., Green, B., Mackenzie, M., & Virnig, M. 2005. Resin-in-pulp and resin-in-solution. Advances in Gold Ore Processing. 15

Krol, J. J. 1997. Monopolar and Bipolar Ion Exchange Membranes - Mass Transport Limitations. University of Twente, Enschede.

Křivčík, J., Neděla, D., & Válek, R. 2014. Ion-exchange membrane reinforcing. Desalination and Water Treatment. 56.

Kubo, S. 1990. Purification process for gold-bearing iodine lixiviant. USA Patent: US5026420A.

Kumar, R. 2014. Strategies of Banks and Other Financial Institutions. Academic Press.

Kumari, A., Jha, M., Lee, Jae-Chun., Singh, R. 2015. Clean process for recovery of metals and recycling of acid from the leach liquor of PCBs. Journal of Cleaner Production. 112.

Lawrence, A., Thollander, P., Andrei, M., & Wallén, M.2019. Specific Energy Consumption/Use in Energy Management for Improving Energy Efficiency in Industry: Meaning, Usage and Differences. Energies. 12.

Le, H., Jeong, J., Lee, J.Ch., Pandey, B.D., Yoo, J.M., & Huyunh, T.H. 2011. Hydrometallurgical Process for Copper Recovery from Waste Printed Circuit Boards (PCBs). Mineral Processing and Extractive Metallurgy Review. 32(2).

Lee, J., Kim, Y., & Lee, J. 2012. Disassembly and physical separation of electric/electronic components layered in printed circuit boards (PCB). Journal of hazardous materials. 241.

Lesakova, L. 2007. Uses and Limitations of Profitability Ratio Analysis in Managerial Practice. In 5th International Conference on Management, Enterprise and Benchmarking, Budapest.

Li, F., Chen, M., Shu, J., Shirvani, M., Li, Y., Sun, Z., Sun, S., Xu, Z., Fu, K., & Chen, S. 2019. Copper and gold recovery from CPU sockets by one-step slurry electrolysis. J. Clean. Prod. 213.

Li, J., Xu, X., & Liu, W. 2012. Thiourea leaching gold and silver from the printed circuit boards of waste mobile phones. Waste management. 32.

Li, J., Lu, H., Guo, j., Xu, Z., & Zhou, Y. 2007. Recycle technology for recovering resources and products from waste printed circuit boards, Environmental Science and Technology. 41(6).

Lin, W., Zhang, R. W., Jang, S. S., Wong, C.P. & Hong, J. I. 2010. "Organic Aqua Regia"-Powerful Liquids for Dissolving Noble Metals. Angewandte Chemie International Edition. 49.

Li, X., & Binnemans, K. 2021. Oxidative Dissolution of Metals in Organic Solvents. Chemical Reviews. 121(8).

Luckham, W. R. 1982. Financial Ratio Analysis for Decision-Making. Journal of Arboriculture. 8(11).

Luda, M. 2011. Recycling of Printed Circuit Boards. Integrated Waste Management. 2.

Magni, C. 2010. Average Internal Rate of Return and Investment Decisions: A New Perspective. Technological University of Bolivar. Documentos de Trabajo. 55.

Mahandra, H., Faraji, F., & Ghahreman, A. 2021. Novel Extraction Process for Gold Recovery from Thiosulfate Solution Using Phosphonium Ionic Liquids. ACS Sustainable Chemistry & Engineering. 9(24).

Majozi, T. 2006. Heat integration of multipurpose batch plants using a continuous-time framework. Applied Thermal Engineering. 26(13).

Makua, P., & Kola, O. 2017. Harmful mining activities, environmental impacts, and effects in the mining communities in South Africa: a critical perspective. Environmental Economics. 8.

Manjengwa, E.R. 2019. Evaluating the economics of and business models for metal recycling from waste printed circuit boards in a South African context. Department of Process Engineering, Stellenbosch University, South Africa.

Marsden, J.O., & Fuerstenau, M. C. 1993. Comparison of Merrill–Crowe precipitation and carbon adsorption for precious metals recovery. Proceedings of XVIII International Mineral Processing Congress. Australasian Institute of Mining and Metallurgy.

Marston, C.R., & Gisch, D.J. 2012. New Selective Strong Base Anion Exchange Resins with Promise for Commercial Gold Cyanidation. In ALTA 2010 Gold Conference.

Marques, A.C., Marrero, J.M.C., & Malfatti, C.D.F. 2013. A review of the recycling of non-metallic fractions of printed circuit boards. Springer Plus. 2.Xiong, J., Yu, S., & Wu, D. 2020. Pyrolysis Treatment of nonmetal fraction of waste printed circuit boards: Focusing on the fate of bromine. Waste Management & Research. 38(11).

Mecucci, A., & Scott, K. 2002. Leaching and electrochemical recovery of copper, lead and tin from scrap printed circuit boards. Journal of Chemical Technology and Biotechnology. 77.

Menad, N. & Van Houwelingen, J., 2011. Identification and recovery of rare metals in electric and electronic scrap: a review. In Thirteenth International Waste Management and Landfill Symposium.

Menetti, R.P. & Tenorio, S.A.J. 1995. Recycling of Precious Metals from Electronic Scraps. In Proceedings of the 50th Annual Congress of ABM.

Meng, Qi., Li, G., Kang, H., Yan, X., Wang, H., & Xu, D. 2019. A Study of the Electrodeposition of Gold Process in Iodine Leaching Solution. Metals. 10.

Meng, Qi ., Li, G., & Yan, X. 2021. Eco-friendly and reagent recyclable gold extraction by iodination leaching-electrodeposition recovery. Journal of Cleaner Production. 323.

Mironov, I. 2012. On the extraction of gold(III) with dibutyl carbitol. Russian Journal of Inorganic Chemistry. 57.

Muthumariappan, S., & Alwin, D. 2019. A study of the chemical composition of copper concentrate and granulated slag. International Journal of Scientific Research and Review. 7.

Nassar, N., Brainard, J., Gulley, A., Manley, R., Matos, G., Lederer, G., Bird, L., Pineault, D., Alonso, E., Gambogi, J., & Fortier, S. 2020. Evaluating the mineral commodity supply risk of the U.S. manufacturing sector. Science Advances. 6.

Nekouei, R., Pahlevani, F., Rajarao, R., Golmohammadzadeh, R., & Sahajwalla, V. 2018. Two-step pre-processing enrichment of waste printed circuit boards: Mechanical milling and physical separation. Journal of Cleaner Production. 184.

Nicol, M.J., Fleming, C.A., & Paul, R.L. 1987. The Extractive Metallurgy of Gold in South Africa. South African Institute of Mining and Metallurgy.7.

Norgate, T., Jahanshahi, S., & Rankin, W. 2006. Assessing the environmental impact of metal production processes. Journal of Cleaner Production. 15.

Nurul, A.R., Faiz, B.M.S., & Mohamed, N. 2017. The use of an electro-generative process as a greener method for recovery of gold(III) from the E-waste. Separation and Purification Technology. 182.

O'Connor, M.P., Zinnerman, J.B., Anastas, P.T., & Plata, D.L. 2016. A strategy for material supply chain sustainability: Enabling a circular economy in the electronics industry through green engineering. ACS Sustain. Chem. Eng. 4.

Ogunseitan, O.A., Schoenung, J.M., Saphores, J.D.M., & Shapiro, A. 2009. The Electronics Revolution: From E-Wonderland to E-Wasteland. Science. 326.

Ogura, K., Haruyama, S., & Nagasaki, K. 1971. The Electrochemical Oxidation and Reduction of Gold. Journal of The Electrochemical Society. 118(4).

Oh, C.J., Lee, S.O., Yang, H.S., Ha, T.J. & Kim, M.J. 2003. Selective Leaching of Valuable Metals from Waste Printed Circuit Boards. Journal of the Air & Waste Management Association. 53(7).

Oliveira, P.C., Cabral, M., Nogueira, C.A. & Margarido, F., 2010. Printed Circuit Boards Recycling: Characterization of Granulometric Fractions from Shredding Process. In Materials Science Forum. 636–637.

Ortuño, N., Conesa, J., Juan A., Moltó, J., Font, R. 2014. Pollutant emissions during pyrolysis and combustion of waste printed circuit boards, before and after metal removal. The Science of the Total Environment. 499 C.

Otunniyi, I., & Vermaak, M. 2007. Improving printed circuit board physical processing - An overview. Proceedings - European Metallurgical Conference. 4.

Parga, T.J., Valenzuela, J., Moreno, C.H., & Pérez, J. 2011. Copper and Cyanide Recovery in Cyanidation Effluents. Advances in Chemical Engineering and Science. 01.

Park, Y.J., & Fray, D.J. 2009. Recovery of High Purity Precious Metals from Printed Circuit Boards, Journal of Hazardous Materials. 164.

Peter, M., & Timmerhaus, K. 2003. Plant Design and Economics for Chemical Engineers. 5. McGraw-Hill.

Petter, P.M.H., Veit, H.M., Bernardes, A.M. 2014. Evaluation of gold and silver leaching from the printed circuit board of cellphones. Waste Management. 34.

Pichtel, J. 2016. Oil and Gas Production Wastewater: Soil Contamination and Pollution Prevention. Applied and Environmental Soil Science. 16.

Pinto, D.V.B.S., & Martins, A.H. 2001. Electrochemical elution of a cation-exchange polymeric resin for yttrium and rare earth recovery using a statistical approach. Hydrometallurgy. 60(1)

Rajesha, D.K, Gohatre, O.K., Biswal, M., Mohanty, S., & Nayak, S.K. 2019. Influence of Non-Metallic Parts of Waste Printed Circuit Boards on the Properties of Plasticised Polyvinyl Chloride Recycled from the Waste Wire. Waste Management & Research. 37(6).

Reichenberg, D. 1953. Properties of Ion-Exchange Resins in Relation to their Structure. III. Kinetics of Exchange. J. Am. Chem. Soc. 75(3).

Reno Cell® Technical Bulletin. 2011. Reviewing the Operations of Gold Electrowinning Cells. Renoware International Inc.

Rovira, M., Hurtado, L., Cortina, J.L., Arnaldos, J. & Sastre, A.M. 1998. Impregnated Resins Containing Di-(2-Ethylhexyl) Thiophosphoric Acid for the Extraction of Palladium (II). I Preparation and Study of the Retention and Distribution of the Extractant on the Resin. Solvent Extraction and Ion Exchange. 16(2).

Ruhmer, W.T. 1996. Handbook on the estimation of metallurgical process costs. Mintek. 2.

Sahin, M., Akcil, A., Erust, C., Altynbek, S., Gahan, C.S., & Tuncuk, A. 2015. A potential alternative for precious metal recovery from e-waste: iodine leaching. Separation Science and Technology. 50(16).

Sander, G., Jiang, D., Wu, Y., & Birbilis, N. 2020. Exploring the possibility of a stainless steel and glass composite produced by additive manufacturing. Materials and Design. 196.

Schow, A.J., Peterson, R.T., & Lamb, J.D. 1996. Polymer inclusion membranes containing macrocyclic carriers for use in cation separations. J. Membr. Sci. 111.

Seider, W.D., Seader, J.D., Lewin, D.R., & Widagdo, S. 2019. Product and Process Design Principles - Synthesis, Analysis, and Evaluation. John Wiley. 4.

Simons, R. 1993. A mechanism for water flows in bipolar membranes. J. Membr. Sci. 82.

Singh, S., & Prasad, B.L.V. 2007. Nearly Complete Oxidation of Au° in Hydrophobized Nanoparticles to Au^{3+} Ions by N-Bromosuccinimide. Phys. Chem. 111.

Sivaramanan, S. 2013. E-Waste Management, Disposal, and Its Impacts on the Environment. UJERT. 2.

Spalvins, E., Dubey, B., & Townsend, T. 2008. Impact of Electronic Waste Disposal on Lead Concentrations in Landfill Leachate. Environmental science & technology. 42.

Steyn, J. & Sandenbergh, R. 2004. A study of the influence of copper on the gold electrowinning process. Journal of The South African Institute of Mining and Metallurgy. 104.

Stickland, A., Irvin, E., Skinner, S., Scales, P., Hawkey, A., & Kaswalder, F. 2016. Filter Press Performance for Fast-Filtering Compressible Suspensions. Chemical Engineering & Technology. 39.

Strathmann, H. 2004. Ion-Exchange Membrane Separation Processes. Elsevier.

Sugiura, M., Kikkawa, M., & Urita, S. 1989. Carrier-mediated transport of rare earth ions through cellulose triacetate membranes. Journal of Membrane Science. 42.

Sun, Y., Wang, Z., Wang, Y., Liu, M., Li, S., Tang, L., Wang, S., Xiangjun, Y., & Ji, S. 2019. Improved transport of gold(I) from aurocyanide solution using a green ionic liquid-based polymer inclusion membrane with in-situ electrodeposition. Chemical Engineering Research and Design. 153.

Suratman, S. 2008. The Recovery of Gold from a Pregnant Gold-Thiosulfate Leach Solution Using Ion Exchange Resin. Indonesian Mining Journal. 11(12).

Szałatkiewicz, J. 2014. Energy Recovery from Waste of Printed Circuit Boards in Plasmatron Plasma Reactor. Polish Journal of Environmental Studies. 23(1).

Tang, H., Chang, T., Chen, C., Nagoshi, T., Yamane, D., Konishi, T., & Machida, K. 2018. Electrodeposition of Gold Alloys and the Mechanical Properties. Intech open.

Teirlinck, P.A.M., & Petersen, F.W. 1995. Factors Influencing the Adsorption of Gold-Iodide onto Activated Carbon, Separation Science and Technology. 30(16).

Thompson, R.C., Moore, C.J., vom Saal, F.S., & Swan, S.H. 2009. Plastics, the environment, and human health: current consensus and future trends. Philosophical Transactions of the Royal Society of London. Series B. Biological sciences. 364.

Thompson, V.S., Gupta, M., Jin, H., Vahidi, E., Yim, M., Jindra, M.A., Nguyen, V., Fujita, Y., Sutherland, J.W., Jiao, Y., & Reed, D.W. 2018. Techno-economic and Life Cycle Analysis for Bioleaching Rare-Earth Elements from Waste Materials. ACS Sustainable Chemistry & Engineering. 6(2).

Towler, G., & Sinnott, R. 2020. Chemical Engineering Design: Principles, Practice and Economics of Plant and Process Design. Elsevier.

Turton, R., Bailie, R.C., Whiting, W.B., Shaewitz, J.A., & Bhattacharyya, D. 2012. Analysis, Synthesis, and Design of Chemical Processes. 4. Prentice-Hall.

Tumuluru, J.S., & Heikkila, D.J. 2019. Biomass grinding process optimization using response surface methodology and a hybrid genetic algorithm. Bioengineering. 6(12).

United Nations University. 2012. E-waste: Annual gold, silver 'deposits' in new high-tech goods worth $21B, less than 15% recovered. Retrieved from https://phys.org/news/2012-07-ewaste-annual-gold-silver-deposits.html.

U.S. Geological Survey. 2021. Mineral Commodity Summaries.

Van Deventer, J 2012. New Developments in Ion Exchange Resins for the Recovery of Gold in Complex Ores. Proceedings of the 7th international Hydrometallurgy symposium. Canadian Institute of Mining, Metallurgy & Petroleum.

Van Deventer, J 2014. New Developments in Ion Exchange Resins for the Recovery of Gold in Complex Ores. Originally presented at Hydrometallurgy 2014. Canadian Institute of Mining, Metallurgy & Petroleum.

Veit, H.M., de Pereira, C.C. & Bernardes, A.M., 2002. Using mechanical processing in recycling printed wiring boards. Jom, 54(6).

Verrett, J., Qiao, R., & Barghout, R.A. 2020. Foundations of Chemical and Biological Engineering I. BCcampus.

Vermesan, H., Tiuc, A., Elena, V., & Purcar, M. 2019. Advanced Recovery Techniques for Waste Materials from IT and Telecommunication Equipment Printed Circuit Boards. Sustainability. 12.

Vidyadhar, A. 2015 A Review of Technology of Metal Recovery from Electronic Waste, Jamshedpur.

Vijayaram, R. & Kavitha, C. 2013. Studies on Metal (Cu and Sn) Extraction from the Discarded Printed Circuit Board by Using Inorganic Acids as Solvents." Journal of Chemical Engineering & Process Technology. 3.

Villaescusa, I., Salvadó, V., & de Pablo, J. 1996. Liquid-liquid and solid-liquid extraction of gold by trioctylmethylammonium chloride (TOMAC1) dissolved in toluene and impregnated on amberlite XAD-2 resin. Hydrometallurgy. 41.

Wu, J., Chen, L., & Qiu, L.J. 2008. Study on selectively leaching gold from waste printed circuit boards with thiourea. Gold. 29(6).

Waldir, B., Renata, F., & Valdelis, A. 2014. Characterization of Printed Circuit Boards for Metal and Energy Recovery after Milling and Mechanical Separation. Materials. 7(6).

Wang, H., Gu, G.H. & Qi, Y.F., 2005. Crushing performance and resource characteristics of printed circuit board scrap. Journal of the Central South University of Technology, 12(5).

Wang, F., Zhao, Y., Zhang, T., Duan, C., Wang, L. 2015. Mineralogical analysis of dust collected from typical recycling line of waste printed circuit boards. Elsevier Ltd. 43.

Wankat, P. 2016. Separation Process Engineering: Includes Mass Transfer Analysis. 4. Prentice Hall.

Wei, Z., Jiakuan, Y., Xu, W., Yuchen, H., Wenhao, Y., Junxiong, W., Jinxin, D., Mingyang, L., Sha, L., Jingping, H., & Ramachandran, K. 2016. A critical review of secondary lead recycling technology and its prospect. Renewable and Sustainable Energy Reviews. 61.

Williams, E. 2011. Environmental effects of information and communications technologies. Nature, 479.

Witt, K., & Radzymińska-Lenarcik, E. 2019. Characterization of PVC-based polymer inclusion membranes with phosphonium ionic liquids. J Therm Anal Calorim. 138.

Wong, D.S., & Lavoie, P. 2019. Aluminium: Recycling and Environmental Footprint. JOM. 71.

Wordsworth, J., Khan, N., Blackburn, J., Camp, J., & Angelis-Demakis, A. 2021. Techno-economic Assessment of Organic Halide Based Gold Recovery from Waste Electronic and Electrical Equipment. Resources. 10.

Xie, F., Lu, D., Yang, H., & Dreisinger, D. 2014. Solvent Extraction of Silver and Gold from Alkaline Cyanide Solution with LIX 7950, Mineral Processing and Extractive Metallurgy Review. 35(4).

Xu, Q., Chen, D. H., Chen, L., & Huang, M. H. 2010. Gold leaching from waste printed circuit board by iodine process. Nonferrous Metals. 62(3).

Xu, T. 2005. Ion exchange membranes: State of their development and perspective. Journal of Membrane Science. 263.

Xu, X.L., & Li, J.Y. 2011. Experimental study of thiourea leaching gold and silver from waste circuit boards. Journal of Qingdao University. 26.

Yang, H., Liu, J., & Yang, J. 2011. Leaching copper from shredded particles of waste printed circuit boards. Journal of Hazardous Materials. 187.

Yannopoulos, J.C. 1991. The Extractive Metallurgy of Gold. Springer, New York. 10.

Yazici, E., Deveci, H., Yazici, R. 2015. Base and precious metal losses in magnetic separation of waste printed circuit boards. Proceeding of EMC 2015, Düsseldorf, Germany.

Yazıcı, E., & Deveci, H. 2016. Economic potential and environmental characterisation of waste of printed circuit boards. Madencilik. 55.

Yedla, S. 2005. Modified landfill design for sustainable waste management. International Journal of Global Energy Issues. 23.

Ylä-Mella, J., Poikela, K., Lehtinen, U., Tanskanen, P., Román, E., Riitta L.K., & Pongrácz, E. 2014. Overview of the WEEE Directive and Its Implementation in the Nordic Countries: National Realisations and Best Practices. Journal of Waste Management. 14.

Yoo, J., Jeong, J., Yoo, K., Lee, J. & Kim, W. 2009. Enrichment of the metallic components from waste printed circuit boards by a mechanical separation process using a stamp mill. Waste Management. 29(3).

Yue, C., Yang, P., Sun, H., Liu, W.J., Deng, X., Guan, B., & Zhang, X. 2017. Environmentally Benign, Rapid and Selective Extraction of Gold from Ores and Waste Electronic Materials. Angewandte Chemie International Edition. 49.

Zaheri, P., & Davarkhah, R. 2020. Selective separation of uranium from sulfuric acid media using a polymer inclusion membrane containing alamine336. Chem. Pap. 74.

Zhang, H., Jeffery, C., & Jeffrey, M. 2012. Ion exchange recovery of gold from iodine–iodide solutions. Hydrometallurgy. 125.

Zhang, X.Y., Chen, L., & Fang, Z.T. 2009. Review on gold leaching from PCB with non-cyanide leach reagents. Nonferrous Metals. 61.

Zhang, Y., Liua, S., Xiea, H., Zengb, X., & Li, J. 2012. Current status on leaching precious metals from waste printed circuit boards. Procedia Environmental Sciences. 16.

Zhao, J., Wu, Z., & Chen, J. 1998. Extraction of gold from thiosulfate solutions using amine mixed with neutral donor reagents. Hydrometallurgy. 48(2).

Zheng, Su & Wang, Yun-yan & Chai, Li-yuan. 2006. Research status and the prospect of gold leaching in alkaline thiourea solution. Minerals Engineering. 19.

Zhu, X., Nie, C., Wang, S., Xie, Y., Zhang, H., Lyu, X., Qiu, J., & Li, L. 2020. A cleaner approach to the recycling of metals in waste printed circuit boards by magnetic and gravity separation. Journal of Cleaner Production. 248.

http://www.astom-corp.jp/en/product/02.html – accessed 15 March 2021.

https://www.ptanode.com/post/2020/04/04/– accessed 23 April 2021.

https://www.tokaicarbon.co.jp/en/products/graphite/ – accessed 23 April 2021.

https://www.iea.org/data-and-statistics/data-tools/cost-of-capital-observatory – 4 January 2022.

https://www.nersa.org.za – 4 January 2022.

https://www.sars.gov.za – 4 January 2022.

https://taxsummaries.pwc.com – 4 January 2022.

https://mbmmllc.com/products/24-x-30-hammer-mill – accessed 13 February 2022.

https://www.purolite.com/product/mta9920 – accessed 16 April 2022.

https://www.suezwaterhandbook.com – accessed 5 May 2022

https://www.xinhaimining.com/product/gold/leaching-agitation-tank – accessed 8 June 2022.

https://www.indmin.com – accessed 19 July 2022.

https://www.chemanalyst.com – accessed 17 September 2022.

https://products.sasol.com/pic/products/home/grades/ZA/5s5718/index.html – 12 October 2022.

https://ishigaki.de/en/products/filter-press-lasta-mc – accessed 29 October 2022.

https://dtsc.ca.gov/disposal-fee – accessed 5 December 2022.

https://www.alliedbuildings.com – accessed 7 October 2023.

https://www.anvilproperty.co.za– accessed 7 October 2023.

https://www.sinusjevi.com/products/hazardous-area-immersion-heaters-type-d-8800/– accessed 26 October 2023.

Appendices

SIZE-REDUCTION CIRCUIT COSTING						
Main Equipment:	**Qty**	**Cost (Per Unit)**	**Cost (Total)**	**Capacity**	**Vendor**	Exchange Rate 1USD = R15.86
Elevator Conveyor (Carbon Steel) - NE800	1	$8 000.00	$8 000.00	200 t/hr	Hebei Taizhe Machinery Equipment Trading	
Hammer Mill (With Screen)	1	$43 425.00	$43 425.00	100 t/hr	Mt. Baker Mining and Metals	
Belt Conveyor - BAICHY1200	1	$12 000.00	$12 000.00	500 t/hr	Henan Baichy Machinery Equipment	
Dust Collection and Cooling Units	1	$24 000.00	$24 000.00	500 t/hr	Shandong Huayu Metal Material Co., Ltd	
		Total	$87 425.00			
Auxiliary Equipment:	**Qty**	**Cost (10% Main Equipment Cost)**				
Holding Bin	1	$8 743				
Feeder Hopper	1					
Buffer Hopper	1					
Miscellaneous (Rails, Pipes, etc.)	N/A					
Total Size-Reduction Circuit Equipment Cost	$96 167.50					
Power/Electricity Consumption						
Energy Demand	32.5 KWh/t WPCB					
Energy Usage Per Day	3250 KWh					
Energy Usage Per Annum	975000 KWh					
Average Electricity Cost (RSA April 2022)	$0.1330 /KWh					
Electricity Cost Per Day	$423					
Electricity Cost Per Annum	$126 750					
Operating Parameters						
Mill Throughput	100 t WPCB/day	50 t WPCB/hr				
Mill Operating Time	2 hr/day					
Final Product Size	2mm/2mm					

LEACHING CIRCUIT COSTING

Main Equipment	**Qty**	**Cost (Per Unit)**	**Cost (Total)**	**Capacity**	**Vendor**		Exchange Rate 1USD = R15.86
SJ8.5x9 Leaching Tank (Including Back Up)	2.00	$73 400.00	$146 800.00	400 kL	XinhaiMineral Processing EPC		
SJ8.5x9 Precipitation Tank (Including Back Up)	2.00	$73 400.00	$146 800.00	400 kL	XinhaiMineral Processing EPC		
D-8800 Immersion Heaters (Including Back Up)	8.00	$11 581.00	$92 648.00	2.5 MW	Sinusjevi		
Ishigaki Laster Filter Press	1.00	$468 750.00	$468 750.00	100 t/hr	Ishigaki		
		Total	$854 998.00				
Auxiliary Equipment	**Cost (20% Main Equipment Cost)**						
Miscellaneous (pumps, pipes, etc.)	$170 999.60						
Storage Tanks, (HDPE)							
Leaching Tank Scrubbers							
Lixiviant Reagent Systems							
Conveyor System							
Total Leaching Circuit Equipment Cost	$1 025 997.60						
Power/Electricity Consumption							
Energy Demand (Leaching Tank)	0.628 KWh/t WPCB						
Energy Demand (Filter Press)	35 KWh/t WPCB						
Energy Demand (Total)	35.628 KWh/t WPCB						
Energy Usage Per day	3563 KWh						
Energy Usage Per Annum	1068900 KWh						
Average Electricity Cost (RSA April 2022)	$0.1329 per KWh						
Electricity Cost Per Day	$463						
Electricity Cost Per Annum	$138 957						
Operating Parameters							
Lixiviant Concentration	2.5g/L I_2, 10 g/L I^-, 10 g/L H_2O_2			0.2M HNO_3	3.5 M HCl	2M H_2SO_4 2M H_2O_2	
S/L ratio	500 g/L			500 g/L	500 g/L	500 g/L	
Filter press operating time	1 hr			1 hr	1 hr	1 hr	
Leaching time	4 hrs			45 min	120 min	3 hr	
Pre-heating time	0 hrs			1.5 hrs	1.5 hrs	0 hrs	
Aggitation speed	18 rpm			18 rpm	18 rpm	18 rpm	
Temperature	25 deg.C			90 deg.C	90 deg.C	25 deg.C	
Capacity	100 t WPCB/ day			100 t WPCB/ day	100 t WPCB/ day	100 t WPCB/ day	
Leach pH	6.00						
Filterpress and scrubber efficiency				100%			

CONCENTRATION-RECOVERY CIRCUIT COSTING									
Main Equipment	**Qty**	**Price Per Unit**	**Cost (Total)**	**Capacity**	**Price Per Unit (Old**	**Capacity (Old)**	**Factor**	**Vendor**	Exchange Rate 1USD = R15.86
Assembled IX-EW Cell (304 SS)	1	$1 200 000.00	$1 200 000.00	520 m^3	$1100000	460 m^3	0.6	Inquip Mineral Industry Equipment	
Anode (Titanium Basket) ASTM B265,	60	$860.00	$51 600.00	2m/2m/50mm	$223	1.4m/0.3m/50mm	0.6	Hangzhou King Titanium	
Cathode (316 SS Sheet)	118	$595.00	$70 210.00	2m/2m/50mm	$289	1.135m/1.062m/50mm	0.6	Tongling Huierpu Technology Co., Ltd.	
AEM (AFX)	116	$770.00	$89 320.00	5m/5m	$130	0.8m/1.6m	0.6	RisingSun Membrane Technology	
IEM (2709g PVC, 4063g Purogold S992, 135L T	118	$80.00	$9 440.00	5m/5m	$70	4m/4m (2167g PVC, 3250g Purogold S992, 108L THF)	0.6	Chemanalyst.com, Sunresin New Materials	
DC Power Supply	1	$10 500.00	$10 500.00	30V/10000A				Green Power Co., Ltd	
		Total	$1 431 070.00						
Auxiliary Equipment	**Cost (20% Main Equipment Cost)**								
Miscellaneous (pumps, pipes, etc.)	$286 214.00								
Au melting furnance									
Conveyor system									
Lixiviant systems									
BM precipitation systems									
Electrolyte solution systems									
Structural equipment (stainless-steel									
pallets and track system, lifting rack, overhead crane,									
nuts, and bolts)									
Power/Electricity Consumption									
Energy Demand	5.53 KWh/t WPCB								
Energy Usage Per day	553 KWh								
Energy Usage Per Annum	165900 KWh								
Average Electricity Cost (RSA April 2022)	$0.1329 per KWh								
Electricity Cost Per Day	$71.89								
Electricity Cost Per Annum	$21567								
Operating Parameters									
Voltage	12.9 V								
Current	7145A								
Current Density	1429 A/m2								
Time	6 hrs								
Electolyte Concentration	2.5g/L I2	10 g/L I-							
Capacity	200 kL WPCB Iodide Leachate/day								
Au Recovery Yield	0.96								
Au Purity	>99%								

PROCESS CONSUMBALES REAGENT COSTING						
Lixiviant Reagents	**Price (100% basis)**	**Qty Per Cycle**	**Qty Per Annum**	**Cost Per Cycle**		**Cost Per Annum**
I_2	$55.00/kg	500 kg	150000	$27 500.00	indmin.com	$8 250 000.00
I- (KI)	$48/kg	2000 kg	600000	$96 000.00	Proto Chemical Industries	$28 800 000.00
H_2O_2	$2.788/kg	11606 kg + 2000 kg	4081800	$37 930.00	Worldwide Commodities LLC	$11 379 000.00
HNO_3	$1.811/kg	2520 kg	756000	$4 564.00	pharmacompass.com	$1 369 200.00
HCl	$0.179/kg	25520 kg	7656000	$4 568.00	chemanalyst.com	$1 370 400.00
H_2SO_4	$0.67	39232 kg	11769600	$26 284.00	Proto Chemical Industries	$7 885 200.00
H_2O	$2.96/kL	800 kL	240000.00	$2 370.00	SA Municiple Tarrifs (2022)	$711 000.00
			Total	$199 216.00		
Electrolyte Reagents	**Price (100% basis)**	**Qty Per Cycle**		**Cost Per Cycle**	**Cost Per Annum**	
I2	$55.00/kg	800 kg		$44 000.00	$13 200 000.00	Indmin.com
I- (KI)	$48/kg	3200 kg		$153 600.00	$46 080 000.00	Proto Chemical Industries
H2O	$2.96/kL	320 kL		$947.00	$284 100.00	SA Municiple Tarrifs (2022)
			Total	$198 547.00		
Electrolyte and Lixiviant Reagent Cost Per Cycle	$397 763.00					
Recovered Reagents	**Price (100% basis)**	**Qty Per Cycle**		**Cost Per Cycle**	**Cost Per Annum**	
I2	$55.00/kg	1066 kg	319 800.00	$58 630.00	$17 589 000.00	Indmin.com
I- (KI)	$48/kg	4628 kg	1 388 400.00	$222 144.00	$66 643 200.00	Proto Chemical Industries
H2O	$2.96/kL	108 kL	32 400.00	$319.68	$95 904.00	SA Municiple Tarrifs (2022)
			Total	$281 093.68		
Cost Saving from Use of Recovered Iodide Reagents Per Cyc	$281 093.68					
Cost Saving from Use of Recovered Iodide Reagents Per Anr	$84 328 104.00					
BM Prec. Reagents	**Price (100% basis)**	**Qty Per Cycle**		**Cost Per Cycle**	**Cost Per Annum**	
NaOH	$6.87/kg	0.8 kg (0.2 kg X 4)		$5.50	$1643.00	miningchem.co.za
BM Prec. Reagent Cost Per Cycle	$5.50					
Total Regeant Costs Per Cycle	$116 674.82					
Total Regeant Costs Per Cycle	$35 002 446.00					

SENSITIVITY ANALYSIS CONDITION 1											
Total Capital Investment		30 585 000									
Bond Amount		30 585 000									
Bond Interest		0.14	per annum								
Bond Term		5	years								
Time Period/Year		1	2	3	4	5	6	7	8	9	10
Depreciation rate		0.4	0.2	0.2	0.2	0	0	0	0	0	0
Asset Book Value		$2 839 000	$567 800	$340 680	$204 408	$122 645	$0	$0	$0	$0	$0
Depreciation allowance		$2 271 200	$227 120	$136 272	$81 763	$0	$0	$0	$0	$0	$0
Annual Revenue		$342 800 000	$342 800 000	$342 800 000	$342 800 000	$342 800 000	$342 800 000	$342 800 000	$342 800 000	$342 800 000	$342 800 000
Annual Production Cost		$237 500 000	$237 500 000	$237 500 000	$237 500 000	$237 500 000	$237 500 000	$237 500 000	$237 500 000	$237 500 000	$237 500 000
Annual Bond Repayments		$8 908 907	$8 908 907	$8 908 907	$8 908 907	$8 908 907	$0	$0	$0	$0	$0
Annual Interest on Bond		$2 791 907	$2 791 907	$2 791 907	$2 791 907	$2 791 907	$0	$0	$0	$0	$0
Taxable Revenue		$100 236 893	$102 280 973	$102 371 821	$102 426 330	$102 508 093	$105 300 000	$105 300 000	$105 300 000	$105 300 000	$105 300 000
Tax rate		0.28	0.28	0.28	0.28	0.28	0.28	0.28	0.28	0.28	0.28
Tax Paid		$28 066 330	$28 575 079	$28 625 954	$28 656 479	$28 702 266	$29 484 000	$29 484 000	$29 484 000	$29 484 000	$29 484 000
Net Cash Flow		$72 170 563	$73 705 894	$73 745 867	$73 769 851	$73 805 827	$75 816 000	$75 816 000	$75 816 000	$75 816 000	$75 816 000
Discount Rate		0.19	0.19	0.19	0.19	0.19	0.19	0.19	0.19	0.19	0.19
Discounted Cash Flow		$60 647 532	$52 048 509	$43 761 964	$36 786 719	$30 928 285	$26 698 023	$22 435 313	$18 853 204	$15 843 029	$13 313 470
Net Present Value	$290 731 049										
ROI	25.25592317										
PBP	0.951866554	321316048.6	32131604.86	0.951866554							
Net Margin	9.373280297	0.1769	0.1518	0.1277	0.1073	0.0902	0.0779	0.0654	0.0550	0.0462	0.0388
Ebitda Margin	18.32082984	0.0937									

SENSITIVITY ANALYSIS CONDITION 2											
Total Capital Investment		40780000									
Bond Amount		40780000									
Bond Interest		0.18	per annum								
Bond Term		5	years								
Time Period/Year		1	2	3	4	5	6	7	8	9	10
Depreciation rate		0.4	0.2	0.2	0.2	0	0	0	0	0	0
Asset Book Value		$2 839 000	$567 800	$340 680	$204 408	$122 645	$0	$0	$0	$0	$0
Depreciation allowance		$2 271 200	$227 120	$136 272	$81 763	$0	$0	$0	$0	$0	$0
Annual Revenue		194400000	$194 400 000	$194 400 000	$194 400 000	$194 400 000	$194 400 000	$194 400 000	$194 400 000	$194 400 000	$194 400 000
Annual Production Cost		$316 600 000	$316 600 000	$316 600 000	$316 600 000	$316 600 000	$316 600 000	$316 600 000	$316 600 000	$316 600 000	$316 600 000
Annual Bond Repayments		$13 040 540	$13 040 540	$13 040 540	$13 040 540	$13 040 540	$0	$0	$0	$0	$0
Annual Interest on Bond		$4 884 540	$4 884 540	$4 884 540	$4 884 540	$4 884 540	$0	$0	$0	$0	$0
Taxable Revenue		-$129 355 740	-$127 311 660	-$127 220 812	-$127 166 304	-$127 084 540	-$122 200 000	-$122 200 000	-$122 200 000	-$122 200 000	-$122 200 000
Tax rate		0.33	0.33	0.33	0.33	0.33	0.33	0.33	0.33	0.33	0.33
Tax Paid		-$42 687 394	-$42 012 848	-$41 982 868	-$41 964 880	-$41 937 898	-$40 326 000	-$40 326 000	-$40 326 000	-$40 326 000	-$40 326 000
Net Cash Flow		-$86 668 346	-$85 298 812	-$85 237 944	-$85 201 423	-$85 146 642	-$81 874 000	-$81 874 000	-$81 874 000	-$81 874 000	-$81 874 000
Discount Rate		0.19	0.19	0.19	0.19	0.19	0.19	0.19	0.19	0.19	0.19
Discounted Cash Flow		-$72 830 543	-$60 235 020	-$50 581 544	-$42 487 287	-$35 680 647	-$28 831 301	-$24 227 984	-$20 359 650	-$17 108 950	-$14 377 269
Net Present Value	-$407 500 196										
ROI	#NUM!										
PBP	-1.112019475	-366720196	-36672019.6	-1.112019475							
Net Margin	-18.86420761	-0.3746	-0.3099	-0.2602	-0.2186	-0.1835	-0.1483	-0.1246	-0.1047	-0.0880	-0.0740
Ebitda Margin	-38.67268661	-0.1886									

ANNUAL PRODUCTION COSTS BASE CASE				
	FCI	17330000		
C	Total Direct Production Cost	1 to 8		**136257620.7**
1	Raw materials and process consumables	CRM&PC		**129100000**
2	Electricity and utilities	CE		**431100**
3	Operating labour	COL		**218100**
4	Direct supervisory and clerical labour	0.18 COL		**39258**
5	Maintenance and repairs	0.06 FCI		**1039800**
6	Operating supplies (including fuel)	0.15 (0.06 FCI)		**155970**
7	Laboratory charges	0.15 COL		**32715**
8	Patents and royalties	0.04 (CRM&PC)+ CE + COL +0.06 FCI +0.15 (0.06 FCI)+ 0.15 COL)		**5240677.72**
D	Total Fixed Production Costs	9 to 10		**1280864.8**
9	Insurance	0.029 FCI		**502570**
10	Plant overhead costs	0.60 (COL + 0.18 COL + 0.06 FCI)		**778294.8**
E	Total General Production Costs	11 to 12		**20775375.65**
11	Administrative costs	0.15 (COL + 0.18 COL +0.06 FCI)		**194573.7**
12	Product distribution and selling costs	0.13 APC		**20580801.95**
	Total Annual Production Costs	C+D+E		**158313861.2**

TOTAL CAPITAL INVESTMENT BASE CASE				
A	Fixed Capital Investment	A1+A2		17327610
A1	Total Direct Plant Costs	1 to 9		13750470
1	Total start-up equipment	CME		2839000
2	Purchased-equipment installation		0.39	1107210
3	Instrumentation & Controls (installed)		0.26	738140
4	Piping (installed)		0.31	880090
5	Electrical (Installed)		0.1	283900
6	Service facilities (installed)		0.55	1561450
7	Land (purchase)			1500000
8	Buildings (including services*)			4500000
9	Yard improvements		0.12	340680
A2	Total Indirect Costs	10 to 14		3577140
10	Design, Engineering and Supervision		0.32	908480
11	Construction Expenses		0.34	965260
12	Legal Expenses		0.04	113560
13	Contractors Fee		0.19	539410
14	Contingency		0.37	1050430
B	Working Capital	0.15TCI		3057813.529
	Total Capital Investment (TCI)	A + B		20385423.53

LEACHING LAB RESULTS

50g WPCB V = 2 L S/L = 25 g/L

WPCB Composition

		T1	T2	T3			T1	T2	T3						1000 g WPCB	
		mg/L	mg/L	mg/L	AVE	STD	mg	mg	mg	mg AVE	STD	g AVE			AVE	STD
HNO3+HCL	Al	1780.21	1720.75	1750.32	1750.43	29.73	3560.42	3441.50	3500.64	3500.85	59.46	3.50	7.00	Al	70017.07	1189.21
	Au	27.21	26.43	28.15	27.26	0.86	54.42	52.86	56.30	54.53	1.72	0.06	0.11	Au	1090.53	34.45
	Cu	13901.00	13906.00	13945.00	13917.33	24.09	27802.00	27812.00	27890.00	27834.67	48.18	27.89	55.78	Cu	556693.33	963.60
	Fe	833.00	804.36	847.21	828.19	21.83	1666.00	1608.72	1694.42	1656.38	43.65	1.69	3.39	Fe	33127.60	873.05
	Ni	402.33	399.89	401.00	401.07	1.22	804.66	799.78	802.00	802.15	2.44	0.80	1.60	Ni	16042.93	48.87

1000g WPCB V = 2 L S/L = 500 g/L

Leaching efficiency at 500 g/L S/L ratio

		T1	T2	T3			T1	T2	T3			T1 % Yield	T2 % Yield	T3 % Yield		
		mg/L	mg/L	mg/L	AVE	STD	mg	mg	mg	AVE	STD				AVE	STD
HNO3	Al	16015.14	15090.57	16028.23	15711.31	537.62	32030.28	30181.14	32056.46	31422.63	1075.24	45.75	43.11	43.11	43.99	1.52
	Au	0.00	0.00	0.00	0.00	0.00	0.00	0.00	0.00	0.00	0.00	0.00	0.00	0.00	0.00	0.00
	Cu	92900.39	92158.14	92517.77	92525.43	371.18	185800.78	184316.28	185035.54	185050.87	742.37	33.38	33.11	33.11	33.20	0.15
	Fe	10306.00	10526.00	10245.00	10359.00	147.81	20612.00	21052.00	20490.00	20718.00	295.61	62.22	63.55	63.55	63.11	0.77
	Ni	3330.00	3040.36	3470.21	3280.19	219.21	6660.00	6080.72	6940.42	6560.38	438.42	41.51	37.90	37.90	39.11	2.08

1000g WPCB V = 2 L S/L = 500 g/L

Leaching efficiency at 500 g/L S/L ratio

		T1	T2	T3			T1	T2	T3			T1 % Yield	T2 % Yield	T3 % Yield		
		mg/L	mg/L	mg/L	AVE	STD	mg	mg	mg	AVE	STD				AVE	STD
HCl	Al	8095.21	7895.21	7789.55	7926.66	155.24	16190.42	15790.42	15579.10	15853.31	310.47	23.12	22.55	22.25	22.64	0.44
	Au	0.00	0.00	0.00	0.00	0.00	0.00	0.00	0.00	0.00	0.00	0.00	0.00	0.00	0.00	0.00
	Cu	47306.00	47926.00	47245.00	47492.33	376.80	94612.00	95852.00	94490.00	94984.67	753.61	17.00	17.22	16.97	17.06	0.14
	Fe	983.01	1006.87	801.63	930.50	112.24	1966.02	2013.74	1603.26	1861.01	224.49	5.93	6.08	4.84	5.62	0.68
	Ni	833.00	804.36	847.21	828.19	21.83	1666.00	1608.72	1694.42	1656.38	43.65	10.38	10.03	10.56	10.32	0.27

1000g WPCB V = 2 L S/L = 500 g/L

Leaching efficiency at 500 g/L S/L ratio

		T1	T2	T3			T1	T2	T3			T1 % Yield	T2 % Yield	T3 % Yield		
		mg/L	mg/L	mg/L	AVE	STD	mg	mg	mg	AVE	STD				AVE	STD
H2SO4 + H2O2	Al	1150.31	1040.73	1132.52	1107.85	58.81	2300.62	2081.46	2265.04	2215.71	117.61	3.29	2.97	2.97	3.08	0.18
	Au	0.00	0.00	0.00	0.00	0.00	0.00	0.00	0.00	0.00	0.00	0.00	0.00	0.00	0.00	0.00
	Cu	77912.45	79128.69	78276.13	78439.09	624.28	155824.90	158257.38	156552.26	156878.18	1248.56	27.99	28.43	28.43	28.28	0.25
	Fe	827.35	658.44	836.65	774.15	100.31	1654.70	1316.88	1673.30	1548.29	200.63	4.99	3.98	3.98	4.32	0.59
	Ni	626.37	599.34	615.18	613.63	13.58	1252.74	1198.68	1230.36	1227.26	27.16	7.81	7.47	7.47	7.58	0.19

1000g WPCB V = 2 L S/L = 500 g/L

Leaching efficiency at 500 g/L S/L ratio

		T1	T2	T3			T1	T2	T3			T1 % Yield	T2 % Yield	T3 % Yield		
		mg/L	mg/L	mg/L	AVE	STD	mg	mg	mg	AVE	STD				AVE	STD
I2 + I + H2O2	Al	0.00	0.00	0.00	0.00	0.00	0.00	0.00	0.00	0.00	0.00	0.00	0.00	0.00	0.00	0.00
	Au	531.22	529.70	538.54	533.15	4.73	1062.44	1059.40	1077.08	1066.31	9.45	97.42	97.15	98.77	97.78	0.87
	Cu	60.77	59.82	60.16	60.25	0.48	121.54	119.64	120.32	120.50	0.96	0.02	0.02	0.02	0.02	0.00
	Fe	0.00	0.00	0.00	0.00	0.00	0.00	0.00	0.00	0.00	0.00	0.00	0.00	0.00	0.00	0.00
	Ni	0.00	0.00	0.00	0.00	0.00	0.00	0.00	0.00	0.00	0.00	0.00	0.00	0.00	0.00	0.00

Cumulative Yields

	T1 % Yield	T2 % Yield	T3 % Yield		
				AVE	STD
Al	72.16	68.63	68.33	69.70	2.13
Au	97.42	97.15	98.77	97.78	0.87
Cu	78.38	78.78	78.53	78.56	0.20
Fe	73.15	73.60	72.36	73.04	0.63
Ni	59.71	55.40	55.94	57.02	2.35